

INFLUENCE OF THE HDL RECEPTOR ON ATHEROSCLEROSIS IN MICE

**THE IMPACT OF THE HDL RECEPTOR, SR-B1, ON CARDIOVASCULAR
PHENOTYPES IN THE MOUSE.**

By MARK FULLER, B.SC (HONOURS)

**A Thesis Submitted to the School of Graduate Studies in Partial Fulfillment
of the Requirements for the Degree Doctor of Philosophy.**

McMaster University

© Copyright by Mark Fuller, 2015

Abstract

Atherosclerosis is a major cause of cardiovascular disease, which is among the leading causes of death globally. Elevated plasma concentration of low density lipoprotein (LDL) cholesterol is a risk factor for atherosclerosis, while a high plasma level of high density lipoprotein (HDL) cholesterol is considered protective. Uptake of HDL cholesterol by hepatocytes during reverse cholesterol transport, and athero-protective signaling induced by HDL in other cells are mediated by the scavenger receptor class B, type 1 (SR-B1).

SR-B1 deficiency in mice that are susceptible to atherosclerosis results in exacerbation of atherosclerosis, and in mice with mutations in apolipoprotein E (apoE), renders mice uniquely susceptible to occlusive coronary artery (CA) atherosclerosis and myocardial infarction.

In this thesis, the impact of a lack of SR-B1 on the development of atherosclerosis is characterized in otherwise wild type mice, and in mice that also lack the LDL receptor (LDLR). We demonstrate that after prolonged feeding of a high fat, high cholesterol cholate-containing diet, SR-B1 knockout (KO) mice develop similar levels of diet-induced atherosclerosis to LDLR KO mice and apoE KO mice in traditionally susceptible arteries, and significantly more atherosclerosis in arteries that are typically resistant to plaque development, such as the CAs. SR-B1/LDLR double KO mice develop extensive occlusive CA atherosclerosis accompanied by myocardial infarction, and exhibit reduced

survival compared to LDLR KO control mice when fed a variety of atherogenic diets.

In both SR-B1 single KO and SR-B1/LDLR dKO mice, CA atherosclerosis is accompanied by splenomegaly, elevated numbers of circulating leukocytes and increased expression of VCAM-1 in CA endothelium. Interestingly, removal of the spleen has no effect on circulating leukocyte numbers or atherosclerosis in SR-B1/LDLR dKO mice, suggesting the enlarged spleens in SR-B1 deficient mice do not influence atherosclerosis in these animals.

We conclude that SR-B1 is important for the protection against atherosclerosis in mice, particularly in CAs. This is likely through roles in multiple cell types including hepatocytes, endothelial cells and bone marrow-derived cells. Future studies should focus on evaluating the impact of cell-specific SR-B1 activity in different cell types on murine atherosclerotic CA disease.

Acknowledgements

The research presented in this thesis would not have been possible without continued support and guidance from Dr. Bernardo (Dino) Trigatti. Dino is a meticulous researcher and a talented communicator and writer; these are among the most important skills that I take away from graduate school and I thank Dino for consistently challenging me and providing multiple opportunities to develop these skills.

My supervisory committee; Dino, Dr. Werstuck, and Dr. Gross; has been nothing but supportive throughout my graduate career. My experiences with them were always positive and I thank them for their encouragement and helpful advice.

My years at McMaster have been the best of my life; this time was made infinitely more positive by the people I've met and the friendships that I've made. Thank you to, among others, my friends at TaARI, my friends from the MiNDs program and the members of the Mighty Chondria and Cereballers softball teams for making this experience so much fun. Thank you especially to Dr. Omid Dadoo, with whom I've worked elbow to elbow on multiple projects, both in and outside of the lab – we made it!

Kelly, you're my best friend and have consistently been there for me for as long as I can remember. Thank you for keeping me grounded and encouraging me to stay focused, while at the same time making sure I always left some time to relax and enjoy family and friends. You've been a constant source of support

and I can't imagine making this journey without you. I love you and I'm excited to move on to the next stage of our lives together.

Finally, I want to thank my parents. My father passed away early in my graduate school career, but he is nevertheless largely responsible for the person I am today. He taught me the value of hard work and led by example. He never missed a graduation, an awards ceremony or sporting event when I was growing up and he took every opportunity to make sure I knew how proud he was of my accomplishments. I'm grateful to have had him as a part of my life for as long as did. My mom is one of the strongest and most selfless people I know. On multiple occasions she has gone, and continues to go out of her way to make my life easier. Like my father, she has been present at every event in my life, big or small, and in many ways I've followed in her academic footsteps. Even after her official retirement, she continues to expand her education and embark on new fields of science and I admire her for her lifelong pursuit of learning.

I couldn't ask for a more supportive group of people in my life and owe my success in part to each and every one of you. Thank you for being who you are!

- Mark

Table of Contents

Abstract	iii
Acknowledgements	v
Table of Contents	vii
List of Figures and Tables	xii
List of Abbreviations	xv
Chapter 1: General Introduction	1
1.1 Epidemiology of Cardiovascular Diseases	1
1.2 Atherosclerosis Overview	1
1.3 Lipids and Lipoproteins	10
<i>Chylomicron, VLDL and LDL metabolism</i>	<i>14</i>
<i>HDL metabolism</i>	<i>19</i>
1.4 Mouse Models of Atherosclerosis	23
<i>Diets used in Atherosclerosis Research</i>	<i>24</i>
<i>ApoE KO Mice</i>	<i>25</i>
<i>LDLR KO Mice</i>	<i>27</i>
1.5 Immune Cells	28
<i>Monocytes</i>	<i>29</i>
<i>Lymphocytes</i>	<i>30</i>
1.6 Endothelial Cells	32
<i>Adhesion molecules in atherosclerosis</i>	<i>33</i>
<i>Regional Specific Endothelial Inflammation</i>	<i>35</i>
1.7 Platelets	36
1.8 Scavenger Receptors	37
1.9 SR-B1	38
<i>SR-B1 function in RCT in vivo</i>	<i>40</i>
<i>The Role of SR-B1 in non-hepatic tissues</i>	<i>42</i>
<i>The effect of SR-B1 on Reproduction</i>	<i>43</i>
<i>The effect of SR-B1 on Red Blood Cells</i>	<i>44</i>
<i>The effect of SR-B1 on Platelets</i>	<i>44</i>
1.10 The effect of SR-B1 on atherosclerosis in mice	46
<i>SR-B1/apoE double knockout mice</i>	<i>47</i>
<i>SR-B1 KO mice with hypomorphic expression of apoE R61</i>	<i>49</i>

<i>SR-B1/ LDLR dKO mice</i>	50
1.11 Beyond Cholesterol Uptake, is Coronary Atherosclerosis in SR-B1 KO Mice a Multi-Cellular Phenomenon?	51
<i>Role in Endothelial Cells and HDL signaling</i>	51
<i>Bone Marrow SR-B1 in Atherosclerosis</i>	55
<i>The role of SR-B1 in Macrophages and Inflammation</i>	56
<i>HDL and SR-B1 in endothelial progenitor cells</i>	58
1.12 Additional Evidence Supporting a Role for HDL Induced Signaling in CA Atherosclerosis Protection	60
<i>eNOS/apoE dKO mice</i>	61
<i>AKT1/apoE dKO mice</i>	61
<i>PDZK1/apoE dKO mice</i>	62
1.13 Overall Context and Objective	63
1.14 Hypothesis	63
1.15 Specific Aims	64
<i>Aim of Chapter 2</i>	64
<i>Aim of Chapter 3</i>	64
<i>Aim of Chapter 4</i>	64
Chapter 2: Extensive Diet-Induced Atherosclerosis in the Aorta and Coronary Arteries of Scavenger Receptor Class B Type 1-Deficient Mice is Associated with Substantial Leukocytosis and Elevated Vascular Cell Adhesion Molecule-1 Expression in Coronary Artery Endothelium.	65
Foreword	65
2.1 Abstract	67
2.2 Introduction	68
2.3 Materials and Methods	71
<i>2.3.1 Animals and Diet</i>	71
<i>2.3.2 Plasma Lipids</i>	71
<i>2.3.3 Atherosclerosis Analysis</i>	72
<i>2.3.4 Histological Characterization of Atherosclerotic Plaques</i>	73
<i>2.3.5 Blood Cell Analysis</i>	73
<i>2.3.6 Cytokine Analysis</i>	74
<i>2.3.7 VCAM-1 Immunofluorescence</i>	74

2.3.8 Statistical Analysis.....	74
2.4 Results	75
2.4.1 Plasma Lipids	75
2.4.2 Aortic Sinus Atherosclerosis and Plaque Composition	80
2.4.4 Blood Cells and Cytokines.....	88
2.4.5 Coronary Artery VCAM-1 Expression	95
2.5 Discussion	98
2.6 References.....	102
2.7 Supplementary Materials.....	108
Chapter 3: The Effects of Diet on Occlusive Coronary Artery Atherosclerosis and Myocardial Infarction in Scavenger Receptor Class B, Type 1/Low-Density Lipoprotein Receptor Double Knockout Mice.	113
Foreword.....	113
3.1 Abstract	115
3.2 Introduction	116
3.3 Results	118
3.3.1 Survival of SR-BI/LDLR dKO Mice Fed Different Atherogenic Diets	118
3.3.2 Atherosclerosis in the Aortic Sinus	119
3.3.3 Atherosclerosis in CAs	123
3.3.4 Myocardial Infarction	127
3.3.5 Plasma Lipoproteins and Cytokines	130
3.3.6 Blood Cells	134
3.3.7 CA Endothelial Cell Activation	138
3.4 Discussion.....	141
3.5 References.....	147
3.6 Supplementary Materials and Methods.....	155
3.6.1 Animals.....	155
3.6.2 Diet Induction of Atherosclerosis	155
3.6.3 Histology.....	156
3.6.4 Immunofluorescence	157
3.6.5 Plasma Lipid and Lipoprotein Analysis.....	158
3.6.5 Triglyceride Production.....	158

3.6.6 Plasma Cytokine Measurements.....	159
3.6.7 Blood Cell Analysis.....	159
3.6.8 Statistical Analysis.....	159
3.7 Supplementary Data	160
Chapter 4: Splenectomy has no Influence on the Development of Occlusive Coronary Artery Atherosclerosis in High Fat, High Cholesterol Diet Fed Scavenger Receptor Class B Type 1/Low Density Lipoprotein Receptor Double Knockout Mice.....	166
Foreword.....	166
4.1 Abstract	168
4.2 Introduction	169
4.3 Materials and Methods	171
4.3.1 Mice, Diet and Splenectomy.....	171
4.3.2 Blood Cell Analysis.....	172
4.3.3 Assessment of Atherosclerosis in the Aortic Sinus and Coronary Arteries.....	172
4.3.4 Assessment of Atherosclerosis in the Descending Aorta	173
4.3.5 Myocardial Infarction	173
4.3.6 Plasma Lipid Analysis.....	173
<i>Plasma was prepared from blood collected after a 4 hour fast at the time of harvest. Total cholesterol (Cholesterol Infinity, Thermo Scientific), HDL cholesterol (HDL Cholesterol E, WAKO), free cholesterol (Free Cholesterol E, WAKO) and triglycerides (L-Type Triglyceride M, WAKO) were measured using the commercially available kits indicated in parentheses following manufacturers' protocols.</i>	<i>174</i>
4.3.7 Plasma Cytokine Analysis	174
4.3.8 Statistical Analysis.....	174
4.4 Results	174
4.4.1 Spleen Size and Leukocytosis in HFC-fed SR-B1/LDLR dKO Mice .	174
4.4.2 The Effect of Splenectomy on Atherosclerosis in the Aortic Sinus and Descending Aorta.....	178
4.4.3 The Effect of Splenectomy on Coronary Artery Atherosclerosis and Myocardial Infarction	181
4.4.4 The Effect of Splenectomy on Plasma Lipids	185
4.4.5 The Effect of Splenectomy on Leukocytosis.....	188

4.4.6 <i>The Effect of Splenectomy on Systemic Inflammation</i>	188
4.4.7 <i>The Effect of Splenectomy on the Liver</i>	192
4.5 Discussion	195
4.6 References	197
4.7 Supplementary Materials	202
Chapter 5: Discussion	203
5.1 Summary of Results in Chapters 2-4	204
5.2 Implications from the Studies Detailed in Chapters 2-4	206
5.2.1 <i>The Role of SR-B1 in the Liver and in Lipoprotein Metabolism</i>	206
5.2.2 <i>The Role of SR-B1 in Immune Cells and Inflammation</i>	210
5.2.3 <i>The Role of SR-B1 in Platelets</i>	214
5.2.4 <i>The Role of SR-B1 in Endothelial and Endothelial Progenitor Cells</i> .	215
5.3 Conclusions	218
References	220

List of Figures and Tables

Figure 1.1 – The development of an atherosclerotic plaque.....	4
Figure 1.2 – Classification of atherosclerotic lesions according to complexity.....	8
Figure 1.3 – Characteristics of lipoproteins.	12
Figure 1.4 – Metabolism of chylomicrons, VLDL and LDL.....	17
Figure 1.5 – Overview of reverse cholesterol transport.	21
Figure 1.6 – SR-B1 signaling in endothelial cells.....	53
Figure 2.1 – Plasma Lipid Parameters in HFCC-fed WT, LDLR KO, apoE KO and SR-B1 KO mice.	78
Figure 2.2 – Size and Composition of Aortic Sinus Atherosclerotic Plaques in HFCC-fed WT, LDLR KO, apoE KO and SR-B1 KO mice.....	82
Figure 2.3 – Atherosclerosis in the Descending Aorta and Coronary Arteries of HFCC-fed WT, LDLR KO, apoE KO and SR-B1 KO mice.....	86
Figure 2.4 – Circulating Immune Cells and Systemic Inflammatory Markers in HFCC-fed WT, LDLR KO, apoE KO and SR-B1 KO mice.....	90
Figure 2.5 – Monocyte Subsets in HFCC-fed WT, LDLR KO, apoE KO and SR-B1 KO mice.	93
Figure 2.6 – Expression of VCAM-1 in Coronary Artery Endothelial Cells in HFCC-fed WT, LDLR KO, apoE KO and SR-B1 KO mice.....	96
Supplementary Figure 2.7 – Plasma lipid parameters in chow-fed wild type, LDLR KO, apoE KO and SR-B1 KO mice.	108
Supplementary Figure 2.8 – Atherosclerosis in the aortic sinus of male wild type, LDLR KO, apoE KO and SR-B1 KO mice fed the HFCC for 20 weeks.	110
Supplementary Table 2.1. Hematology profiles for wild type, LDLR KO, apoE KO and SR-B1 KO mice fed either chow or HFCC diet for 20 weeks.....	112
Figure 3.1 – SR-B1/LDLR dKO mice exhibit diet dependent reduced survival and develop larger atherosclerotic plaques in their aortic sinuses compared to similarly treated LDLR KO control mice.....	121

Figure 3.2 – SR-BI/LDLR dKO mice develop occlusive CA atherosclerosis with evidence of platelet accumulation.....	125
Figure 3.3 – Large myocardial infarctions are observed in SR-BI/LDLR dKO mice fed diets that are very high in cholesterol.	128
Figure 3.4 – SR-BI/LDLR dKO mice fed atherogenic diets have lower plasma cholesterol levels but higher levels of circulating inflammatory cytokines than LDLR KO mice fed the same diets for the same length of time.	132
Figure 3.5 – SR-BI/LDLR dKO mice exhibit increased circulating monocyte and lymphocyte numbers and proportionally larger populations of Ly6Chi monocytes compared to control LDLR KO mice when fed the HFCC diet.	136
Figure 3.6 – Larger proportions of CA’s stain positively for endothelial activation markers VCAM-1 and ICAM-1 in SR-BI/LDLR dKO mice compared to control LDLR KO mice fed each of the atherogenic diets.....	139
Supplementary Figure 3.7 – Atherosclerosis and associated phenotypes in normal chow fed SR-BI/LDLR dKO and control LDLR KO mice.....	160
Supplementary Table 3.1 – Plasma lipid parameters in LDLR KO and SR-BI/LDLR dKO mice fed different diets.....	162
Supplementary Figure 3.8 – Hepatic VLDL triglyceride secretion is reduced in SR-BI/LDLR dKO mice compared to LDLR KO control mice fed HF and HFCC diets.....	163
Supplementary Table 3.2 – Spleen weights.	165
Supplementary Table 3.3 – Hematology profiles of Chow- and HFCC-fed SR-BI/LDLR dKO and control LDLR KO mice.	165
Figure 4.1 – SR-B1/LDLR dKO mice have enlarged spleens and elevated monocyte and lymphocyte counts in circulation compared to LDLR KO mice when fed a high fat, high cholesterol diet.	176
Figure 4.2 – Splenectomy does not reduce HFC diet accelerated atherosclerosis in the aortic sinus or descending aorta of SR-B1/LDLR dKO mice.....	179
Figure 4.3 – Splenectomy does not influence the development of HFC diet induced coronary artery atherosclerosis or myocardial infarction in SR-B1/LDLR dKO mice.....	183

Figure 4.4 – Splenectomy has little effect on plasma lipid levels in HFC fed SR-B1/LDLR dKO mice.	186
Figure 4.5 – Splenectomy does not alter circulating monocyte, lymphocyte or cytokine levels in HFC fed SR-B1/LDLR dKO mice.....	190
Figure 4.6 – Splenectomy results in enlargement of the liver in HFC fed SR-B1/LDLR dKO mice.	193
Supplementary Table 4.1 – Hematology profiles of HFC-fed non-surgical LDLR KO and SR-B1/LDLR dKO mice, and sham operated or splenectomized SR-B1/LDLR dKO mice.	202

List of Abbreviations

ABCA1	adenosine triphosphate binding cassette transporter A1
ABCG1	adenosine triphosphate binding cassette transporter G1
ACTH	adrenocorticotrophic hormone
ANOVA	analysis of variance
apoA1	apolipoprotein A1
apoB	apolipoprotein B
apoC2	apolipoprotein C2
apoE	apolipoprotein E
B1/E dKO	SR-B1/apoE double knockout
BMT	bone marrow transplantation
CA	coronary artery
CAD	coronary artery disease
CCR2	C-C chemokine receptor type 2
CCR5	C-C chemokine receptor type 5
CD115	cluster of differentiation 115
CD11b	cluster of differentiation 11b
CD36	cluster of differentiation 36
CD41	cluster of differentiation 41/ integrin alpha chain 2B
CD68	cluster of differentiation 68
CE	cholesterol ester
CHO	chinese hamster ovary

CM	chylomicron
CVD	cardiovascular disease
ELISA	enzyme-linked immunosorbant assay
eNOS	endothelial nitric oxide synthase
EPC	endothelial progenitor cell
ER	endoplasmic reticulum
ERK	extracellular signal-regulated kinases
FA	fatty acid
FC	free cholesterol
FFA	free fatty acid
FPLC	fast protein liquid chromatography
H&E	hematoxylin and eosin
HC	high cholesterol
HDL	high density lipoprotein
HF	high fat
HFC	high fat, high cholesterol
HFCC	high fat, high cholesterol, cholate
HL	hepatic lipase
HMG-CoA	3-hydroxy-3-methylglutaryl-coenzyme A
HSC	haematopoietic stem cell
HypoE	apoE R61 hypomorphic
ICAM-1	intercellular adhesion molecule 1

IDL	intermediate density lipoprotein
IFN γ	interferon gamma
IgG	immunoglobulin G
IgM	immunoglobulin M
I κ B	inhibitor of kappa B
IL10	interleukin 10
IL-6	interleukin-6
KO	knockout
LCAT	lecithin-cholesterol acyltransferase
LDL	low density lipoprotein
LDLR	low density lipoprotein receptor
LIMP-2	lysosomal integral membrane protein type 2
LPL	lipoprotein lipase
LPS	lipopolysaccharide
LRP-1	low density lipoprotein receptor related protein 1
MAPK	mitogen activated protein kinase
MCP-1	monocyte chemoattractant protein-1
MI	myocardial infarction
MMP	matrix metalloproteinases
mRNA	messenger ribonucleic acid
MTP	microsomal triglyceride transport protein

NF- κ B	nuclear factor kappa B
NK	natural killer
NPC1L1	Niemann-Pick C1-like 1
OCT	optimal cutting temperature
oxLDL	oxidized low density lipoprotein
PCSK9	proprotein convertase subtilisin/kexin type 9
PDZK1	pdz domain containing 1
PI3K	phosphatidylinositol 3 kinase
POMx	pomegranate extract
RAG2	recombinant activating gene 2
RANTES	regulated on activation, normal T cell expressed and secreted
RBC	red blood cell
RCT	reverse cholesterol transport
S1P1	sphingosine-1-phosphate receptor-1
siRNA	small inhibiting ribonucleic acid
SMA	smooth muscle actin
SPx	Splenectomy
SR	scavenger receptor
SR-A1	scavenger receptor class A type 1
SR-B1/SR-BI	scavenger receptor class B, type 1

SR-B2	scavenger receptor class type 2
SR-B3	scavenger receptor class B type 3
TC	total cholesterol
TG	triglyceride
TGF β	transforming growth factor beta
Th	t-helper
TNF α	tumor necrosis factor alpha
TUNEL	terminal deoxynucleotidyl transferase dUTP nick end labeling
VCAM-1 D4D	VCAM-1 domain 4-deficient
VCAM-1	vascular cell adhesion molecule 1
VLDL	very low density lipoprotein
WT	wild type

Chapter 1: General Introduction

1.1 Epidemiology of Cardiovascular Diseases

Cardiovascular diseases (CVDs) are among the leading causes of morbidity and mortality and account for a major burden on the health of Canadians and citizens of other developed nations (Libby, 2002). In Canada in 2011, diseases of the circulatory system were the second leading cause of mortality, accounting for 27.3% of all deaths, of which approximately half were a result of ischemic heart diseases (Statistics Canada). In 2005, the estimated cost of cardiovascular diseases to the Canadian economy was \$20.5 billion; this figure is expected to reach \$28.3 billion by 2020 (Conference Board of Canada). Atherosclerosis, characterized by a build-up of cholesterol rich plaque in the walls of small and medium sized arteries, is a major cause of ischemic cardiovascular diseases such as heart attack and stroke (Libby, 2002).

1.2 Atherosclerosis Overview

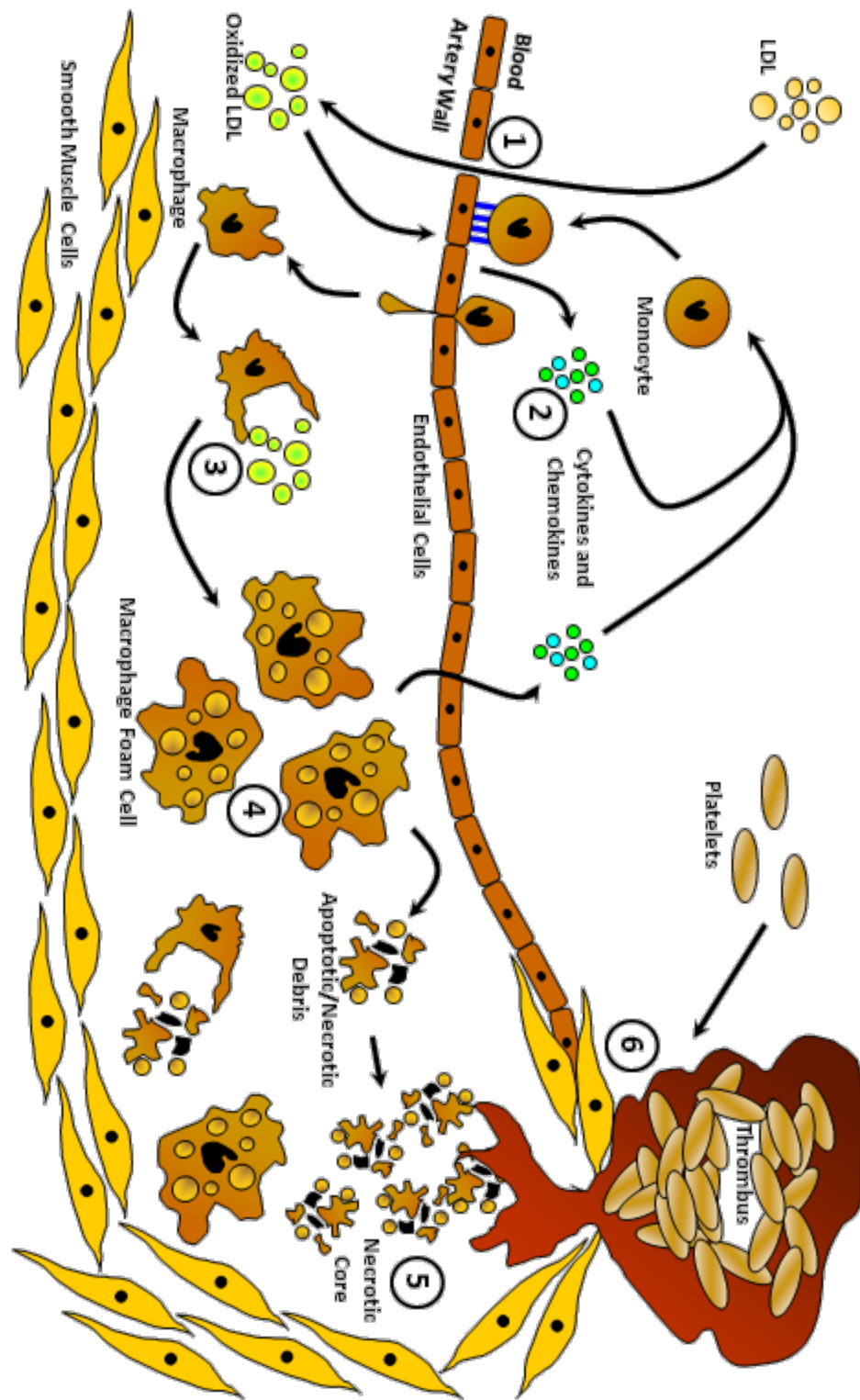
Atherosclerosis is a dynamic process involving multiple cell types and risk factors including hyperlipidemia, the immune system and inflammation, and the cells of the vasculature (Libby, 2002). Atherosclerosis is initiated by infiltration of the sub-endothelial space of the artery wall by cholesterol-carrying low density lipoprotein (LDL) particles from the circulation (Lusis, 2000). This tends to occur at sites along the vasculature where blood flow is non-laminar, which increases the permeability of the endothelial barrier and promotes the expression of adhesion

molecules by endothelial cells, creating sites that favor monocyte attachment (Chatzizisis et al., 2007). The prevailing view is that LDL particles can get trapped in the artery wall and become oxidized, generating oxidized (ox)LDLs, inflammatory particles that activates endothelial cells to secrete a variety of pro-inflammatory cytokines and chemokines, and further increase expression of adhesion molecules on the cell surface (Steinberg, 1997). This collectively results in the recruitment and attachment of monocytes, which migrate into the artery wall, differentiate into macrophages and phagocytose oxLDL particles (Libby, 2002). Cholesterol from oxLDL is stored in lipid droplets inside the macrophage, giving rise to macrophage foam cells, the characteristic cell type of early stage atherosclerotic lesions termed fatty streaks (X. H. Yu, Fu, Zhang, Yin, & Tang, 2013). Foam cells eventually die or undergo apoptosis (Tabas, 2010). It is thought that the resulting debris is initially cleared by neighboring macrophages in the plaque; however, as the plaque becomes more advanced and healthy macrophages are unable to keep up with necrosis and apoptosis of foam cells, a lipid rich necrotic core develops (Tabas, 2010). Smooth muscle cells lining the vessel proliferate and migrate into very advanced lesions, and lay down collagen on the surface of the plaque, forming a fibrous cap that stabilizes the lesion and protects the necrotic core (Hopkins, 2013). Atherosclerotic plaques may be asymptomatic for decades prior to an acute clinical manifestation. It is erosion of the fibrous cap by proteases secreted by macrophage foam cells and released by necrotic foam cells that makes a plaque

vulnerable to rupture (Libby, 2009). Plaque rupture exposes the highly pro-thrombotic contents of the lesion to the bloodstream, leading to formation of a thrombus on top of the lesion, completely blocking blood flow and triggering a clinical event such as a heart attack or stroke (Libby, 2009) (See Figure 1.1).

Figure 1.1 – The development of an atherosclerotic plaque.

The formation of an atherosclerotic plaque begins with the deposition and retention of LDL in the subendothelial space of the artery wall at sites of endothelial dysfunction (1). Oxidation of LDL creates an inflammatory particle (oxLDL) that activates overlying endothelial cells to secrete pro-inflammatory cytokines and chemokines, and express adhesion molecules (2). This results in recruitment and attachment of monocytes which migrate across the endothelium, differentiate into macrophages, and endocytose oxLDL (3). Cholesterol derived from oxLDL is stored in lipid droplets in the macrophages, giving rise to lipid-laden macrophage foam cells, the characteristic cell type in early stage atherosclerotic lesions (4). Foam cells secrete additional cytokines and chemokines, driving the continued recruitment of monocytes and proliferation of the plaque. Eventually, foam cells undergo apoptosis or necrosis. In early lesions, cellular debris is cleared by neighbouring macrophages, however in more complex lesions this debris accumulates in the form of an acellular, lipid-rich necrotic core (5). Eventually, smooth muscle cell proliferation and migration into the plaque creates a fibrous cap overlaying the lesion. Rupture of this fibrous cap exposes the contents of the lesion to the thrombotic machinery in the blood, resulting in the formation of a thrombus, which can occlude the vessel and lead to an acute clinical event (6).



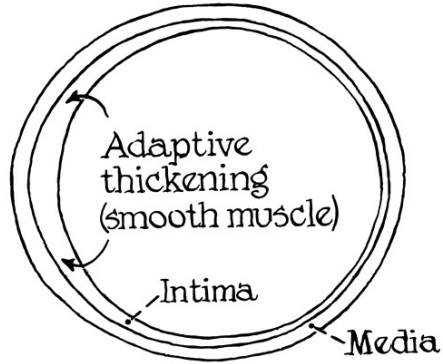
Clinically, atherosclerotic lesions are classified from class I to class VI (Stary et al., 1995; Stary et al., 1994), with each successive class representing a more advanced stage of atherosclerosis than the preceding class (See Figure 1.2). Type I lesions can be detected in human infants, and are characterized by isolated macrophage foam cells or small groups of foam cells in the artery wall. These are often macroscopically invisible (Stary et al., 1994). Type II lesions include those that are commonly referred to as fatty streaks and can be detected in the aortas of children as young as two years of age. These lesions are visible to the naked eye and consist of larger groups of macrophages and foam cells that form a thin layer in the artery wall (Stary et al., 1994). While macrophages are the dominant cell type in type II lesions, these lesions may also be characterized by lipid accumulation in the smooth muscle cells and by the presence of other immune cells such as T-lymphocytes (Stary et al., 1994). Type III lesions are similar in cellular composition to type II lesions in that they are dominated by macrophage foam cells (Stary et al., 1994). Type III lesions can be found in young adults; they are larger than type II lesions and contain more extracellular lipid found in droplets between the macrophage and smooth muscle layers, as well as throughout the smooth muscle cells (Stary et al., 1994). These are the last class of lesion that are not considered to be clinically dangerous. Type IV lesions are the first class of lesions characterized by an extracellular lipid-rich core. Bordering the lipid core are macrophage foam cells and lymphocytes, with minimal fibrous tissue (Stary et al., 1995). These lesions are

thicker than type III lesions but are generally characterized by outward remodeling of the vessel wall, such that the vessel lumen remains unobstructed (Stary et al., 1995). Type IV lesions evolve into type V lesions when a fibrous cap forms over the lipid core. Fibrous caps in type V lesions are characterized by accumulation of smooth muscle cells and collagen above the lipid core (Stary et al., 1995). These lesions tend to narrow the vessel. Both type IV and V lesions are clinically dangerous because they can rupture, leading to thrombosis and complete occlusion of the vessel (Stary et al., 1995). Lesions characterized by thrombosis or intraplaque hemorrhage are classified as type VI lesions (Stary et al., 1995). These lesion classes will be referred to throughout this introduction.

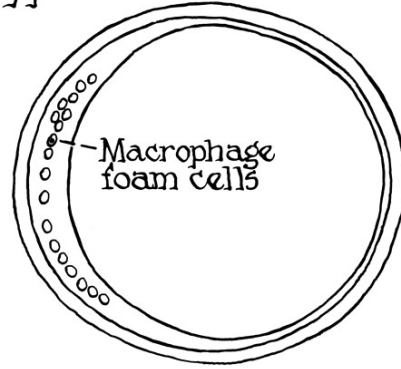
Figure 1.2 – Classification of atherosclerotic lesions according to complexity. An illustration of the progression of an atherosclerotic lesion from type I to type VI according to Stary et al, 1995. Latent lesions (type I-III) are characterized by macrophage foam cells and small extracellular lipid droplets. As these lesion progress to clinically dangerous plaques (type IV-VI), they develop lipid-rich cores and a fibrous cap, which eventually ruptures leading to thrombosis.

Reprinted with permission from: Stary, H. C., Chandler, A. B., Dinsmore, R. E., Fuster, V., Glagov, S., Insull, W., Jr., Rosenfeld, M. E., Schwartz, C. J., Wagner, W. D., Wissler, R. W. (1995). A definition of advanced types of atherosclerotic lesions and a histological classification of atherosclerosis. A report from the Committee on Vascular Lesions of the Council on Arteriosclerosis, American Heart Association. *Circulation*, 92(5), 1355-1374. (License #: 3543320324735)

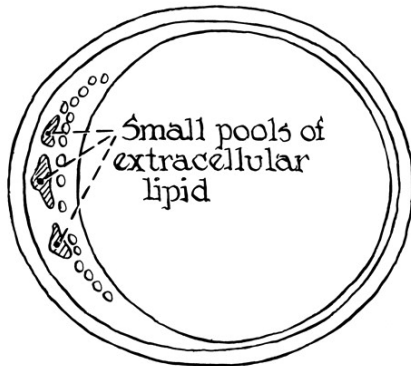
Coronary artery at lesion-prone location



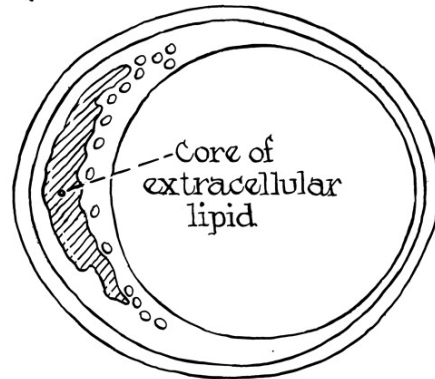
Type II lesion



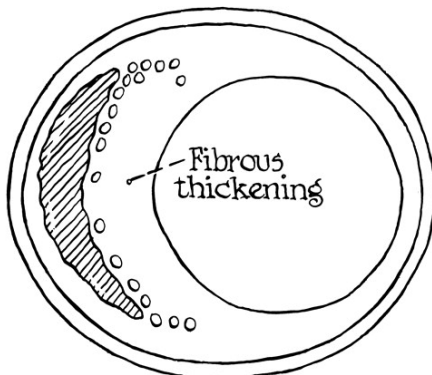
Type III (preatheroma)



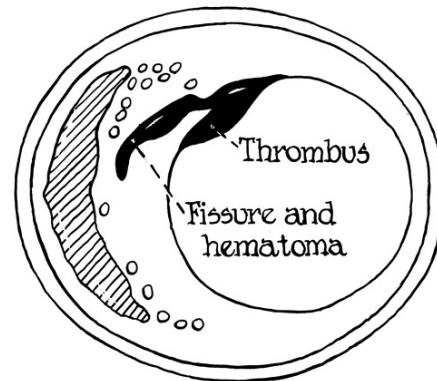
Type IV (atheroma)



Type V (fibroatheroma)



Type VI (complicated lesion)



1.3 Lipids and Lipoproteins

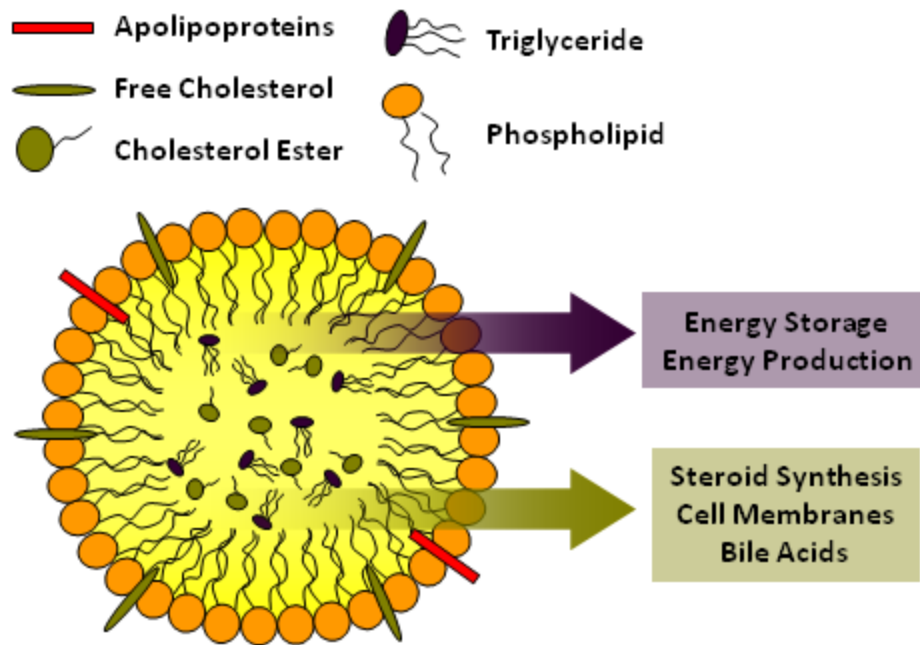
Perhaps the most clinically relevant lipids in atherosclerosis are cholesterol and triglycerides (TG) (Hegele, 2009). Cholesterol is a tetracyclic lipid (Nes, 2011) that has a number of biological roles as a component of cell membranes, and as a precursor in the synthesis of steroid hormones and bile acids (Hegele, 2009). While cholesterol is essential in many biological processes, the concentration of cholesterol in human blood tends to be much higher than is actually necessary (LaRosa, Pedersen, Somaratne, & Wasserman, 2013). This is problematic as high levels of cholesterol in blood plasma, particularly cholesterol in complex with LDL particles, is strongly correlated with the development of atherosclerosis (described above) (LaRosa et al., 2013). Cholesterol can be absorbed from the diet, or produced endogenously in the endoplasmic reticulum (ER) of all cells through a complicated biosynthetic process involving more than 30 enzymes (Herman, 2003). The rate limiting enzyme in this pathway, HMG-CoA Reductase, is the target of statins, the most commonly prescribed class of cholesterol lowering drugs (Hegele, 2009).

TGs are composed of a glycerol molecule and three fatty acid (FA) molecules and represent a major source of energy for the body (Hegele, 2009). TG molecules are assembled in the intestinal enterocytes and liver hepatocytes and are hydrolyzed in circulation to supply free (F)FAs to peripheral tissues for energy production through β -oxidation or energy storage through reassembly of TG (Hegele, 2009).

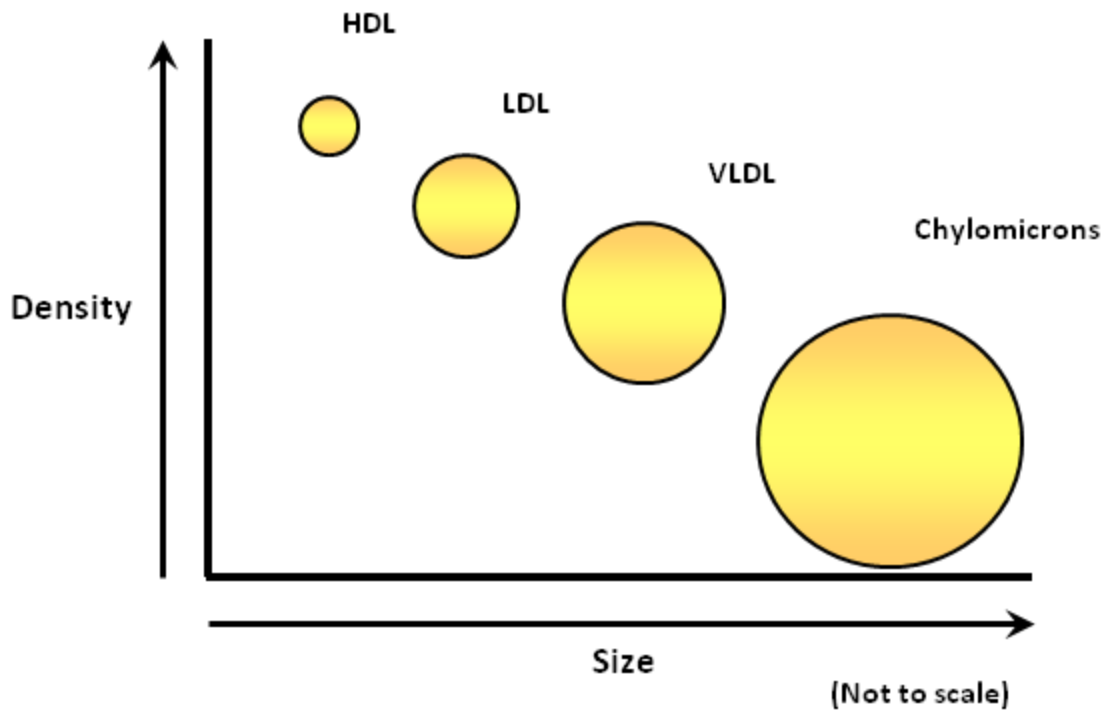
Cholesterol and TG in plasma travel through the circulation as components of lipoproteins, which are spherical particles with a hydrophilic surface and hydrophobic core. The surface of lipoproteins is comprised mainly of a monolayer of phospholipids, unesterified cholesterol (free cholesterol, FC) and associated proteins called apolipoproteins (Hegele, 2009). The cargo of lipoproteins is carried in the core and consists of mainly TG and esterified cholesterol (CE) (Ridker, 2014) (Figure 1.3A). There are several different classes of lipoproteins that differ in structure and function, and can be broadly classified based on density. Chylomicrons are the largest and least dense lipoproteins, followed by very low density lipoproteins (VLDLs), LDLs and finally high density lipoproteins (HDLs) (Ridker, 2014) (Figure 1.3B). The surface apolipoproteins and the ratio of TG:CE in the cores of lipoproteins vary depending on the type of lipoprotein (Ridker, 2014). The structure, metabolism and major metabolic roles of different lipoproteins will be discussed in the sections that follow.

Figure 1.3 – Characteristics of lipoproteins. A) Lipoproteins supply biologically important lipids (mainly cholesterol and triglycerides [TG]) to the cells of the body. Cholesterol is used in the synthesis of steroid hormones and bile acids, and as a component of cell membranes; while TG are used in the production and storage of energy. Lipoproteins are spherical particles with a hydrophilic surface and a hydrophobic core. The surface is comprised of phospholipid head groups, various apolipoproteins and free cholesterol. The cargo of a lipoprotein exists in the hydrophobic core and consists mainly of esterified cholesterol and TG. The ratio of cholesterol to TG in the core, and the assortment of apolipoproteins on the surface of the lipoprotein vary depending on the type of lipoprotein. B) Lipoproteins are classified based on their density, which is inversely proportional to their size. High density lipoproteins (HDL) are the smallest and most dense of the lipoproteins, and have the highest protein to lipid ratio. In terms of increasing density, HDLs are followed by low density lipoproteins (LDL), which are larger and less dense; very low density lipoproteins (VLDL), which even larger and less dense than LDLs; and finally, chylomicrons, the largest and least dense of the lipoproteins. Chylomicrons and VLDL are major carriers of TG, while LDL and HDL are major carriers of cholesterol.

A. Basic structure of lipoproteins



B. Classes of lipoproteins by size and density



Chylomicron, VLDL and LDL metabolism

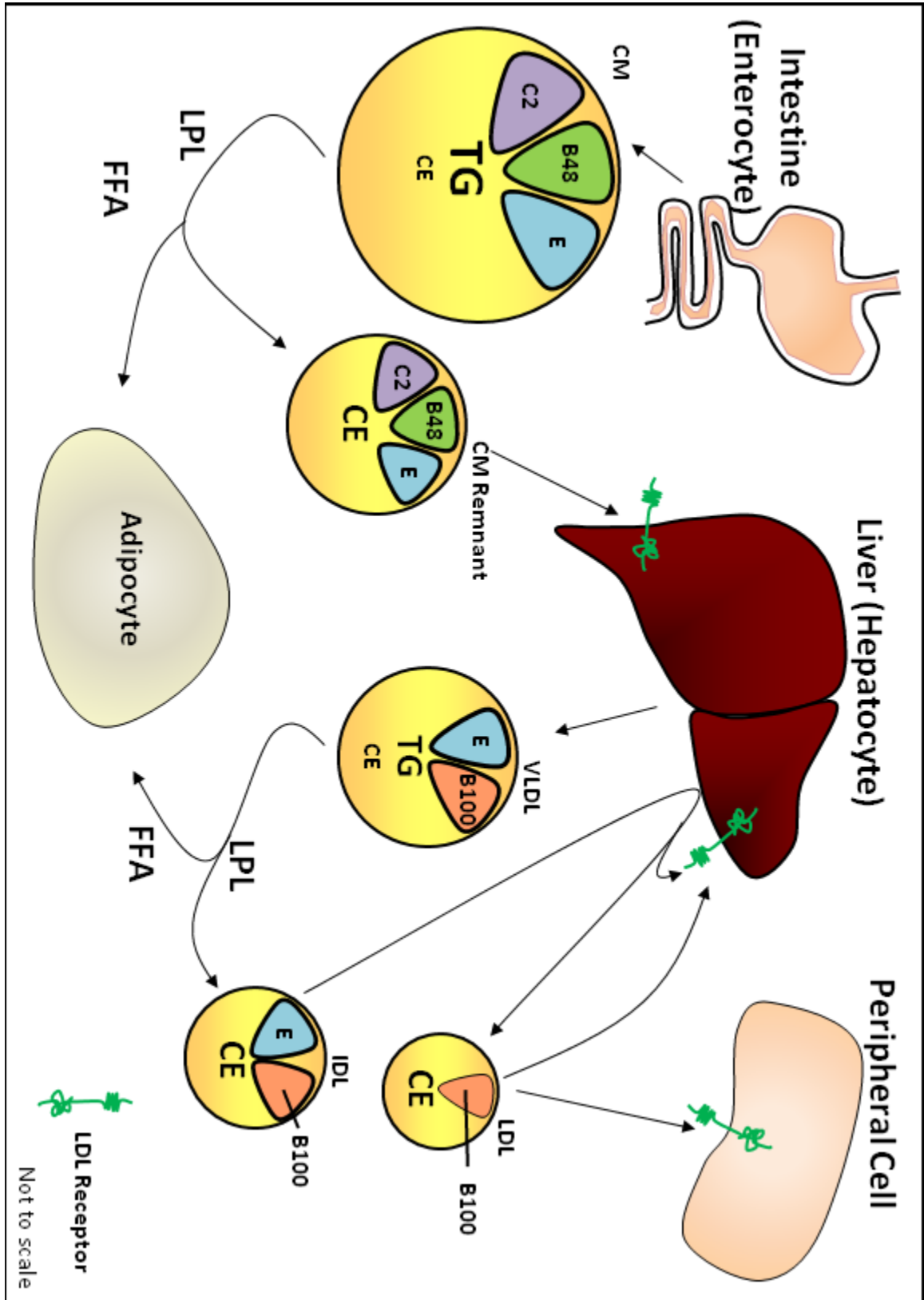
Dietary TG and cholesterol are packaged into chylomicrons in the ER of intestinal enterocytes (Xiao, Hsieh, Adeli, & Lewis, 2011). Cholesterol is absorbed by the enterocyte from the intestinal lumen through the Niemann-Pick C1-like 1 (NPC1L1) transporter, while FFAs are absorbed through FA transporters and used to synthesize TG in the intestinal enterocyte (Hegele, 2009). NPC1L1 is the target of the drug Ezetimibe, which blocks absorption of dietary cholesterol. Microsomal triglyceride transfer protein (MTP) mediates the assembly of chylomicrons by packaging TG and CE with phospholipid and apolipoprotein B48 (apoB48: a truncated isoform of apoB) (Hegele, 2009). Nascent chylomicrons are secreted from enterocytes into the lymph and travel through the lymphatic system into the circulation where HDLs donate apolipoprotein C2 (apoC2) and apolipoprotein E (apoE) to form mature chylomicrons (Daniels, Killinger, Michal, Wright, & Jiang, 2009). Chylomicrons circulate dietary lipid through the bloodstream and deliver TG to peripheral tissues. Lipoprotein lipase (LPL), an enzyme tethered to endothelial cells (Hegele, 2009), hydrolyzes TG associated with chylomicrons in an apoC2 dependent manner (Xiao et al., 2011), releasing FFAs into circulation for uptake by peripheral tissues. After LPL hydrolysis, apoC2 is returned to HDL and the remaining particles, called chylomicron remnants, are taken up by liver hepatocytes via the LDL receptor (LDLR) and the LDLR related protein (LRP)-1 and broken down (Daniels et al., 2009). The LDLR

binds to both apoB and apoE on the surface of lipoproteins and mediates their internalization (discussed in more detail below).

Some circulating FFAs are taken up by the liver and reassembled into TG. The liver packages TG and cholesterol into VLDL particles (Hegele, 2009). The TG incorporated into VLDL is derived from FFAs that come from a variety of sources including uptake and breakdown of remnant lipoprotein particles, circulating FFAs and FFAs synthesized de novo (Xiao et al., 2011). Similar to the assembly of chylomicrons, MTP mediates the packaging of TG and CE with apoB100 (full length) in the hepatocyte ER (Xiao et al., 2011). VLDL is secreted directly into the circulation, where it acquires apoC2 from HDL, and interacts with LPL to supply FFAs to the periphery (Daniels et al., 2009). VLDL remnant particles are called intermediate density lipoproteins (IDL); IDLs can be taken up and degraded by hepatocytes through LDLR/LRP dependent mechanisms, or converted to LDL by hepatic lipase, an enzyme produced and secreted by the liver that hydrolyzes IDL phospholipids and most of the remaining TG to produce a smaller, denser, CE-rich particle (Lusis, Fogelman, & Fonarow, 2004). The only remaining apolipoprotein retained on LDL after conversion from IDL is apoB100 (Lusis et al., 2004). The major function of LDL is to deliver cholesterol to peripheral cells. Peripheral cells acquire cholesterol from LDL by receptor mediated endocytosis of the entire particle; this is mediated by the LDLR, which binds apoB100 on the surface of LDL.

The LDLR is a cell-surface receptor that localises to clathrin-coated pits in the cell membrane (Goldstein & Brown, 2009). Binding of LDL to the LDLR results in the internalization of the LDL:LDLR complex in clathrin-coated endocytic vesicles, which deliver the LDL particle to the lysosome where it is degraded while LDLRs are recycled back to the cell surface (Goldstein & Brown, 2009). The LDLR is the major avenue for LDL removal from the blood stream; loss of function mutations in the gene that encodes the LDLR are among the main causes of familial hypercholesterolemia (Goldstein & Brown, 2009), in which heterozygous patients have very high levels of LDL in their blood stream, and exhibit symptoms of CVD in their 30's, while homozygous patients have severely high levels of LDL and experience heart attacks at a very young age (Goldstein & Brown, 2009).

Figure 1.4 – Metabolism of chylomicrons, VLDL and LDL. Chylomicrons (CMs) are generated in the intestinal enterocyte and are composed of TG and cholesterol absorbed from the diet. The major apolipoproteins carried by mature CMs are apoC2, apoB48 and apoE. CMs deliver TG to peripheral tissues through interaction with lipoprotein lipase (LPL), which hydrolyzes free fatty acids (FFA) from CM TG. Cholesterol ester (CE)-rich CM remnants are taken up by the liver via the LDLR. The liver packages TG and cholesterol into VLDL particles, which are similar to but smaller than CMs, and carry the full length isoform of apoB (apoB100). VLDLs also deliver FFA to peripheral tissues via LPL hydrolysis. The remaining CE-rich particles are called IDLs, which can be taken up by the liver via the LDLR, or converted to LDL particles by hepatic lipase (HL). LDL particles carry only apoB100, and deliver cholesterol to the periphery via the LDLR. Excess LDL is clear by the liver via LDLR.

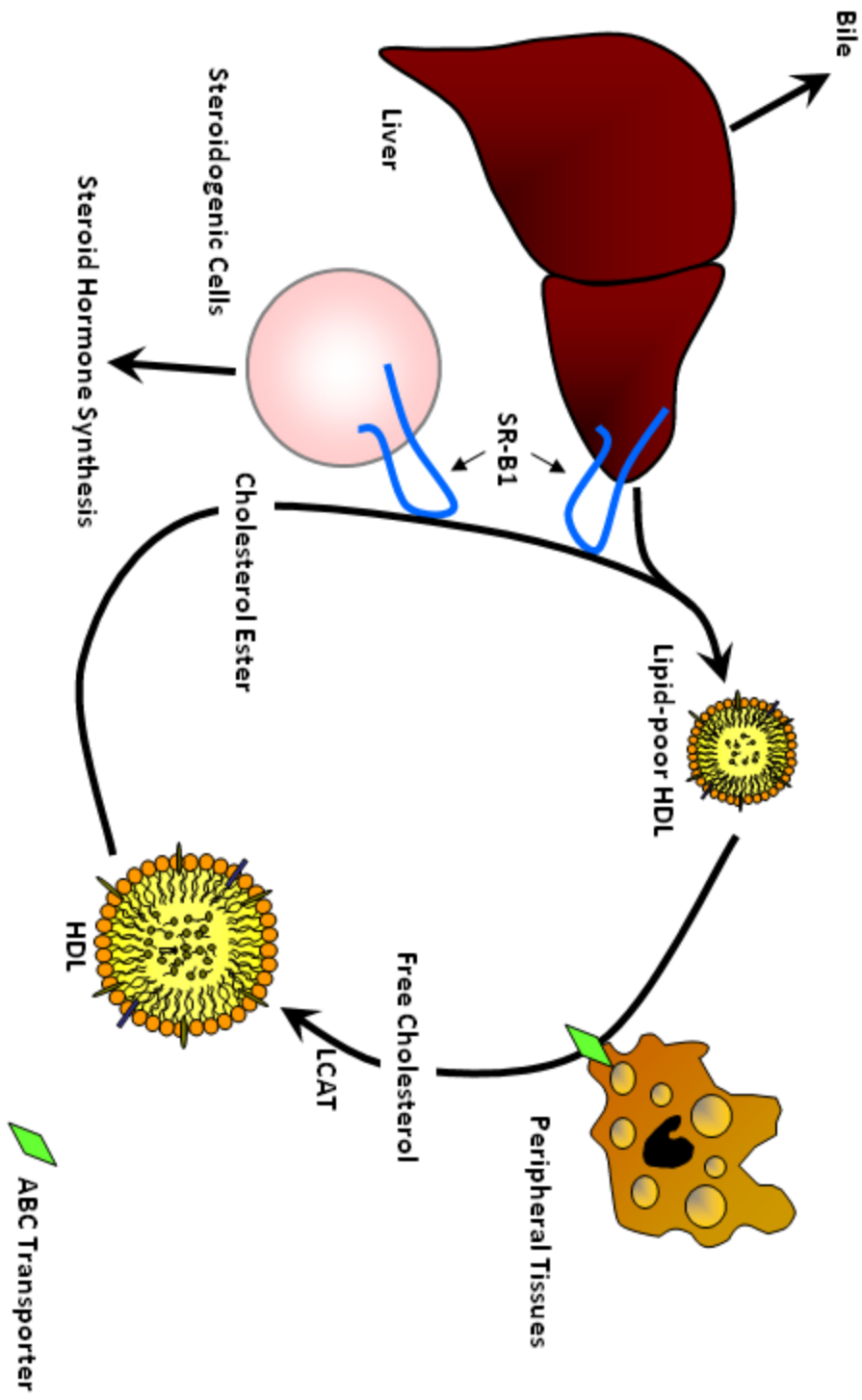


HDL metabolism

While LDL functions in cholesterol delivery, the major function of HDL is in removal of cholesterol from peripheral tissues, and transport of that cholesterol back to the liver for disposal in bile or repackaging (Linsel-Nitschke & Tall, 2005). This process, called reverse cholesterol transport (RCT), is thought to be protective against CVD and account for much of the protective effects of HDL (Krieger, 1999). HDL is the smallest of the lipoproteins, and HDL particles can be further sub-divided into different classes from discoidal particles containing no core lipids (pre- β HDL), to partially lipidated particles (α -HDL3), to fully lipidated spherical α -HDL2 particles with CE-rich cores (Asztalos, Tani, & Schaefer, 2011). The major apolipoprotein on the surface of HDL is apoA1. Pre- β discoidal HDL is released from the liver as a disc composed of a bilayer of phospholipids and apoA1 molecules arranged in a belt around the otherwise exposed fatty acid tails of the phospholipids at the periphery of the disc (Phillips, 2013). These particles gain free cholesterol from the liver through interactions with ATP binding cassette transporter (ABC) A1 on the surface of hepatocytes (Rader & Daugherty, 2008). Free cholesterol is then esterified by lecithin-cholesterol acyltransferase (LCAT) and the accumulating CE moves to the hydrophobic interior of the disc to form the hydrophobic core of a spherical HDL particle (Rader & Daugherty, 2008). HDL particles circulate through the body and extract cholesterol from peripheral tissues through ABCA1- and ABCG1-mediated efflux at the cell surface (Rader & Daugherty, 2008). Fully lipidated HDL circulates back to the liver, where it

deposits its cholesterol through a process called selective cholesterol transfer, mediated by a receptor called the scavenger receptor class B, type 1 (SR-B1) expressed on the surface of hepatocytes (Linsel-Nitschke & Tall, 2005). The uptake of cholesterol from HDL through SR-B1 differs from the receptor mediated endocytosis of LDL particles in that CE and FC are transferred from the HDL core and surface, respectively, to the cell without net internalization and degradation of the entire HDL particle (Krieger, 1999). Thus, fully lipidated HDL offloads its core CE, and the particle is recycled to continue extracting CE from peripheral tissues (Krieger, 1999). CE taken up from HDL is then hydrolyzed and excreted in the bile either as FC or as bile acid (Linsel-Nitschke & Tall, 2005) (Figure 1.5).

Figure 1.5 – Overview of reverse cholesterol transport. Lipid-poor HDL (either pre- β HDL or delipidated α -HDL) is released into the circulation by the liver, where it acquires free cholesterol from peripheral cells through interactions with ABCA1 and ABCG1 at the cell surface. Lecithin-cholesterol acyltransferase (LCAT) esterifies free cholesterol into cholesterol ester (CE), which accumulates in the core of the HDL particle. HDL cholesterol is taken up by cells through a process called selective cholesterol uptake, in which cholesterol is transferred from the HDL particle to the cell without net internalization of the entire HDL particle. This is mediated by scavenger receptor class B, type 1 (SR-B1). The tissues that exhibit the highest HDL selective cholesterol uptake activity, and highest SR-B1 expression, are the liver and steroidogenic tissues. HDL-derived cholesterol taken up by steroidogenic cells is used as a precursor in steroid hormone synthesis, while HDL cholesterol taken up by the liver is either repackaged into other lipoproteins or secreted into the bile.



1.4 Mouse Models of Atherosclerosis

Targeted mutagenesis of genes involved in LDL and VLDL clearance, such as apoE and the LDLR, has given rise to very useful models of experimental atherosclerosis (Daugherty, 2002) which will be discussed further below. These mice will develop complex atherosclerotic plaques in their larger arteries in regions where blood flow is non-laminar (Reardon & Getz, 2001). Atherosclerosis in these animal models is routinely measured in the aortic sinus (Whitman, 2004); the three leaflet valve structure which separates the left ventricle of the heart from the ascending aorta. Other sites where atherosclerosis is commonly measured in mice include the aortic arch, the brachiocephalic artery, and the descending aorta (Whitman, 2004). CAs in mice are generally resistant to development of atherosclerosis, even in genetically susceptible models (Braun et al., 2002). Wild type mice will not develop spontaneous atherosclerosis (Daugherty, 2002), likely due to their favorable lipoprotein profile, in which the majority of their plasma cholesterol is concentrated in HDL particles (Daugherty, 2002). However, if fed a high fat, very high cholesterol diet supplemented with sodium cholate, wild type C57BL/6 mice will develop small atherosclerotic plaques in their aortic sinuses (Paigen, Morrow, Brandon, Mitchell, & Holmes, 1985). This appears to be strain dependent, as other inbred strains were much less susceptible (Paigen et al., 1985). Because of this, mice used in atherosclerosis studies, even those lacking expression of apoE, LDLR and/or

other genes of interest, are most often on a C57BL/6 inbred background (Whitman, 2004).

Diets used in Atherosclerosis Research

Standard laboratory diets for mice are comprised of approximately 6% fat by weight and contain negligible amounts of cholesterol (e.g. Teklad 2018 Global 18% Protein Rodent Diet). Many studies on atherosclerosis involving mice rely on the use of diets with elevated levels of fat and/or cholesterol to induce or accelerate atherosclerosis. There are multiple variations on each type of atherogenic diet, but for simplicity, four broad categories of atherogenic diet will be referred to throughout this thesis; the high fat (HF) or Western type diet, the high cholesterol (HC) diet, the high fat, high cholesterol (HFC) diet, and the HFC diet containing sodium cholate (HFCC), commonly referred to as the Paigen diet. The most widely used atherogenic diets in the literature are the Western type diets (Getz & Reardon, 2006), which are typically comprised of approximately 21% fat and 0.15% cholesterol by weight (e.g. Dyets Inc. 112286 (Plump et al., 1992)). Cholesterol in this type of diet is elevated compared to normal rodent chow, however it is relatively low compared to the other three types of atherogenic diet that will be discussed. In addition to hypercholesterolemia, mice fed the Western type diets develop hypertriglyceridemia, insulin resistance and obesity; confounding variables that can be avoided through use of the HC diet (Hartvigsen et al., 2007). HC diets are normal chow diets supplemented with

additional cholesterol to final concentrations of 1-2% by weight, without any added fat (e.g. Teklad TD.01383). The HFC and HFCC diets generally contain approximately 16% fat and 1.25% cholesterol by weight with the latter containing 0.5% sodium cholate (e.g. Teklad TD.94059 [HFC] and TD.88051 [HFCC]). The primary source of fat in these diets is cocoa butter. The use of both of these types of diet is fairly common, however, the use of dietary sodium cholate has met with some controversy because of its exacerbating effects on hyperlipidemia, and its activating effects on genes involved in chronic inflammation and hepatic fibrosis (Getz & Reardon, 2006; Vergnes, Phan, Strauss, Tafuri, & Reue, 2003). Despite these drawbacks, sodium cholate is a useful tool that can be used to rapidly accelerate plaque development, and drive the development of complex atherosclerotic lesions in animals that do not otherwise develop them.

ApoE KO Mice

ApoE KO mice were first described as a model for experimental atherosclerosis by two independent groups in publications released on the same day in 1992 (Plump et al., 1992; S. H. Zhang, Reddick, Piedrahita, & Maeda, 1992), both of which describe development of atherosclerotic lesions in the aortic sinus in normal chow-fed mice at a relatively young age (3-5 months). Commercially available apoE KO mice that are used in most current atherosclerosis studies were originally generated by N. Maeda by homologous recombination to carry a mutation that disrupts a region of the apoE gene spanning from a portion of exon

3 through a portion of intron 3, replacing it with a neomycin resistance cassette (Piedrahita, Zhang, Hagan, Oliver, & Maeda, 1992). ApoE deficient mice have a lipoprotein profile that resembles human type III hyperlipoproteinemia, with elevated plasma cholesterol associated with large lipoproteins, consistent with the role of apoE as an important ligand for chylomicron and VLDL remnant clearance. Since its initial description as a model of experimental atherosclerosis, the apoE KO mouse has rapidly become one of the two most widely used animal models in atherosclerosis research and it has been extensively characterized. On a normal chow diet, cholesterol levels are elevated to ~10-15mM compared to ~2mM in wild type mice (Breslow, 1996; S. H. Zhang et al., 1992). ApoE KO mice begin to develop stage I lesions in their aortic sinus at around 2 months of age (Whitman, 2004), progressing to macrophage-rich stage III lesions as early as 7 months (Whitman, 2004). Complex and fibrotic stage IV and stage V lesions can be observed from 8 months onward (Whitman, 2004). Hyperlipidemia and lesion development in these mice are exacerbated by Western type diet (21% fat, 0.15% cholesterol) feeding, such that cholesterol levels range from ~40mM to ~50mM (Breslow, 1996) and stage IV lesions develop within 20 weeks of feeding (Whitman, 2004). Stage VI lesions characterized by intraplaque hemorrhage in apoE KO mice are rare, but have been reported in complex lesions in the brachiocephalic artery (Whitman, 2004). A single instance of thrombosis on a plaque in the coronary ostia has been reported in an apoE KO mouse fed a Western type diet supplemented with methionine (Zhou et al., 2001), however

plaque rupture and thrombosis are not routinely detected in these mice (Whitman, 2004). ApoE KO mice fed a sodium cholate-containing HFCC diet develop even larger lesions, approximately 50% larger after 8 weeks of feeding compared to mice fed a Western type diet (Chamberlain et al., 2009).

LDLR KO Mice

Unlike in apoE KO mice, in which plasma cholesterol is concentrated in VLDL-sized lipoproteins; in humans, the majority of plasma cholesterol is associated with LDL particles. The LDLR KO mouse was developed to mimic the phenotype of human familial hypercholesterolemia (Fazio & Linton, 2001), in which one or both of the *ldlr* alleles are dysfunctional. The LDLR KO mouse was originally described as a model of hypercholesterolemia in 1993 (Ishibashi et al., 1993) and as a model of diet-accelerated atherosclerosis in 1994 (Ishibashi, Goldstein, Brown, Herz, & Burns, 1994). The mouse *ldlr* gene was targeted by insertion of a neomycin resistance cassette in exon 4, which completely ablates expression of the LDLR protein (Ishibashi et al., 1993). When fed a normal chow diet, LDLR KO mice have moderately (approximately 2-3 fold) elevated plasma cholesterol (~6mM), with the majority of additional cholesterol associated with LDL sized particles (Ishibashi et al., 1993). Normal chow-fed LDLR KO mice begin to develop stage I lesions much later than apoE KO mice, at around 6-7 months of age (Whitman, 2004), and these lesions will progress to larger stage III lesions after 1 year (Whitman, 2004). However, advanced lesions are generally not

observed without dietary intervention. In the original publication describing LDLR KO mice as a model for experimental atherosclerosis, mice were fed a HFCC diet (15.8% fat, 1.25% cholesterol, 0.5% sodium cholate) for 7-8 months (Ishibashi et al., 1994). Plasma cholesterol was elevated from ~6mM to ~50mM, extensive atherosclerosis was observed throughout the descending aorta and stage V lesions were observed in the aortic sinus and proximal coronary arteries (Ishibashi et al., 1994). LDLR KO mice fed the more moderate Western type diet have since been described (Daugherty, 2002) and are routinely used in atherosclerosis research today. Western diet-fed LDLR KO mice begin to develop stage I lesions after 4-6 weeks of feeding (Whitman, 2004), which progress to macrophage-rich stage III lesions between 12 and 16 weeks of feeding, and begin to develop features of advanced lesions after prolonged feeding (Whitman, 2004).

1.5 Immune Cells

It was originally thought that atherosclerosis was a result of passive accumulation of LDL in the artery wall; it is now well appreciated that the immune system plays a major role in the development of an atherosclerotic plaque (Swirski & Nahrendorf, 2013). The immune system protects the body from dangerous pathogens such as bacteria, viruses and other foreign material; as well as damaged or unwanted endogenous material (Swirski & Nahrendorf, 2013). A functional immune system is therefore essential to the health of humans and

other complex organisms. Unfortunately, atherosclerosis is an example of an instance in which the immune system contributes to the progression of disease. In the case of atherosclerosis, the major immune stimulus is thought to be oxLDL that is retained in the artery wall (Libby, Ridker, & Maseri, 2002). The role of the immune system in atherogenesis is complex, and the roles of different immune cells will be discussed in the subsections that follow. The immune system is made up of leukocytes, which originate from hematopoietic stem cells in the bone marrow and in some cases the spleen (Swirski & Nahrendorf, 2013). Leukocytes can be subdivided into a number of different cell types, all of which have been associated with either the pathogenesis of or protection against atherosclerosis (Swirski & Nahrendorf, 2013). The major categories of immune cells that are relevant to this thesis are monocytes and lymphocytes.

Monocytes

Monocytes give rise to macrophages and eventually foam cells, the most abundant cell type in early lesions (Swirski & Nahrendorf, 2013). Monocytosis, characterized by high levels of monocytes in the blood, is a documented risk factor for CVD and atherosclerosis in humans and animal models (Tall, Yvan-Charvet, Westerterp, & Murphy, 2012). Monocytes in mouse blood can be broadly categorized into two groups based on their level of expression of a surface protein called Ly6C (Swirski & Nahrendorf, 2013). Ly6C^{high} or “inflammatory” monocytes express CCR2, the receptor for monocyte chemotactic

protein -1 (MCP-1) (Weber, Zernecke, & Libby, 2008), and are actively recruited to sites of inflammation; while Ly6C^{low} monocytes, also termed resident monocytes, do not express CCR2 and are thought to patrol healthy tissues and migrate to sites of inflammation through CCR5, the receptor for the chemokine RANTES (Weber et al., 2008). Evidence suggests that both monocyte subtypes may contribute to the progression of atherosclerosis; however mice with hypercholesterolemia exhibit monocytosis associated with a marked expansion of the Ly6C^{high} monocyte population (Swirski et al., 2007; Swirski & Nahrendorf, 2013; Weber et al., 2008). In these mice, the spleen serves as a reservoir for inflammatory monocytes and contributes to a substantial proportion of the monocytes incorporated into developing atherosclerotic plaques (Robbins et al., 2012).

Lymphocytes

Lymphocytes include T-cells, B-cells and Natural Killer (NK) cells, all of which have been implicated in either development or protection against atherosclerosis. T-cells are the second most abundant cell type in atherosclerotic plaques after monocyte-derived cells (J. Li & Ley, 2015), and while substantially outnumbered by monocyte-derived cells, they play a major role in atherosclerosis by regulating local inflammation (Weber et al., 2008). T-cells can be further divided into different sub-classes which have different effects on the progression of atherosclerosis. Th1 cells are the most abundant and most atherogenic T-cells in

atherosclerotic plaques (J. Li & Ley, 2015). Th1 cells are producers of interferon γ ($\text{IFN}\gamma$) and $\text{TNF}\alpha$, which are activators of local macrophages (J. Li & Ley, 2015). Both down-regulating Th1 cell response and reducing $\text{IFN}\gamma$ levels reduce atherosclerosis in mouse models, while inducing Th1 response and increasing $\text{IFN}\gamma$ augments atherosclerosis (J. Li & Ley, 2015). Other T-cell sub-types are Th2 cells, which are rarely detected in plaques and have an unclear effect on atherosclerosis (J. Li & Ley, 2015); Th17 cells, which appear to promote atherosclerosis but their specific role is not well understood (J. Li & Ley, 2015); regulatory T-cells, which have a protective role in atherogenesis through production of anti-atherogenic cytokines interleukin 10 ($\text{IL}10$) and transforming growth factor β ($\text{TGF}\beta$)(J. Li & Ley, 2015); NK T-cells, which promote early lesion formation (J. Li & Ley, 2015); and CD8 T-cells, which promote advanced atherosclerosis by promoting macrophage apoptosis (J. Li & Ley, 2015).

B-cells are antibody producing cells and can be sub-divided into B-1 cells and B-2 cells, which have opposing effects on atherosclerosis (J. Li & Ley, 2015). B-1 cells produce mainly IgM antibodies, which are thought to be atheroprotective. In support of this, IgMs that bind the oxidised phospholipid on oxLDL block scavenger receptor-mediated uptake of oxLDL by macrophages (Witztum & Lichtman, 2014). Additionally, splenectomy reduces B cells and IgM titers in the plasma and significantly increases atherosclerosis in apoE KO mice (Caligiuri, Nicoletti, Poirier, & Hansson, 2002). Transfer of B-1 cells, but not B-2 cells into splenectomised apoE KO mice protects against splenectomy-induced

increased atherosclerosis, and this protection is dependent on the ability of the B-1 cells to secrete IgM (Kyaw et al., 2011). B-2 cells produce mainly IgG antibodies and are considered atherogenic. IgG titers correlate with levels of atherosclerosis in mice, and specific depletion of B-2 cells reduces atherosclerosis in mouse models (Witztum & Lichtman, 2014).

NK cells are found in both human and mouse atherosclerotic plaques and play an atherogenic role by promoting necrotic core formation through granzyme-b and perforin mediated apoptosis (Selathurai et al., 2014). Depletion of NK cells in mice reduces atherosclerosis, while adoptive transfer of NK cells into lymphocyte deficient mice increases atherosclerosis in a granzyme-b and perforin dependent manner (Selathurai et al., 2014).

1.6 Endothelial Cells

Vascular endothelial cells are small cells that form a monolayer, termed the endothelium, which separates the lumen of a blood vessel from the vessel wall. A functional endothelium has a vital role in haemostasis as it is involved in a number of vascular processes including regulation of vascular tone and blood pressure, prevention of coagulation and thrombosis, and regulation of vascular inflammation (Deanfield, Halcox, & Rabelink, 2007). Endothelial dysfunction is thought to be the initiating factor leading to the development of an atherosclerotic plaque (Weber et al., 2008). While the entire circulatory system is exposed to systemic risk factors for atherosclerosis, plaques preferentially develop at

bifurcations, branch points and curvatures in blood vessels (Chatzizisis et al., 2007). In these regions of the vasculature, endothelial cells are exposed to non-laminar blood flow and experience low shear stress (Chatzizisis et al., 2007). There are a number of mechanoreceptors on the luminal surface of endothelial cells that sense shear stress and direct the cellular response to different shear stress conditions (Chatzizisis et al., 2007). In regions experiencing low shear stress, a number of pro-atherogenic responses are activated including down-regulation of endothelial nitric oxide synthase (eNOS), reducing the bioavailability of NO; increased permeability to LDL particles; increased expression of oxidative enzymes and reduced expression of reactive oxygen species scavengers, increasing oxidative stress in the artery wall; and up-regulation of inflammatory genes including adhesion molecules and chemokines, promoting recruitment and attachment of inflammatory cells (Chatzizisis et al., 2007).

Adhesion molecules in atherosclerosis

A series of studies have demonstrated that atherosclerosis prone regions of the arterial tree correlate with elevated inflammatory and adhesion molecule gene expression in endothelial cells of those regions prior to plaque initiation. In LDLR KO mice fed a HFCC diet, vascular cell adhesion molecule 1 (VCAM-1) expression is elevated in endothelial cells near the edges of established atherosclerotic plaques, but is concentrated within the lesion (Iiyama et al., 1999). However, in both normal chow-fed LDLR KO mice and C57BL/6 mice,

VCAM-1 expression is elevated in the endothelial cells of the lesser curvature of the aortic arch, a region that experiences low shear stress and is prone to plaque development in hypercholesterolemic mice (Iiyama et al., 1999). In contrast, endothelial cells in the greater curvature, which is not susceptible to atherosclerosis, do not express detectable levels of VCAM-1 (Iiyama et al., 1999). Similar observations were made in rabbits. Expression of intercellular adhesion molecule 1 (ICAM-1) is not as restricted to lesion prone sites as VCAM-1 expression, however it is measurably higher in arterial regions where atherosclerosis tends to develop (Iiyama et al., 1999). VCAM-1 deficiency is embryonic lethal, however mice with the domain 4-deficient (D4D) mutation in the VCAM-1 gene are viable even though they have very low levels of the mutated VCAM-1 protein (Cybulsky et al., 2001). LDLR KO mice homozygous for the VCAM-1 D4D mutation develop less HFC diet-induced aortic atherosclerosis than LDLR KO controls with wild type VCAM-1 (Cybulsky et al., 2001). Similarly, chow-fed apoE KO mice with the VCAM-1 D4D mutation developed smaller aortic sinus atherosclerotic plaques at 16 weeks of age and exhibited reduced leukocyte attachment to aortic arch endothelium compared to apoE KO mice with normal VCAM-1 (Dansky et al., 2001). The effect of ICAM-1 deficiency on atherosclerosis is not as well established. In apoE KO mice, ICAM-1 deficiency reduces atherosclerosis in the aortic arch in both chow and Western diet-fed mice at multiple stages of plaque development (Bourdillon et al., 2000), however in HFC-fed LDLR KO mice, ICAM-1 deficiency has no effect on the development

of atherosclerosis in the aorta (Cybulsky et al., 2001). Therefore, while both VCAM-1 and ICAM-1 may influence plaque development, VCAM-1 appears to be more robustly associated with the initiation of atherosclerosis in mice.

Regional Specific Endothelial Inflammation

In addition to elevated adhesion molecule expression, arterial regions prone to plaque development exhibit a pro-inflammatory gene expression pattern. In wild type mice, expression of eNOS mRNA and protein is higher in the greater curvature than in the lesser curvature of the aortic arch (Won et al., 2007). Additionally, eNOS phosphorylation is higher in the greater curvature compared to the lesser curvature (Won et al., 2007). Conversely, expression and activation of the nuclear factor kappa B (NF- κ B) transcription factor is higher in the lesser curvature of the aortic arch compared to the greater curvature (Hajra et al., 2000). The NF κ B transcription factor consists of three subunits; p65, p50 and I κ B (inhibitor of κ B). In inactive states, I κ B is not phosphorylated and is bound to p65 and p50, keeping the complex in the cytoplasm. Phosphorylation of I κ B releases the other two subunits, allowing them to translocate into the nucleus and activate transcription of inflammatory genes. Higher levels of the p65 subunit and the I κ B subunit are detectable in the lesser curvature compared to the greater curvature of the aortic arch in C57BL/6 mice (Hajra et al., 2000). Nuclear translocation of p65 is induced by HFC diet feeding in LDLR KO mice. While activation of NF κ B in response to these stimuli occurs to the same extent in both the lesser and

greater curvature, the absolute levels of activated p65 are much higher in the lesser curvature (Hajra et al., 2000). These observations were replicated in cultured endothelial cells exposed to different flow conditions. In porcine endothelial cells, uniform flow induced eNOS expression and reduced p65 expression to a greater extent than disturbed flow (Won et al., 2007). Similarly, in human aortic endothelial cells, laminar shear stress induced eNOS mRNA expression and reduced p65 mRNA expression (Won et al., 2007).

1.7 Platelets

Platelets affect the development of atherosclerosis through all stages of the disease. In the initial stages of plaque formation, platelets accelerate monocyte recruitment to activated endothelial cells (Ley, Miller, & Hedrick, 2011). Platelets adhere to the endothelium in regions of disturbed blood flow in a manner mediated by integrins and selectins expressed on the surface of both platelets and endothelial cells (Langer & Gawaz, 2008). Adherent platelets form a bridge between endothelial cells and circulating monocytes as platelets express P-selectin, which binds P-selectin glycoprotein ligand-1 on the surface of monocytes. Platelet-specific deficiency of integrins and selectins involved in platelet adherence to monocytes and endothelial cells delays atherosclerosis in mouse models (Ley et al., 2011). Platelets can also transiently adhere to the endothelium on established atherosclerotic plaques and affect local inflammation through secretion of a number of chemokines such as platelet factor 4 and

RANTES, and by stimulation of inflammatory gene expression in endothelial cells through secretion of CD40 ligand (Davi & Patrono, 2007; Langer & Gawaz, 2008). CD40 ligand also stimulates the release of matrix metalloproteases (MMPs) by endothelial cells, macrophages and smooth muscle cells; MMPs contribute to the breakdown of the fibrous cap (Langer & Gawaz, 2008), and are also released by activated platelets themselves (Davi & Patrono, 2007). Finally, platelet aggregation on top of a ruptured atherosclerotic plaque is the driver of thrombus formation that ultimately causes a heart attack or stroke (Davi & Patrono, 2007).

1.8 Scavenger Receptors

Scavenger receptors (SRs) were first identified as macrophage cell surface receptors that bind to modified lipoproteins; they are thought to be responsible for the unregulated accumulation of cholesterol in macrophage foam cells in the artery wall (Kzhyshkowska, Neyen, & Gordon, 2012). While originally defined by their ability to bind and internalize modified LDL, it is now recognized that SRs bind a diverse range of ligands and have a variety of functions in several cellular processes including clearance of foreign pathogens such as bacterial endotoxin, and clearance of unwanted or damaged endogenous material including modified host proteins and apoptotic cells (Canton, Neculai, & Grinstein, 2013). SRs are classified based on the structural motifs in their protein structures, whereby members of the same class have similar structures and share sequence

homology, while different classes have very little sequence overlap (Canton et al., 2013). The most widely studied SRs in atherosclerosis are the type A SRs, SR-A1/1.1, and the class B SRs, CD36 (SR-B2), and SR-B1/1.1.

1.9 SR-B1

SR-B1 was originally identified as a SR due to its ability to bind modified LDL (Krieger, 1999). It belongs to the class B family of SRs and shares a high level of sequence homology with the other members of this family CD36 (SR-B2) and LIMP-2 (SR-B3) (Krieger, 1999). The gene encoding SR-B1 in mice is located on chromosome 5, syntenic to chromosome 12 in humans (Krieger, 1999). The SR-B1 gene gives rise to a 509 amino acid protein with a predicted molecular weight of 57 kDa; however the protein is heavily post-translationally modified, and fatty acylation and N-glycosylation of the mature protein contributes to the observed molecular weight of 82 kDa (Krieger, 1999). SR-B1 is expressed at low levels in multiple cell types including macrophages, endothelial cells and cardiomyocytes, among others; however the highest levels of expression of SR-B1 protein are detected in steroidogenic cells and hepatocytes (Acton et al., 1996). Like other class B SRs, SR-B1 is a cell surface receptor anchored to the plasma membrane by two transmembrane domains next to its short N and C terminal cytoplasmic domains; the bulk of the protein comprises a large, 403 amino acid extracellular domain (Krieger, 1999). Alternative splicing of the SR-B1 gene by exclusion of exon 12 gives rise to a splice variant, SR-B1.1, with an

identical extracellular domain but a different C-terminal domain (Webb et al., 1998). The crystal structure of SR-B3 has recently been established and has been used to predict the structure of SR-B1 and other class B SRs. There are two important features in the extracellular domain of class B SRs; the ligand binding site characterized by a cluster of α -helices, and a hydrophobic channel that runs through the center of the structure (Neculai et al., 2013). SR-B1 protein expression is concentrated in small, cholesterol-rich microdomains in the membrane called caveolae, giving it a punctate expression pattern when observed under immunofluorescence microscopy (Babitt et al., 1997). The C-terminal cytoplasmic domain of SR-B1 associates with its cytoplasmic adapter protein PDZK1, a four-PDZ domain containing protein that stabilizes SR-B1 expression in hepatocytes (Silver, 2002), and appears to be essential for many SR-B1 functions in other cell types (Al-Jarallah, Chen, Gonzalez, & Trigatti, 2014; Al-Jarallah & Trigatti, 2010). The importance of PDZK1 will be discussed in more detail later in this introduction. In addition to modified LDL, SR-B1 has been shown to bind native LDL, maleylated albumin, apoptotic bodies via phosphatidyl serine and importantly, HDL (Krieger, 1999). The ability of SR-B1 to bind HDL with high affinity was first described in 1997 in Idl-A cells (CHO cells lacking the LDLR) transfected with murine SR-B1 (Acton et al., 1996). Association of SR-B1 with protein components of HDL saturated within an hour, however HDL derived lipid continued to accumulate in the cells over 5 hours, suggesting transfer of the lipid component of HDL to the cell without net internalization of the entire HDL

particle, giving rise to the notion of SR-B1 mediated selective lipid uptake from HDL to cells (Acton et al., 1996). The expression pattern and sub-cellular localization of SR-B1.1 are similar to those of SR-B1, however in most tissues SR-B1.1 is expressed at much lower levels than SR-B1 and does not mediate cholesterol uptake as efficiently (Webb et al., 1998). Nevertheless, conclusions that are drawn from studies involving SR-B1 deficient mice should take into account the absence of both splice variants in those mice.

The precise mechanism of selective lipid uptake mediated by SR-B1 is not well understood, but it is thought to involve the initial transfer of cholesterol to the plasma membrane caveolae through the hydrophobic channel in SR-B1 prior to internalization (Krieger, 1999; Neculai et al., 2013; Rodrigueza et al., 1999). The high levels of SR-B1 expression found in tissues known to selectively take up cholesterol from HDL, such as steroidogenic tissues and the liver, suggested that SR-B1 was a physiologically relevant HDL receptor, and that SR-B1-facilitated selective cholesterol transfer may be important for RCT (Krieger, 1999). Genetic knockout studies would later confirm this.

SR-B1 function in RCT in vivo

Studies in genetically modified mice confirmed the crucial role of SR-B1 in RCT. Mice with a targeted disruption in the SR-B1 gene were first described in 1997. These mice were created by germline targeted mutagenesis of the first coding exon of the SR-B1 gene by insertion of a neomycin resistance cassette, resulting

in complete whole-body deficiency of SR-B1 protein (Rigotti et al., 1997). These mice exhibited significantly increased plasma cholesterol concentrations associated predominantly with HDL. The increase in HDL particle size and the absence of a difference in plasma apo-A1 levels suggested that elevated cholesterol in SR-B1 deficient mice is not due to an increase in HDL particle number, but an increase in cholesterol associated with oversized HDL particles, a result of an impaired ability to remove cholesterol from the core of the HDL particle (Rigotti et al., 1997). This is consistent with the notion that SR-B1 mediated hepatic selective lipid transfer is a critical step in functional RCT. Similar observations were made in mice with hypomorphic hepatic SR-B1 expression; in addition to increased HDL cholesterol in plasma, these mice also showed reduced CE clearance and reduced cholesterol concentrations in the bile (Ji et al., 1999). In contrast, hepatic overexpression of SR-B1 via adenovirus results in significant reductions in HDL cholesterol in plasma and significant increases in biliary cholesterol (Ji et al., 1999; Kozarsky et al., 1997), consistent with more efficient RCT. *In vitro* evidence suggests that SR-B1 is also capable of mediating bidirectional lipid transfer between HDL and cells (Ji et al., 1997; Jian et al., 1998), leading to the postulation that SR-B1 may play an additional role in cholesterol efflux from peripheral tissues to HDL in earlier stages of RCT. However, *in vivo* RCT studies in SR-B1 deficient mice demonstrated that SR-B1 mediated cholesterol efflux is not essential for functional RCT in mice (Wang et al., 2007).

The Role of SR-B1 in non-hepatic tissues

While the liver accounts for the highest SR-B1 protein expression in absolute terms, the relative expression of SR-B1 is highest in steroidogenic tissues, such as the adrenal gland, which exhibit the highest selective cholesterol uptake activity from HDL (Rigotti, Miettinen, & Krieger, 2003; B. Trigatti, Rigotti, & Krieger, 2000). SR-B1 expression in the adrenal gland is regulated by intracellular cholesterol levels as well as adrenocorticotrophic hormone (ACTH) (Cao et al., 1999; Rigotti et al., 1996; Sun, Wang, & Tall, 1999). Cholesterol is essential for steroid hormone synthesis, and in rodents, HDL is an important source of cholesterol in steroidogenic tissues (B. Trigatti et al., 2000). This is evident by depletion of cholesterol in the adrenal glands and ovaries in SR-B1 deficient mice (Rigotti et al., 1997; B. Trigatti et al., 1999; B. L. Trigatti, Krieger, & Rigotti, 2003). As a result of reduced cholesterol storage in adrenocortical cells, SR-B1 KO mice have an impaired ability to produce glucocorticoid hormones in response to stress. Under basal conditions, corticosterone levels in SR-B1 KO mice are maintained within the physiological range (Rigotti et al., 2003), however, in response to stresses such as fasting (Hoekstra et al., 2008) or lipopolysaccharide (LPS) administration (Cai, Ji, de Beer, Tannock, & van der Westhuyzen, 2008), SR-B1 KO mice are unable to upregulate production of corticosterone leading to an overproduction of inflammatory cytokines in the liver, due to the lack of a suppressive effect of corticosterone. This makes SR-B1 KO mice unable to resolve inflammation and hypersensitive to inflammatory stimuli.

As such, SR-B1 KO mice, as well as mice lacking SR-B1 specifically in adrenal glands, experience drastically increased mortality in response to LPS-induced endotoxemia (X. A. Li, Guo, Asmis, Nikolova-Karakashian, & Smart, 2006) and experimental sepsis (Gilibert et al., 2014; Guo et al., 2009).

The effect of SR-B1 on Reproduction

Female SR-B1 KO mice are infertile (B. Trigatti et al., 1999). Aside from a reduction in ovarian cholesterol content, their ovaries appear normal, they have normal estrus cycles and they ovulate a normal number of oocytes, suggesting that the reduced lipid accumulation in ovaries does not affect production of steroid hormones (B. Trigatti et al., 1999). However, preimplantation single cell embryos and oocytes from SR-B1 KO females have abnormal morphology in culture, and the embryos do not develop beyond single or two-cell stages (B. Trigatti et al., 1999). Ovarian transplantation experiments revealed that SR-B1 KO ovaries were capable of producing viable oocytes in the context of normal lipoprotein cholesterol profiles in recipient mice (Miettinen, Rayburn, & Krieger, 2001). Additionally female infertility in SR-B1 KO mice is corrected by the lipid lowering drug probucol, which reduces cholesterol associated with abnormal HDL, suggesting that infertility is a consequence of impaired HDL metabolism in SR-B1 KO mice (Miettinen et al., 2001). This was confirmed in a recent study showing that oocytes in SR-B1 KO mice accumulated large amounts of cholesterol *in vivo*, and prematurely activate in culture. This effect is phenocopied

by normal oocytes that are loaded with cholesterol in vitro (Yesilaltay et al., 2014).

The effect of SR-B1 on Red Blood Cells

SR-B1 KO mice have fewer red blood cells (RBCs), low hematocrit and hemoglobin levels, and their RBCs are abnormally shaped, significantly larger, and have a shorter lifespan in plasma compare to those of wild type mice (Holm et al., 2002; Meurs et al., 2005). These abnormalities are exacerbated by diet (high cholesterol) - or genetically-induced (apoE KO) hypercholesterolemia (Holm et al., 2002). SR-B1 KO RBCs stain more positively for cholesterol, which increases with increasing hypercholesterolemia; accumulate autophagolysosomes, and exhibit features of immature reticulocytes (Holm et al., 2002). Infusion of SR-B1 KO RBCs into wild type mice facilitates expulsion of autophagolysosomes and maturation of immature reticulocytes, correcting the abnormal RBC phenotype (Holm et al., 2002). These results suggest that the abnormal lipid environment in SR-B1 KO mice is the major cause of the unusual anemia induced by SR-B1 deficiency.

The effect of SR-B1 on Platelets

Similar to RBCs, platelets in SR-B1 deficient mice accumulate cholesterol in the context of unusually high plasma FC:total cholesterol ratios, and have significantly reduced survival in plasma. As a result, platelet counts are

significantly reduced in SR-B1 KO mice and further reduced with combined SR-B1 and apoE deficiency (Dole et al., 2008). The abnormal lipid environment in SR-B1 KO mice appears to be responsible for this, as reciprocal infusion experiments revealed that wild type and SR-B1 KO platelets are not different from one another in terms of survival and cholesterol content when exposed to the same lipid environments (Dole et al., 2008). The effect of SR-B1 on platelet activation is complex. SR-B1 deficient platelets exhibit impaired aggregation *ex vivo*, however platelets in SR-B1 KO mice circulate in an active state and SR-B1 KO mice are more susceptible to thrombosis. This also appears to be a result of the abnormal lipid environment in these mice (Korporaal et al., 2011). Another study demonstrated that SR-B1 deficient platelets have an enhanced activation response to thrombin, but a blunted response to other platelet agonists. The same study demonstrated that in the lipid environment of SR-B1 KO mice, SR-B1 expression on platelets actually promotes thrombosis. Conversely, platelet SR-B1 deficiency in the lipid environment of wild type mice is associated with reduced activation responses to all agonists (Ma, Ashraf, & Podrez, 2010). The results of these two studies suggest that SR-B1 deficiency impacts platelet function directly as well as through its effects on lipid metabolism in opposing manners.

1.10 The effect of SR-B1 on atherosclerosis in mice

Full body SR-B1 KO mice are susceptible to atherosclerosis induced by a variety of diets (Harder, Lau, Meng, Whitman, & McPherson, 2007; Hildebrand et al., 2010; Van Eck et al., 2003); however large stage III-V plaques have only been described in SR-B1 KO mice fed a HFCC diet (Huby et al., 2006). Despite their susceptibility to advanced atherosclerosis, these mice are not a routinely used experimental model. Chapter 3 of this thesis is focussed on the characterization of HFCC-fed SR-B1 KO mice as a model of diet-inducible atherosclerosis, comparing their disease characteristics to those of conventional atherosclerotic mouse models. Hepatic over-expression of SR-B1 either in transgenic mice or through adenovirus mediated gene transfer limits the development of atherosclerosis in various atherosclerosis mouse models (Arai, Wang, Bezouevski, Welch, & Tall, 1999; Kozarsky, Donahee, Glick, Krieger, & Rader, 2000; Ueda et al., 2000). On the other hand, atherosclerosis is substantially increased in mice with liver specific deletion of SR-B1 (Huby et al., 2006). The above studies confirmed that SR-B1's role in the liver is at least partly responsible for its ability to protect against atherosclerosis. In addition to work outlined above, SR-B1's effect on atherosclerosis has been tested in a number of atherosclerosis-susceptible mouse models.

SR-B1/apoE double knockout mice

The importance of SR-B1 in the protection against murine atherosclerosis was first made evident by the generation of mice lacking both SR-B1 and apoE. SR-B1/apoE double KO (B1/E dKO) mice have exacerbated hypercholesterolemia, with approximately two-fold higher concentration of VLDL-associated cholesterol in plasma compared to apoE single KO mice (B. Trigatti et al., 1999). In addition, B1/E dKO mice have abnormally high plasma levels of free cholesterol, accounting for 80% of total plasma cholesterol, compared to 25% observed in apoE KO mice (Braun et al., 2003). B1/E dKO mice rapidly develop atherosclerosis in their aortic sinuses with stage II to stage III plaques observed between 5 and 7 weeks of age (B. Trigatti et al., 1999). Interestingly, in addition to increased aortic sinus atherosclerosis, B1/E dKO mice develop spontaneous occlusive coronary artery atherosclerosis in both proximal and distal coronary arteries associated with cardiac enlargement, myocardial fibrosis and impaired heart function, consistent with the occurrence of myocardial infarction (MI). As a result, these mice have a severely shortened lifespan of between 5 and 8 weeks of age (Braun et al., 2002). Deposition of fibrin was detected in CA atherosclerotic plaques (Braun et al., 2002), raising the possibility that acute thrombosis on top of atherosclerosis may be a feature of disease in these mice; however presence of platelet-rich thrombi was never confirmed. Addition of probucol to the diet dramatically improves the phenotype of these mice, delaying early onset atherosclerosis and cardiac dysfunction, partially correcting

cholesterol and lipoprotein abnormalities, and extending their lifespan to 25 to 60 weeks (Braun et al., 2003). Several other factors have been identified that modulate the severity of coronary artery atherosclerosis in B1/E dKO mice.

The NCP1L1 inhibitor, Ezetimibe, blocks the absorption of cholesterol from the small intestine and is often used as a complimentary lipid-lowering treatment along with statins (Montecucco, Quercioli, & Mach, 2009). Treatment of B1/E dKO mice with Ezetimibe lowered LDL associated cholesterol, reduced atherosclerosis in the aortic sinus and coronary arteries at 6 weeks of age, reduced myocardial fibrosis and extended the median lifespan of the mice from ~6 weeks to ~8 weeks. Treatment with an inhibitor of bile acid absorption had a similar effect on lipoprotein cholesterol levels and survival (Braun et al., 2008).

Hepatic lipase (HL) deficiency delays MI and extends the lifespan of dKO mice from ~6 weeks to ~9 weeks. At 6 weeks of age, despite an increase in VLDL associated cholesterol in plasma, HL deficient dKO mice developed less aortic sinus and CA atherosclerosis compared to HL-expressing controls, and exhibited minimal cardiac enlargement and no evidence of myocardial fibrosis (Karackattu, Trigatti, & Krieger, 2006).

Treatment with antioxidant polyphenol-rich pomegranate extract (PomX) reduced atherosclerosis in the aortic sinus and CAs of 6 week old B1/E dKO mice. PomX treatment also reduced myocardial fibrosis and cardiac enlargement, and delayed development of conductance abnormalities. These effects were associated with reductions in markers of oxidative stress and lower

levels of MCP-1 in the aortic sinus and coronary arteries; and again, occurred despite an increase in plasma cholesterol associated with VLDL and LDL sized lipoproteins in PomX-treated mice (Al-Jarallah et al., 2013). The results of these latter two studies illustrate that the CA atherosclerosis in B1/E dKO mice cannot be attributed simply to the exacerbation of hypercholesterolemia resulting from a lack of SR-B1, and may involve effects of SR-B1 in extrahepatic tissues and/or more complicated alterations to the compositions of the lipoproteins themselves. It is important to note that in both of the above studies in which increased VLDL-associated cholesterol was associated with reduced atherosclerosis, the ratio of free cholesterol to total cholesterol in plasma was reduced by the atheroprotective condition (Al-Jarallah et al., 2013; Karackattu et al., 2006).

SR-B1 KO mice with hypomorphic expression of apoE R61

While the B1/E dKO mouse provides a unique model of spontaneous occlusive CA atherosclerosis and MI that resembles human CA disease, use of the model in practice is limited by rapid development of the disease and the severely truncated lifespan of the mice. In 2005, a related model was reported in which SR-B1 KO mice were crossed to the apoE R61 hypomorphic (HypoE) mouse (S. Zhang et al., 2005). HypoE mice have a mutated apoE gene with a threonine to arginine point mutation at amino acid 61, and a floxed neomycin resistance cassette that interrupts intron 3. The result is low level expression (~5% of wild type levels) of a mutant form of apoE which exhibits reduced clearance (Raffai &

Weisgraber, 2002). These mice develop aortic sinus atherosclerosis when fed a cholate-containing atherogenic diet, and have been used as a model to study atherosclerotic plaque regression (Raffai, Loeb, & Weisgraber, 2005). SR-B1 KO/HypoE mice exhibit a healthy phenotype when maintained on a normal chow diet, but rapidly develop increased aortic sinus atherosclerosis and occlusive CA atherosclerosis when placed on a HFCC diet, and die within 3 to 4.5 weeks from the onset of feeding. Like B1/E dKO mice, these mice exhibit cardiac enlargement, fibrosis and impaired heart function (S. Zhang et al., 2005). Removal of cholate from the diet extends the survival of these mice to ~9 weeks, while mice fed a Western type diet survive beyond 11 weeks (Nakagawa-Toyama, Zhang, & Krieger, 2012). Disease severity is also affected by housing conditions, such that mice housed in groups survive significantly longer than mice housed individually (Nakagawa-Toyama et al., 2012). SR-B1 KO/HypoE mice are therefore a flexible and convenient model of mouse CA atherosclerosis in which the onset and severity of the disease can be manipulated according to experimental needs.

SR-B1/ LDLR dKO mice

In LDLR KO mice fed a Western type diet, SR-B1 deficiency increases atherosclerosis in the aorta, but paradoxically lowers plasma cholesterol associated with LDL. No macroscopic evidence of MI was observed in these mice (Covey, Krieger, Wang, Penman, & Trigatti, 2003). Chapter 4 of this thesis

is focused on comprehensive characterization of SR-B1/LDLR dKO mice as a model of diet-accelerated occlusive CA atherosclerosis.

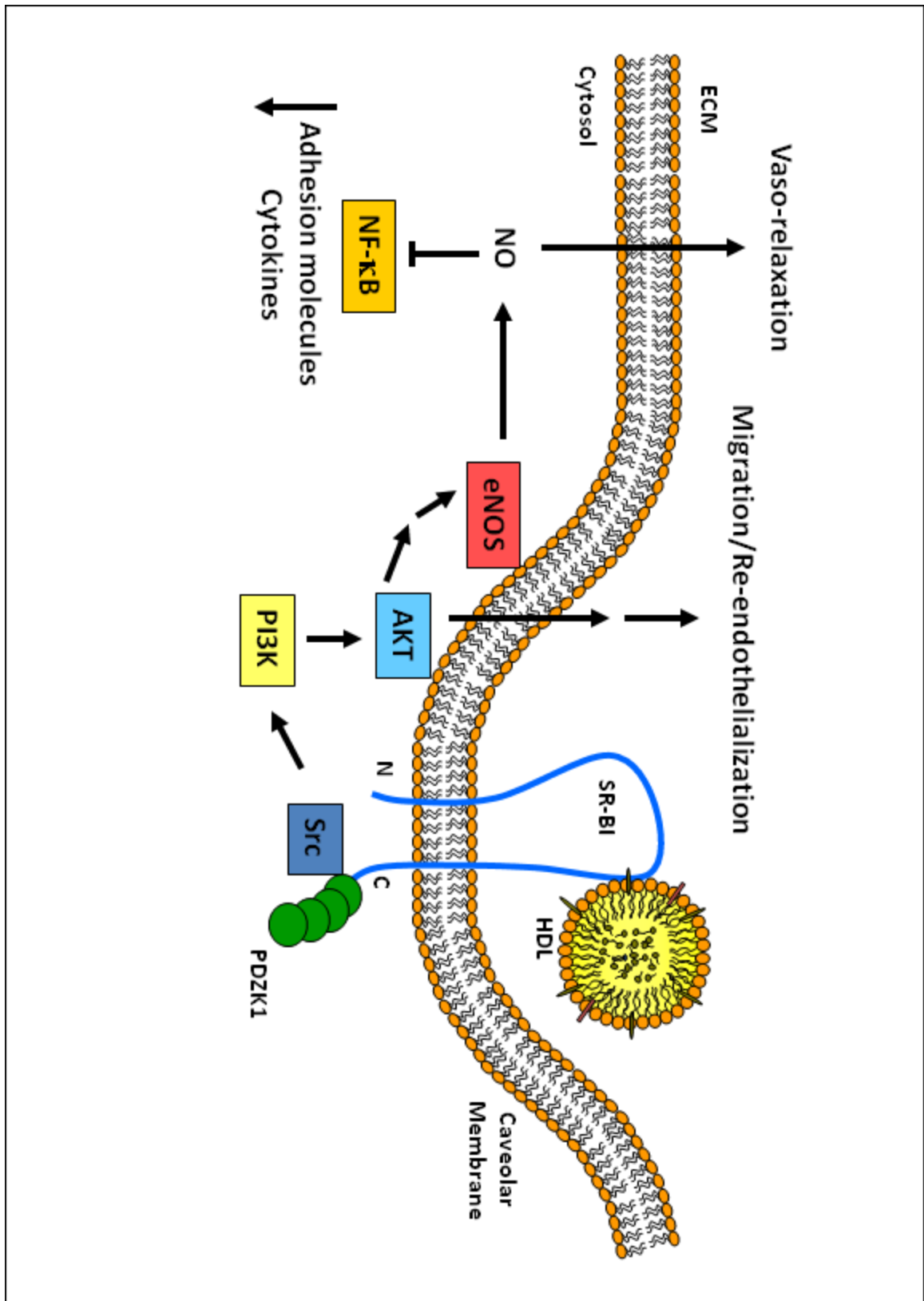
1.11 Beyond Cholesterol Uptake, is Coronary Atherosclerosis in SR-B1 KO Mice a Multi-Cellular Phenomenon?

Role in Endothelial Cells and HDL signaling

In addition to major roles in RCT in the liver and steroidogenic tissues, SR-B1 appears to play important roles in HDL signal transduction in vascular cells. In endothelial cells, SR-B1 is enriched in plasma membrane caveolae and is responsible for HDL-induced enhancement of eNOS activity. HDL maintains the sub-cellular localization of eNOS in caveolae in an SR-B1 dependent manner by preventing redistribution of eNOS from caveolae in response to oxLDL (Uittenbogaard, Shaul, Yuhanna, Blair, & Smart, 2000). Binding of HDL to SR-B1 also induces phosphorylation of serine 1179 of the eNOS protein, leading to activation and production of the anti-inflammatory and vaso-dilatory molecule NO (X. A. Li et al., 2002; Yuhanna et al., 2001). HDL activation of eNOS is dependent on SR-B1-mediated cholesterol flux, SR-B1's C-terminal transmembrane and cytoplasmic domains, and association with PDZK1 (Assanasen et al., 2005; Zhu et al., 2008). HDL binding to SR-B1 induces the downstream activation of a kinase signaling cascade involving Src, phosphatidylinositol 3 kinase (PI3K), and AKT, which ultimately phosphorylates S1179 of eNOS (Mineo, Yuhanna, Quon, & Shaul, 2003). The activation of eNOS

by HDL/SR-B1 leads to at least two favorable outcomes: NO dependent vasodilation (Yuhanna et al., 2001), and NO dependent suppression of adhesion molecule expression (Kimura et al., 2006). HDL binding to SR-B1 also leads to the NO independent stimulation of endothelial cell migration in a PI3K/AKT- and MAP kinase-dependent manner, which leads to enhancement of endothelial repair *in vivo* (Seetharam et al., 2006).

Figure 1.6 – SR-B1 signaling in endothelial cells. In endothelial cells, HDL binding to SR-B1 on the cell surface activates an intracellular signaling cascade that leads to several atheroprotective responses. These include the activation of eNOS and production of NO, leading to vaso-relaxation and suppression of adhesion molecule expression and cytokine production; and induction of cell migration and enhancement of the endothelial repair process. Intracellular signaling activated by SR-B1 flows through a kinase cascade involving phosphatidylinositol 3 kinase (PI3K), AKT and the non-receptor tyrosine kinase Src, and is dependent on its C-terminal adapter protein, PDZK1.



Bone Marrow SR-B1 in Atherosclerosis

In addition to its roles in the liver and endothelial cells, there is an abundance of evidence to support an atheroprotective role for SR-B1 in bone marrow derived cells. Bone marrow transplantation (BMT) of lethally irradiated LDLR KO mice with SR-B1 KO donor BM has no effect on lipoprotein cholesterol profiles but increases atherosclerosis in the aorta and aortic sinus after prolonged Western diet feeding (Covey et al., 2003). Similarly, BMT of apoE KO mice with B1/E dKO BM increases aortic sinus atherosclerosis by ~2-fold without affecting lipoprotein cholesterol levels or cholesterol efflux to HDL (W. Zhang et al., 2003).

Conversely, transplantation of B1/E dKO mice with wild type bone marrow (BM) partially corrected lipoprotein abnormalities, drastically reduced aortic sinus atherosclerosis, and extended their lifespan beyond a year after BMT (H. Yu et al., 2006). This study did not evaluate the roles of BM apoE and BM SR-B1 separately; however, in support of an atheroprotective role of SR-B1 in BM derived cells, our lab has reported that restoration of SR-B1 expression alone in BM of SR-B1 KO/HypoE mice reduced HFCC diet-accelerated aortic sinus atherosclerosis and occlusive CA artery atherosclerosis without affecting plasma lipoprotein cholesterol (Pei et al., 2013). However, chimeric mice with SR-B1 expressing BM had lower levels of circulating interleukin-6 (IL-6), implying that SR-B1 in BM cells may influence overall inflammation (Pei et al., 2013).

Interestingly, deficiency of B- and T- lymphocytes in recombinant activating gene 2 (RAG2) deficient B1/E dKO mice had no effect on atherosclerosis or

spontaneous MI (Karackattu, Picard, & Krieger, 2005), suggesting that SR-B1 deficient lymphocytes do not drive the development of CA atherosclerosis in SR-B1 KO mouse models, and that the protective effects of BM SR-B1 are likely due to its function in other BM cells such as monocytes and monocyte-derived cells. In support of this, SR-B1 KO/HypoE monocytes bind VCAM-1 and ICAM-1 adhesion molecules better and are recruited more readily to atherosclerotic plaques *in vivo* than SR-B1 expressing HypoE monocytes (Pei et al., 2013). Other BM cell types that express SR-B1 and may influence the development of atherosclerosis include platelets, which are involved in both the initiation of atherosclerosis as well as late stage thrombosis leading to tissue ischemia (Davi & Patrono, 2007); and endothelial progenitor cells (EPCs), which can play a role in repair of damaged endothelium (Du et al., 2012).

The role of SR-B1 in Macrophages and Inflammation

The migration of macrophages may influence the dynamics of an atherosclerotic plaque, as an impaired ability to migrate could result in retention of macrophages in the plaque and impaired regression of atherosclerosis (Llodra et al., 2004). HDL stimulates cell migration and lamellipodia formation in wild type, but not in SR-B1 KO mouse peritoneal macrophages. Similarly, SR-B1 blocking antibody and an inhibitor of SR-B1-mediated lipid transfer prevent HDL-stimulated migration of Raw264.7 cells, a mouse macrophage-like tumor cell line (Al-Jarallah et al., 2014). Similar results with respect to HDL-stimulated migration

were observed in PDZK1 KO macrophages (Al-Jarallah et al., 2014), which express normal levels of SR-B1 implicating PDZK1 as an important downstream effector of HDL signaling through SR-B1 in macrophages. HDL-stimulated macrophage migration is also dependent on PI3K activity and phosphorylation of AKT1 at serine 473 (Al-Jarallah et al., 2014), suggesting that HDL binding to SR-B1 stimulates downstream intracellular signaling events through the PI3K-AKT1 signaling cascade that lead to cell migration.

SR-B1 KO mice have elevated levels of IL-6 and TNF α in their circulation compared to wild type mice under basal conditions (H. Feng et al., 2011). This is exacerbated by endotoxemia induced by LPS (Cai et al., 2008; Gilibert et al., 2014) and in response to surgically-induced sepsis via cecal ligation and puncture surgery (Guo et al., 2009). Both endotoxemia and sepsis were significantly more lethal to SR-B1 KO mice than to wild type mice (Cai et al., 2008; Gilibert et al., 2014; Guo et al., 2009; X. A. Li et al., 2006). Much of the protective effect of SR-B1 against endotoxemia and sepsis can be attributed to its roles in adrenal tissues and the liver; however there is evidence that SR-B1 also influences cytokine production in macrophages (Cai, Wang, Meyer, Ji, & van der Westhuyzen, 2012; Guo et al., 2009).

Transplantation of wild type mice with SR-B1 KO BM increases circulating IL-6 and TNF α levels after LPS injection, whereas restoration of SR-B1 expression in the BM of SR-B1 deficient mice reduces circulating IL-6 and TNF α after LPS stimulation (Cai et al., 2012). In cultured mouse bone marrow derived

macrophages, SR-B1 deficiency leads to increased production of IL-6 and TNF α in response to LPS compared to wild type macrophages (Cai et al., 2012; Guo et al., 2009). In contrast, in mouse macrophage-like J774 cells, over-expression of SR-B1 blunts the production of IL-6 and TNF α in response to LPS (Cai et al., 2012). Increased cytokine production by SR-B1KO macrophages treated with LPS was associated with enhanced activation of P38 and JNK kinases (Cai et al., 2012). Whether or not the anti-inflammatory effects of SR-B1 in macrophages are dependent on HDL induced signaling through SR-B1 remains to be determined. SR-B1 can reportedly bind to LPS and may play a role in its clearance, possibly explaining the above results (Guo, Zheng, Ai, Huang, & Li, 2014).

HDL and SR-B1 in endothelial progenitor cells

Circulating EPCs play an important role in repair of the endothelium, maintaining vascular integrity and endothelial function. The number of circulating EPCs in humans and mice is associated with the concentration of HDL cholesterol in the bloodstream (Noor et al., 2007; Petoumenos, Nickenig, & Werner, 2009). Studies in rodents have shown that treatments that increase HDL levels can increase the incorporation of EPCs into the vessel wall and improve repair of damaged endothelium. In apoE KO mice, intravenous infusion of reconstituted HDL increases the number of stem cell antigen-1-expressing EPCs that are incorporated into the endothelium (Tso et al., 2006). Similarly, treatment with

reconstituted HDL improves angiogenesis in wild type mice with hindlimb ischemia, and increases the number of BM-derived EPCs that are incorporated into the ischemic hindlimb (Sumi et al., 2007). Additionally, injection with reconstituted HDL increases circulating EPC populations in wild type mice and improves re-endothelialization of the common carotid artery after electric wire injury (Petoumenos et al., 2009). Increasing HDL levels in apoE KO mice by overexpression of human apoA1 via adenovirus increases the number of EPCs in circulation, the BM and the spleen; and enhances the incorporation of BM-derived EPCs into vascular allografts, reducing allograft associated atherosclerosis (Y. Feng et al., 2008). Elimination of SR-B1 in the BM of wild type mice reverses the protective effect of human apoA1 gene transfer on allograft vasculopathy, suggesting that the effect of HDL on EPC mediated endothelial repair is dependent on SR-B1 (Y. Feng et al., 2009).

In vitro, HDL increases eNOS expression and induces NO production by EPCs in a manner dependent on SR-B1 and ERK signaling. HDL also stimulates the migration of EPCs in an SR-B1 dependent manner that is blocked by the PI3K inhibitor wortmanin, the ERK inhibitor U0126, and the NOS inhibitor LNMA (Y. Feng et al., 2009). These results suggest that in EPCs, similar to its effects on mature endothelial cells, HDL activates eNOS activity via signaling through SR-B1, which leads to EPC migration. HDL has also been shown to promote the differentiation of EPCs from mononuclear cells (Petoumenos et al., 2009), increase the proliferation of EPCs (Petoumenos et al., 2009; Q. Zhang, Yin, Liu,

Zhang, & She, 2010) and prevent EPC apoptosis (Petoumenos et al., 2009) by inhibiting activation of caspase-3 (Noor et al., 2007). While the involvement of SR-B1 in these effects has not been tested, some additional parallels can be drawn between the signaling pathways activated by HDL in EPCs and signaling pathways activated by HDL through SR-B1 in other cell types. Reconstituted HDL increases phosphorylation of AKT in mononuclear cells, and HDL-stimulated differentiation of mononuclear cells into EPCs is blocked by LY294002 (Sumi et al., 2007), implicating a dependence on the PI3K/AKT signaling cascade. Similarly, in rat EPCs, HDL stimulates AKT phosphorylation and cyclin-D1 expression, presumably leading to EPC proliferation. HDL-induced cyclin-D1 upregulation is blocked by LY294006 and knock-down of AKT1 and AKT2 by siRNA. Furthermore, HDL-stimulated tube formation is blocked by LY294006 and siRNA against AKT1 and AKT2 (Q. Zhang et al., 2010). Since EPCs originate from the bone marrow, it is possible that the atheroprotective effects of restoring SR-B1 in bone marrow derived cells can be explained by SR-B1's role in EPCs.

1.12 Additional Evidence Supporting a Role for HDL Induced Signaling in CA Atherosclerosis Protection

In multiple relevant cell types, HDL binding to SR-B1 activates a number of intracellular signaling pathways leading to atheroprotective responses. Notably, SR-B1 signaling activates the PI3K-AKT signaling pathway in a number of cell types in a PDZK1 dependent manner (Al-Jarallah & Trigatti, 2010). Interestingly,

although not to the extent of complete SR-B1 deficiency, CA artery atherosclerosis has been reported in mice lacking several of the components of these signaling pathways.

eNOS/apoE dKO mice

Mice deficient in both eNOS and apoE develop significantly increased atherosclerosis in the aortic sinus and abdominal aorta compared to apoE KO controls after being fed a high fat diet for 16 weeks. Occlusions of the distal coronary arteries and myocardial fibrosis were also observed in all eNOS/apoE dKO mice. However, no reduction in lifespan was reported and no differences in plasma lipoprotein profiles were found compared to apoE KO mice (Kuhlencordt et al., 2001).

AKT1/apoE dKO mice

AKT1/apoE dKO mice fed a high cholesterol diet for 14 weeks exhibit exacerbated atherosclerosis in the brachiocephalic artery, aortic sinus and abdominal aorta compared to apoE KO controls. This was also accompanied by occlusive CA atherosclerosis, and approximately 1/4 of the AKT1/apoE dKO mice died prematurely. This phenotype was associated with reduced eNOS activation and increased adhesion molecule expression in endothelial cells from AKT/apoE dKO mice. Additionally, similar to SR-B1 KO macrophages, AKT1 deficient macrophages exhibited increased susceptibility to cholesterol loading-

induced apoptosis, and more apoptotic cells were observed in atherosclerotic plaques from AKT1/apoE dKO mice compared to apoE KO mice. AKT1 deficiency did not affect plasma lipoprotein profiles in these mice (Fernandez-Hernando et al., 2007).

PDZK1/apoE dKO mice

Mice deficient in both PDZK1 and apoE develop significantly increased atherosclerosis in the aortic sinus compared to apoE KO controls, but exhibit no evidence of coronary artery atherosclerosis when fed Western type diet for 3 months (Kocher et al., 2008). However, when challenged with a HFCC diet, PDZK1/apoE dKO mice developed multiple coronary artery occlusions and large MIs after 3 months of feeding (Yesilaltay, Daniels, Pal, Krieger, & Kocher, 2009). Interestingly, plasma lipoprotein profiles were unaffected by PDZK1 deficiency in apoE KO mice fed the western diet (Kocher et al., 2008), and only a slight increase in cholesterol associated with VLDL-sized particles was seen in PDZK1/apoE dKO mice fed the HFCC diet (Yesilaltay et al., 2009). This may reflect low level SR-B1 expression in the livers of these mice.

1.13 Overall Context and Objective

Whole body deficiency of SR-B1 exacerbates atherosclerosis in the aortic sinus in a variety of mouse models, and in apoE KO and HypoE mice, results in spontaneous or diet-inducible occlusive CA atherosclerosis, myocardial infarction and early death. However, CA atherosclerosis has never been described in SR-B1 deficient mice in the context of normal apoE expression. In addition, although SR-B1 deficiency is associated with multiple pro-atherogenic effects in a variety of cell types, and coronary artery atherosclerosis is observed in a number of mouse models lacking components of the SR-B1 signaling pathway, the majority of the literature on coronary artery atherosclerosis in SR-B1 KO mice emphasizes the influence of a lack of SR-B1 on lipoprotein metabolism. The objective of this thesis is to comprehensively characterize the cardiovascular phenotypes of SR-B1 KO mice on atherosclerosis-susceptible backgrounds with normal apoE expression, with emphasis on non-hepatic effects of SR-B1 deficiency that may influence the development of atherosclerosis.

1.14 Hypothesis

SR-B1 is a major factor that influences both the extent and the distribution of atherosclerosis in mouse arteries. Accordingly, SR-B1 deficient mice on a variety of atherosclerosis-prone genetic backgrounds will be susceptible to exacerbated atherosclerosis in multiple arteries. Furthermore, SR-B1 deficiency will have observable pro-atherogenic effects in multiple cell types which may be

collectively responsible for increased susceptibility of SR-B1 KO mice to the development of atherosclerosis in different arterial regions. Finally, removal of the enlarged spleens in SR-B1/LDLR dKO mice will impact leukocyte phenotypes and influence atherosclerosis in these mice.

1.15 Specific Aims

Aim of Chapter 2

Evaluate the relative effect of SR-B1 deficiency, compared to apoE deficiency and to LDLR deficiency, on the development of atherosclerosis in C57BL/6 mice fed a HFCC diet for 20 weeks.

Aim of Chapter 3

Evaluate the effects of SR-B1 deficiency and of different atherogenic diets on the development of occlusive coronary artery atherosclerosis and MI in mice that also lack the LDLR.

Aim of Chapter 4

Evaluate the effect of splenectomy on HFC diet-induced leukocytosis, occlusive coronary artery atherosclerosis and MI in SR-B1/LDLR dKO mice.

Chapter 2: Extensive Diet-Induced Atherosclerosis in the Aorta and Coronary Arteries of Scavenger Receptor Class B Type 1-Deficient Mice is Associated with Substantial Leukocytosis and Elevated Vascular Cell Adhesion Molecule-1 Expression in Coronary Artery Endothelium.

Author List: Mark Fuller, Omid Dadoo, Pardh Chivukula, Melissa MacDonald and Bernardo Trigatti.

Foreword

This manuscript compares the effects of HFCC diet feeding in wild type, LDLR KO, apoE KO and SR-B1 KO mice in terms of atherosclerosis in the aortic sinus, over the length of the aorta and in coronary arteries. It also explores the influence of the HFCC diet on plasma lipid levels, blood leukocyte numbers, systemic inflammation and endothelial cell activation. We demonstrate that despite no increase in total plasma cholesterol levels compared to wild type mice, SR-B1 KO mice develop extensive atherosclerosis in their aortic sinuses, aortas and coronary arteries to levels similar to or exceeding those of LDLR KO and apoE KO mice fed equivalently. SR-B1 deficient mice had substantial leukocytosis and elevated expression of VCAM-1 in their coronary artery endothelial cells, which may explain their susceptibility to atherosclerosis.

This manuscript will be submitted for publication in early 2015. This project was conceived and designed by Mark Fuller with input from Bernardo Trigatti.

Ph.D. Thesis – M. Fuller
McMaster University – Biochemistry and Biomedical Sciences.

The manuscript was written by Mark Fuller with guidance from Bernardo Trigatti. All data was analyzed and interpreted by Mark Fuller under the guidance of Bernardo Trigatti. The majority of the data was collected by Mark Fuller. Omid Dadoo assisted with sample collection, flow cytometry and cytokine measurements. Pardh Chivukula measured atherosclerosis in the aortic sinus and some en face aortas under the supervision of Mark Fuller. Melissa Macdonald assisted with animal care, sample collection and the remaining en face analysis of atherosclerosis in aortas.

2.1 Abstract

High levels of LDL cholesterol and low levels of HDL cholesterol are additive risk factors for cardiovascular disease. Mice that lack genes involved in the clearance of LDL from the bloodstream, such as the LDL receptor and apolipoprotein E, are widely used models of experimental atherosclerosis. Conversely, mice that lack the HDL receptor, SR-B1, and therefore have disrupted HDL functionality, also develop diet-inducible atherosclerosis but are a seldom used disease model. In this study, we compared atherosclerosis and associated phenotypes in SR-B1 knockout mice with those of wild type, LDLR knockout, and apolipoprotein E knockout mice after 20 weeks of being fed an atherogenic diet containing sodium cholate. We found that while SR-B1 knockout mice had substantially lower plasma cholesterol than LDLR and apolipoprotein E knockout mice, they developed similarly sized atherosclerotic plaques in their aortic sinuses, and more extensive atherosclerosis in their descending aortas and coronary arteries. This was associated with elevated TNF alpha levels in SR-B1 knockout mice compared to wild type and LDLR knockout mice, and lymphocytosis, monocytosis, and elevated VCAM-1 expression in coronary artery endothelial cells in SR-B1 knockout mice compared to all other mice examined. We conclude that extensive atherosclerosis in arteries that are not generally susceptible to atherosclerosis in SR-B1 knockout mice is driven by factors in addition to hypercholesterolemia, including inflammation, dysregulation of the immune system and increased sensitivity of endothelial cells in arteries that are normally

resistant to atherosclerosis. SR-B1 knockout mice fed a cholate containing atherogenic diet may prove to be a useful model to study mechanisms of atherosclerosis and evaluate treatments that rely on intact LDL clearance pathways.

2.2 Introduction

The ratio of the concentrations of low density lipoprotein (LDL) cholesterol to high density lipoprotein (HDL) cholesterol in plasma is positively correlated with the incidence of atherosclerosis¹, a major cause of cardiovascular disease globally². Atherosclerosis is an inflammatory disease characterized by the build up of cholesterol rich plaque in the walls of affected arteries². The development of an atherosclerotic plaque is initiated at sites along the vasculature where the endothelium is disrupted by non-laminar blood flow³. At these sites, the endothelium is more permeable to components of the blood such as LDL particles³. Moreover, the endothelial cells in these regions tend to express high levels of vascular cell adhesion molecule 1 (VCAM-1)⁴, which creates favorable sites for the attachment of circulating monocytes³. Monocytes give rise to macrophages, which phagocytose trapped LDL particles that have been oxidatively modified, resulting in the formation of cholesterol engorged macrophage foam cells², the major cell type that characterizes early stage atherosclerotic lesions⁵.

While high levels of LDL in the blood stream drive atherosclerosis, HDL levels are inversely correlated with cardiovascular disease⁶. This is thought to be in large part due to their role in facilitating cholesterol efflux from peripheral tissues and subsequent transport to the liver for excretion, a process collectively called reverse cholesterol transport⁷. In addition to their role in reverse cholesterol transport, HDLs have been shown to suppress expression of VCAM-1 on endothelial cells⁸, and induce the migration of macrophages⁹, which may contribute to the regression of atherosclerotic plaques¹⁰. The HDL receptor, scavenger receptor class b type 1 (SR-B1) is required in all of these functions.

Genetic disruptions of lipoprotein metabolism through targeted knockout (KO) of the LDL receptor (LDLR)¹¹ or apolipoprotein E (apoE)¹², a major ligand for lipoprotein receptors, has given rise to the conventional mouse models of atherosclerosis that are widely used in basic atherosclerosis research today¹³. These mice have elevated LDL cholesterol and very LDL (VLDL) cholesterol, and develop atherosclerotic lesions either spontaneously (apoE KO) or when fed a high fat diet (LDLR KO) in major arteries such as the aortic sinus, aortic arch and branch points along the descending aorta; sites where blood flow is non-laminar¹³. When SR-B1 is knocked out in these conventional models, the resulting double KO mice are uniquely susceptible to development of occlusive coronary artery atherosclerosis and myocardial infarction causing early death^{14,15}. Interestingly, diet induced coronary artery atherosclerosis in SR-B1/LDLR dKO mice is correlated with increased expression of VCAM-1 in

coronary arteries, elevated monocyte and lymphocyte counts in blood, and high levels of inflammatory cytokines in plasma compared to LDLR KO mice that are fed the same diets¹⁵. This severe phenotype occurs despite a reduction in plasma VLDL and LDL cholesterol¹⁵, suggesting that whole body SR-B1 deficiency affects multiple drivers of atherosclerosis independent of VLDL and LDL cholesterol.

Few studies have used atherogenic diet fed SR-B1 single KO mice as animal models to study atherosclerosis¹⁶⁻¹⁹. While long-term feeding of a Western type diet^{17, 18} or a high fat, high cholesterol diet¹⁶ leads to the development of small atherosclerotic plaques in the aortic sinus in SR-B1 KO mice; a high fat, high cholesterol diet containing sodium cholate (HFCC diet) generates large plaques in the aortic sinus after 11 weeks¹⁹. However, SR-B1 KO mice have never been comprehensively characterized as a model of experimental atherosclerosis. In this study, we compared the effects of HFCC diet feeding in wild type (WT), LDLR KO, apoE KO and SR-B1 KO mice. We demonstrate that atherosclerotic plaque size in the aortic sinus of SR-B1 KO mice after 20 weeks of HFCC is similar to that of LDLR KO and apoE KO mice, while atherosclerosis in the descending aorta and coronary arteries is significantly higher in SR-B1 KO mice. This corresponds with higher VCAM-1 expression in coronary arteries of SR-B1 KO mice, and is despite substantially lower plasma cholesterol levels. We conclude that HFCC diet fed SR-B1 KO mice are a model of wide-spread experimental atherosclerosis.

2.3 Materials and Methods

2.3.1 Animals and Diet

All experiments involving mice were approved by the McMaster University Animal Research Ethics Board and were carried out following guidelines set by the Canadian Council on Animal Care. C57BL/6J wild type mice and LDLR KO and apoE KO mice on C57BL/6J backgrounds were originally purchased from Jackson Labs, and bred in house. SR-B1 KO mice were originally obtained from M. Krieger at the Massachusetts Institute of Technology and crossed 10+ times onto a C57BL/6J background in house. For the majority of experiments, only female mice were used in this study.

Mice were aged to 10-12 weeks old and then fed a diet (Harlan Teklad, TD.88051) consisting of 15.8% fat (7.5% from cocoa butter), 1.25% cholesterol and 0.5% sodium cholate (HFCC diet) for 20 weeks. After 20 weeks of feeding, mice were fasted for a minimum of 4 hours and blood and tissues were collected for analysis.

2.3.2 Plasma Lipids

Plasma was prepared from blood collected by cardiac puncture at the time of harvest. Total cholesterol (Cholesterol Infinity, Thermo Fisher Scientific, Ottawa, ON, Canada), free cholesterol (Free Cholesterol E, WAKO Diagnostics, Mountain View, CA, USA), HDL cholesterol (HDL Cholesterol E, WAKO Diagnostics,

Mountain View, CA, USA) and Triglyceride (L-Type Triglyceride M, WAKO Chemicals, Richmond, VA, USA) were measured using the indicated commercial assay kits and following manufacturers' instructions. Non-HDL cholesterol was calculated as total cholesterol – HDL cholesterol.

2.3.3 Atherosclerosis Analysis

For analysis of atherosclerosis in the aortic sinus and coronary arteries, hearts were excised, fixed overnight in 10% formalin, and prepared and sectioned as described previously^{15, 20}. 10 μ m-thick transverse cryosections were collected from the middle of the heart to the base of the aortic sinus in 0.5mm intervals, then in 100 μ m intervals to the top of the valve leaflets. Atherosclerotic plaque was detected by oil red-O staining; nuclei were visualized with Meyer's hematoxylin stain. ImageJ software was used to measure the cross-sectional area of atherosclerotic plaque in the section best represented by 3 intact valve leaflets. Atherosclerosis in CAs was evaluated by counting the CAs in at least 3 cryosections that contained raised plaque which occluded all, or a portion of the lumen of the artery.

Atherosclerosis in en face prepared-aortas was assessed as previously described²⁰. Briefly, aortas were excised, fixed in 10% formalin, cleaned and stained with Sudan-IV stain. Aortas were opened longitudinally and mounted on a glass slide with aqueous mounting medium and a cover slip. Aortas were imaged with a Nikon digital SLR camera, and plaque coverage as a percentage

of total vessel area was measured manually using ImageJ software. Anatomical boundaries were used to define the aortic arch, the thoracic aorta and the abdominal aorta. The arch was defined as the region from the top of the heart to the end of the lesser curvature. The thoracic aorta was defined as the region from the aortic arch to the attachment point of the diaphragm. The abdominal aorta was defined as the region from the diaphragm to the iliac bifurcation.

2.3.4 Histological Characterization of Atherosclerotic Plaques

Necrotic cores in aortic sinus atherosclerotic plaques were defined as regions of the plaque that contained no nuclei in hematoxylin and eosin (H&E) stained sections, and were measured manually using ImageJ software. Collagen was detected as blue-stained tissue in Masson's trichrome (Sigma, Oakville, ON, Canada) stained sections and measured using the colour deconvolution and threshold functions in ImageJ software. CD68 and smooth muscle actin (SMA) were detected by immunofluorescence using rat anti-mouse CD68 (Ab Serotec) and rabbit anti-mouse SMA (AbCam) primary antibodies and Alexa 594 goat anti-rat, and Alexa 488 goat anti-rabbit secondary antibodies (Life Technologies), respectively. Nuclei were visualized with DAPI counterstain. CD68- and SMA-positive areas were measured using the threshold function in ImageJ software.

2.3.5 Blood Cell Analysis

Blood was collected from the tail veins of mice after 6 weeks of HFCC feeding. Fresh, heparin anti-coagulated blood was run on a Hemavet Multi-Species Hematology System as described previously¹⁵. Ly6C expression was assessed by flow cytometry of whole blood as described previously¹⁵. CD11b and CD115 double-positive monocytes were identified then analyzed for Ly6C expression using FITC-, PE- and APC-conjugated antibodies (BD Pharmingen), respectively.

2.3.6 Cytokine Analysis

Interleukin 6 (IL-6) and Tumor Necrosis Factor alpha (TNF α) were measured in plasma after 20 weeks of HFCC feeding. IL-6 and TNF α were measured using commercial ELISA kits (BioLegend, San Diego, CA, USA) following manufacturer's protocols.

2.3.7 VCAM-1 Immunofluorescence

VCAM-1 was detected by immunofluorescence as described previously¹⁵, using cell culture supernatants from rat B-lymphocyte hybridoma cells that produce mouse VCAM-1 antibody, and Alexa 594 goat anti-rat secondary antibody (Life Technologies). The artery wall auto fluoresces green and nuclei were detected with DAPI counterstain.

2.3.8 Statistical Analysis

All data sets were analyzed by one-way ANOVA and Tukey's Multiple Comparisons Post-Hoc test using GraphPad Prism software. When appropriate, data was transformed ($Y=\log[y]$) prior to statistical analysis. Data was considered statistically significant if $P<0.05$.

2.4 Results

2.4.1 Plasma Lipids

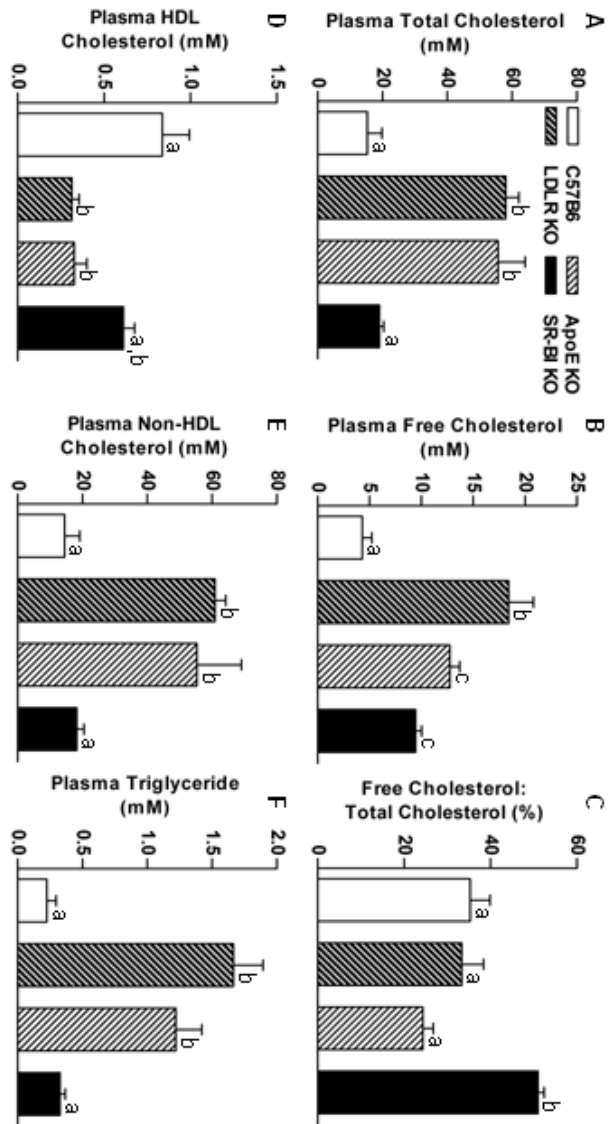
At 10-12 weeks of age, plasma was collected from the tail veins of mice for analysis of plasma lipid levels prior to HFCC diet feeding. (Supplementary Figure 2.7). Plasma total cholesterol levels were elevated by approximately 5-fold in LDLR KO and apoE KO mice compared to WT mice in mice fed a chow diet. Total plasma cholesterol in chow-fed SR-B1 KO mice was significantly higher (~2-fold) than that of WT mice, and significantly lower than in LDLR KO and apoE KO mice (Supplementary Figure 2.7A). Plasma free cholesterol levels were also significantly higher in chow-fed LDLR KO and apoE KO mice compared to both WT and SR-B1 KO mice; levels in chow-fed SR-B1 were significantly higher than levels in WT mice (Supplementary Figure 2.7B). The ratios of free cholesterol:total cholesterol (FC:TC ratios) were significantly higher in chow-fed SR-B1 KO mice than in all other groups. WT mice had the lowest FC:TC ratio while LDLR KO and apoE KO mice did not have significantly different FC:TC ratios when fed a chow diet (Supplementary Figure 2.7C). HDL cholesterol levels were lowest in chow-fed apoE KO mice, and were not significantly different

among chow-fed WT, LDLR KO and SR-B1 KO mice (Supplementary Figure 2.7D). Notably, the difference in HDL cholesterol levels between SR-B1 KO and WT mice approached statistical significance, and a significant increase in HDL cholesterol levels in SR-B1 KO vs. WT mice has been documented previously²¹. A larger sample size may be needed to uncover this difference. Non-HDL cholesterol was significantly higher in chow-fed LDLR KO and apoE KO mice than in WT and SR-B1 KO mice (Supplementary Figure 2.7E). Triglycerides were significantly higher in LDLR KO mice than in all other groups of mice when fed a chow diet (Supplementary Figure 2.7F).

WT, LDLR KO, apoE KO and SR-B1 KO mice were fed a HFCC diet starting at 10-12 weeks of age for 20 weeks. Plasma was prepared from blood collected by cardiac puncture after a 4 hour fasting period at the time of harvest. In general, the HFCC diet was associated with substantially higher total cholesterol and free cholesterol levels and lower HDL cholesterol levels (compare Figure 2.1 with Supplementary Figure 2.7). Total cholesterol levels were significantly (~3.5 fold) higher in both LDLR KO and apoE KO mice than in WT and SR-B1 KO mice when fed the HFCC diet (Figure 2.1A). Total cholesterol was not significantly different in HFCC-fed SR-B1 KO mice compared to WT mice (Figure 2.1A). The vast majority of total cholesterol after HFCC feeding was non-HDL cholesterol (Figure 2.1E). Free cholesterol was significantly higher in plasma from HFCC-fed LDLR KO, apoE KO and SR-B1 KO mice compared to WT mice (Figure 2.1B). Absolute levels of free cholesterol in plasma were

significantly lower in SR-B1 KO mice than in LDLR KO mice and not significantly different between SR-B1 KO and apoE KO mice when fed a HFCC diet (Figure 2.1B). However, the ratio of free cholesterol to total cholesterol in HFCC-fed SR-B1 KO mice (>50%), was significantly higher than the 24-36% observed in either WT, LDLR KO or apoE KO mice, which were not significantly different from each other (Figure 2.1C). In HFCC-fed mice, HDL cholesterol was highest in plasma from WT mice after 20 weeks of HFCC feeding, and similarly significantly lower in LDLR KO and apoE KO mice. SR-B1 KO mice had an intermediate level of HDL cholesterol, which was not significantly different from WT or from LDLR KO and apoE KO HDL levels (Figure 2.1D). Plasma Triglyceride levels were similarly significantly elevated in both HFCC-fed LDLR KO and apoE KO mice compared to WT and SR-BI KO mice, while not significantly different between WT and SR-BI KO mice (Figure 2.1F).

Figure 2.1 – Plasma Lipid Parameters in HFCC-fed WT, LDLR KO, apoE KO and SR-B1 KO mice. Mice were fed a HFCC diet for 20 weeks and plasma was prepared from blood collected at the time of harvest following a minimum of 4 hours of fasting. Average plasma lipid levels from WT (N=6-13), LDLR KO (N=8-14), apoE KO (N=9-15), and SR-B1 KO mice are shown for A) total cholesterol, B) free cholesterol, C) free cholesterol: total cholesterol ratio, D) HDL cholesterol, E) non-HDL cholesterol, and F) triglyceride. Bars with different letters are statistically significantly different from one another by one-way ANOVA with Tukey's post-hoc test ($P < 0.05$).

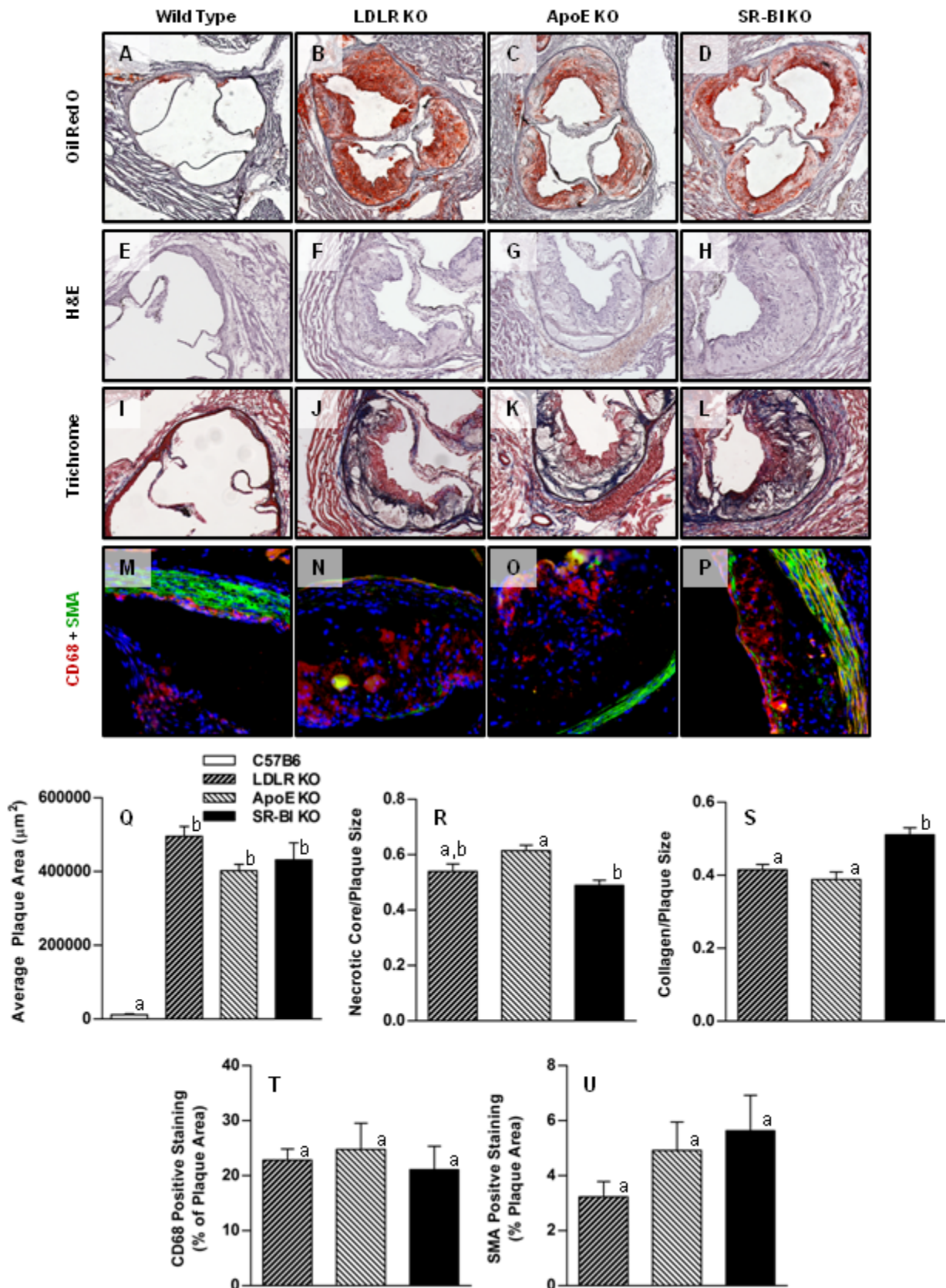


2.4.2 Aortic Sinus Atherosclerosis and Plaque Composition

Figure 2.2 (A-D) show representative images of oil red O stained aortic sinuses from female WT, LDLR KO, apoE KO, and SR-B1 KO mice after 20 weeks of HFCC feeding. Atherosclerotic plaque development was minimal in WT mice, while extensive atherosclerosis was observed in the aortic sinuses of each of the three knockout groups. In female mice, there were no significant differences in average plaque area among the three KO groups (Figure 2.2Q). However, in male mice, plaques from SR-B1 KO mice were significantly smaller than plaques from LDLR KO and apoE KO mice, but significantly larger than those of WT mice (Supplementary Figure 2.8). Figure 2.2 (E-H) show representative hematoxylin and eosin stained aortic sinus plaques from each of the four groups of mice. Necrotic cores were identified as regions of the plaque that contained no nuclei. No necrotic cores were observed in WT plaques, while large necrotic cores were observed in the plaques from all three of the KO groups. Normalized to plaque size, necrotic cores in plaques from apoE KO mice were slightly, but significantly larger than in plaques from SR-B1 KO mice, but not significantly different from those of LDLR KO mice (Figure 2.2R). Necrotic core size was not significantly different between SR-B1 KO and LDLR KO mice (Figure 2.2R). Figure 2.2 (I-L) show representative images of Masson's trichrome stained aortic sinus plaques from each group of mice. Collagen-rich fibrous regions of plaque are represented in blue. Plaques from SR-B1 KO mice contained the highest amount of collagen as a proportion of plaque size, with a significantly greater ratio of collagen:plaque

area compared to both LDLR KO and apoE KO plaques (Figure 2.2S). Plaques from LDLR KO and apoE KO mice were not significantly different in terms of collagen content (Figure 2.2S). Figure 2 (M-P) show representative immunofluorescence images of CD68 (macrophages) and smooth muscle actin (SMA) (smooth muscle cells) co-stained aortic sinus plaques from each of the four groups of mice. Plaques from LDLR KO, apoE KO and SR-B1 KO mice did not differ significantly in terms of macrophage content or smooth muscle cell content (Figure 2.2T,U). Most plaques from all knockout groups displayed SMA-positive staining near the luminal surface of the plaque, suggesting smooth muscle cell infiltration and formation of fibrous caps. Plaques from WT mice were difficult to identify reproducibly in trichrome or immunofluorescence images and were not quantitatively analyzed for collagen, CD68 or SMA.

Figure 2.2 – Size and Composition of Aortic Sinus Atherosclerotic Plaques in HFCC-fed WT, LDLR KO, apoE KO and SR-B1 KO mice. Representative images of transverse cryosections of the aortic sinus from mice in the indicated genotype groups stained with oil red-O (A-D), H&E (E-H), Masson's trichrome (I-L) and by immunofluorescence for CD68 (red) and smooth muscle actin (green) (M-P) are shown. Q) Average atherosclerotic plaque size in the aortic sinus. R) Necrotic core size as a fraction of plaque size measured as acellular regions in H&E stained sections. S) Collagen as a fraction of plaque size measured as blue-stained tissue in Masson's trichrome-stained sections. T) CD68-positive area as a fraction of plaque size as measured by immunofluorescence. U) SMA-positive area as a fraction of plaque size as measured by immunofluorescence. All data is represented as average + SEM from a minimum of 8 mice per group. Only plaque size was measured in WT mice due to difficulty reproducibly identifying plaques in images stained for other parameters. Bars with different letters are significantly different from one another by one-way ANOVA with Tukey's post-hoc test ($P < 0.05$).



2.4.3 Atherosclerosis in the Descending Aorta and Coronary Arteries

We measured atherosclerosis in other arteries to determine if there is a difference in the distribution of plaque in the different strains of mice examined here. Atherosclerosis in descending aorta was measured en face by Sudan IV staining. Representative images of Sudan IV stained aortas from each genotype of mouse are shown in Figure 2.3 (A-D). Surprisingly, there was a significant ~2-fold greater level of atherosclerotic plaque coverage in the descending aortas of SR-B1 KO mice compared to those of LDLR KO and apoE KO mice, which were not significantly different from each other (Figure 2.3E). All three knockout groups developed significantly more aortic plaque than WT control groups, which developed very little aortic atherosclerosis. For a more detailed analysis of plaque development along the descending aorta, we divided the aorta into three regions; the arch, the thoracic aorta (from the end of the arch to the diaphragm) and the abdominal aorta (from the diaphragm to the iliac bifurcation). In both apoE and LDLR KO mice, atherosclerotic plaque coverage (40%) was highest in the arch (Figure 2.3F) but dropped off significantly in the thoracic (15-20% coverage, Figure 2.3G) and the abdominal (<10% coverage, Figure 2.3H). Likewise, plaque coverage in the aortic arch of SR-B1 KO mice averaged 40% (Figure 2.3G), similar to that in apoE and LDLR KO mice, but in contrast, plaque coverage did not drop off in the SR-B1 KO mice in the thoracic aorta (~40%, Figure 2.3G) and decreased only moderately (<20%) in the abdominal portion (Figure 2.3H) of the aorta, extending right to the iliac bifurcation, which was

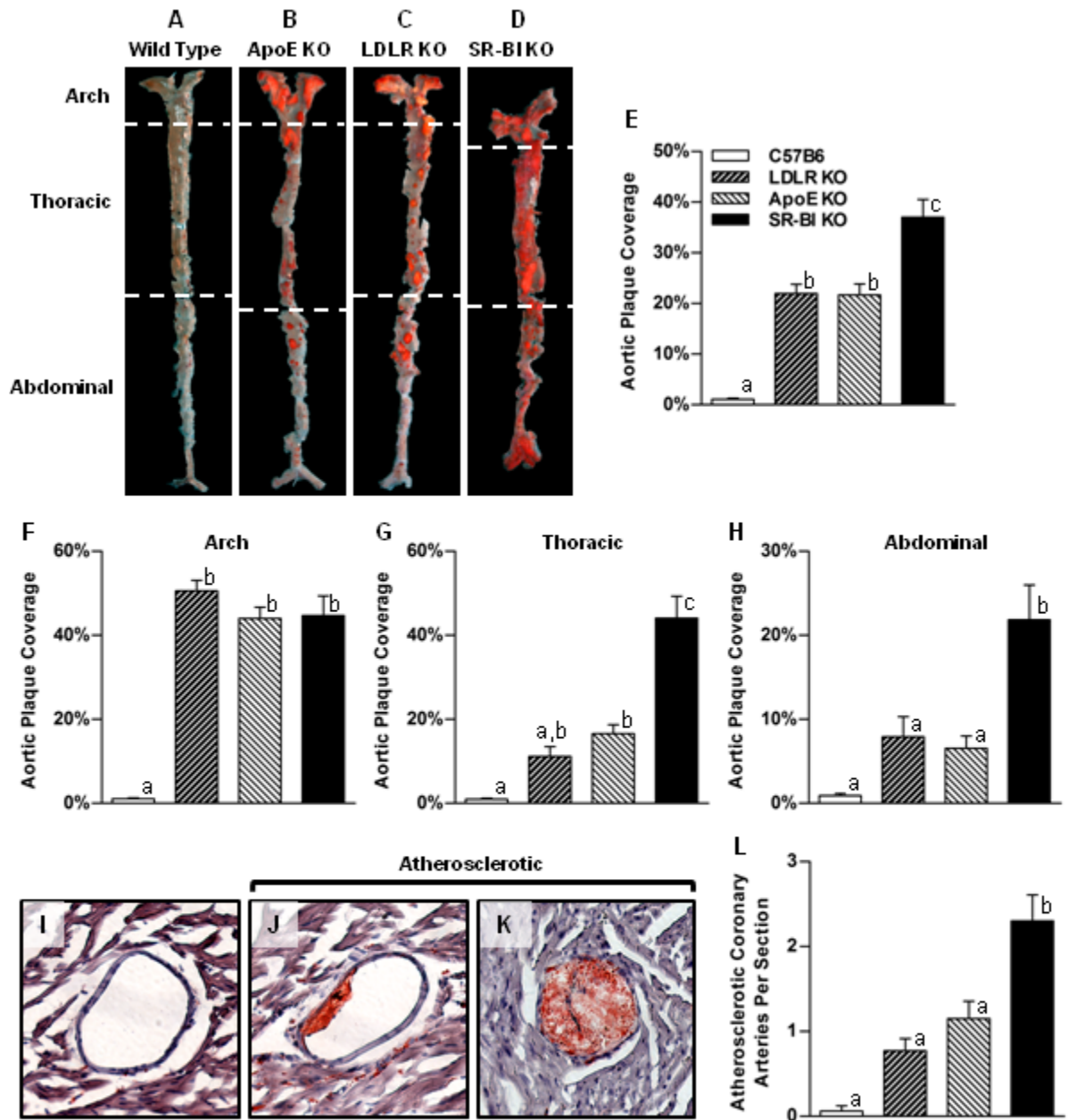
generally atherosclerosis free in the LDLR and apoE KO mice. Therefore SR-B1 deficiency, even in otherwise WT mice, appears to cause regions of the aorta that are typically relatively atherosclerosis resistant to become more susceptible to atherosclerosis development.

Since SR-B1 deficiency renders other atherosclerotic mouse strains susceptible to coronary artery atherosclerosis, we analyzed atherosclerosis in coronary arteries as well. Coronary arteries were counted in 3-4 transverse cardiac sections, spaced 0.5mm apart from the middle of the heart to the aortic sinus, and classified as either non-atherosclerotic, or atherosclerotic. Images of coronary arteries representing these categories are shown in Figure 2.3 (I-K). SR-B1 KO mice had, on average, ~2 times as many atherosclerotic coronary arteries per heart section as both LDLR KO mice and apoE KO mice (Figure 2.3L). As expected, all three knockout strains developed significantly more coronary artery atherosclerosis than WT mice (Figure 2.3L).

Figure 2.3 – Atherosclerosis in the Descending Aorta and Coronary

Arteries of HFCC-fed WT, LDLR KO, apoE KO and SR-B1 KO mice. A-D)

Representative en-face images of Sudan-IV-stained whole aortas from mice in the indicated genotype group. Dashed white lines indicate the boundaries of regions defined as the aortic arch, thoracic aorta and abdominal aorta. E-H) Plaque coverage as a percentage of entire en-face vessel area in the whole aorta (E) (N=8-11 per group), the aortic arch (F) (N=10-17 per group), the thoracic aorta (G) (N=10-16 per group) and the abdominal aorta (H) (N=8-11 per group). (I-K) Representative images of oil red-O-stained coronary arteries that are plaque free (I) or partially (J) or fully (K) occluded with atherosclerotic plaque. All plaque-containing (atherosclerotic) coronary arteries were counted in at least 3 transverse myocardial cross-sections from each mouse spaced at least 0.5mm apart. The graph in (L) represents the average number of atherosclerotic coronary arteries observed per myocardial cross-section (N= 4(WT) or 11(LDLR KO, apoE KO and SR-B1 KO). Bars with different letters are statistically significantly different from one another by one-way ANOVA with Tukey's post-hoc test.

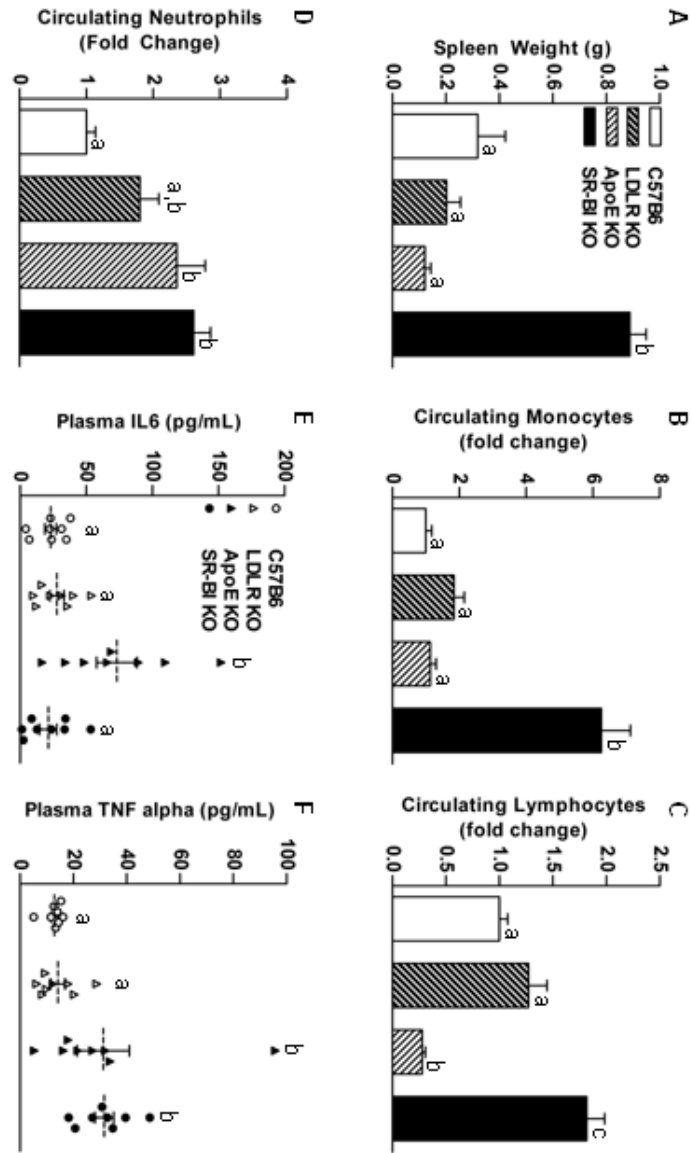


2.4.4 Blood Cells and Cytokines

Given that HFCC-fed SR-B1 KO mice developed more extensive atherosclerosis than LDLR KO and apoE KO mice fed the same diet despite having much lower plasma cholesterol levels, and that immune cells and inflammation are major factors that influence atherosclerosis, we measured aspects of immune system, including analysis of blood cells and cytokines. We noticed that spleens from SR-B1 KO mice fed the HFCC diet were markedly larger than those from WT, LDLR KO or apoE KO mice (Figure 2.4A). Blood cells were counted using a Hemavet multi species hematology analyzer. Red blood cells in chow-fed SR-B1 KO mice were slightly larger than those of WT, LDLR KO and apoE KO mice, and platelet counts were significantly lower in chow-fed SR-B1 KO mice compared to WT and LDLR KO mice. However, when fed a HFCC diet, SR-B1 KO mice exhibited substantially lower red blood cell counts and substantially larger red blood cells compared to WT, LDLR and apoE KO mice (supplementary table 2.1). In chow-fed 10-12 week old mice, aside from a slightly higher lymphocyte count in LDLR KO mice compared to SR-B1 KO mice, there were no significant differences in circulating neutrophils, lymphocytes or monocytes between any of the genotype groups (data not shown). Strikingly, monocytes in HFCC-fed SR-B1 KO mice were ~6 fold higher than observed in WT and apoE KO mice, and ~3-fold higher than in LDLR KO mice (Figure 2.4B). Lymphocytes in HFCC-fed SR-B1 KO mice were significantly elevated compared to all 3 of the other groups (~1.8 fold compared to WT) (Figure 2.4C). Interestingly, lymphocytes in HFCC-fed apoE

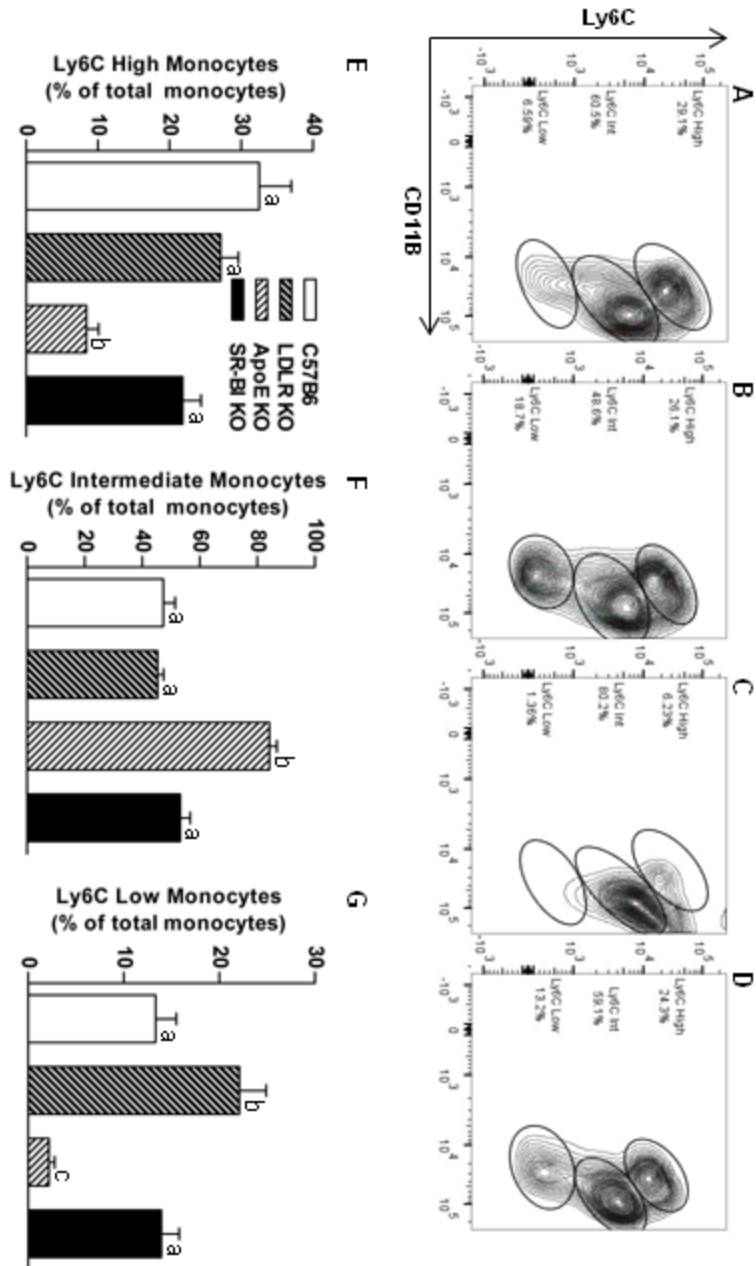
KO mice were significantly lower than in all other mice (Figure 2.4C). Neutrophils in apoE KO and SR-B1 KO mice were elevated to a similar extent compared to WT (~2.5 fold) and LDLR KO (~50%) mice after 6 weeks of HFCC feeding (Figure 2.4D). Interleukin-6 and TNF alpha levels in plasma were measured by ELISA. IL-6 and TNF α levels in all groups of mice were below the limit of detection of the assay prior to the onset of HFCC feeding. After 20 weeks of being fed a HFCC diet, IL-6 levels in apoE KO mice were significantly elevated compared to the other 3 groups of mice by ~2 fold, there were no significant differences in plasma IL-6 concentration between WT, LDLR KO and SR-B1 KO mice (Figure 2.4D). Plasma TNF α concentration was significantly higher (~2 fold) in both apoE KO and SR-B1 KO mice compared to the other 2 groups, there was no significant difference in plasma TNF α levels between apoE KO and SR-B1 KO mice. Plasma TNF α was similarly low in both WT and LDLR KO mice (Figure 2.4E).

Figure 2.4 – Circulating Immune Cells and Systemic Inflammatory Markers in HFCC-fed WT, LDLR KO, apoE KO and SR-B1 KO mice. A) Spleens were collected and weighed after 20 weeks of HFCC feeding. Blood cells were analyzed from whole blood collected from the tail veins of mice after 6 weeks of HFCC feeding using a Hemavet Multi-species Cell Analyzer. Average levels + SEM of circulating monocytes (B) lymphocytes (C) and neutrophils (D) in each genotype group are shown, normalized to levels observed in WT mice (N=8-11 per group). E&F) Levels of circulating IL-6 and TNF α in plasma were measured by ELISA after 20 weeks of HFCC feeding. Average concentration + SEM are shown for 8 mice per group. For all graphs, bars with different letters are statistically significantly different from one another by one-way ANOVA with Tukey's post-hoc test (P<0.05).



We measured Ly6C expression levels in monocytes by flow cytometry. SR-BI KO, LDLR KO and WT mice exhibited similar proportions of Ly6C^{high}, Ly6C^{int} and Ly6C^{low} monocytes. In contrast, apoE KO mice mainly exhibited Ly6C^{int} monocytes in circulation, with much lower levels of Ly6C^{high} monocytes. Therefore, by virtue of the higher numbers of circulating monocytes, the absolute numbers of circulating Ly6C^{high} monocytes are higher in SR-BI KO mice, than in LDLR KO, apoE KO or control WT mice.

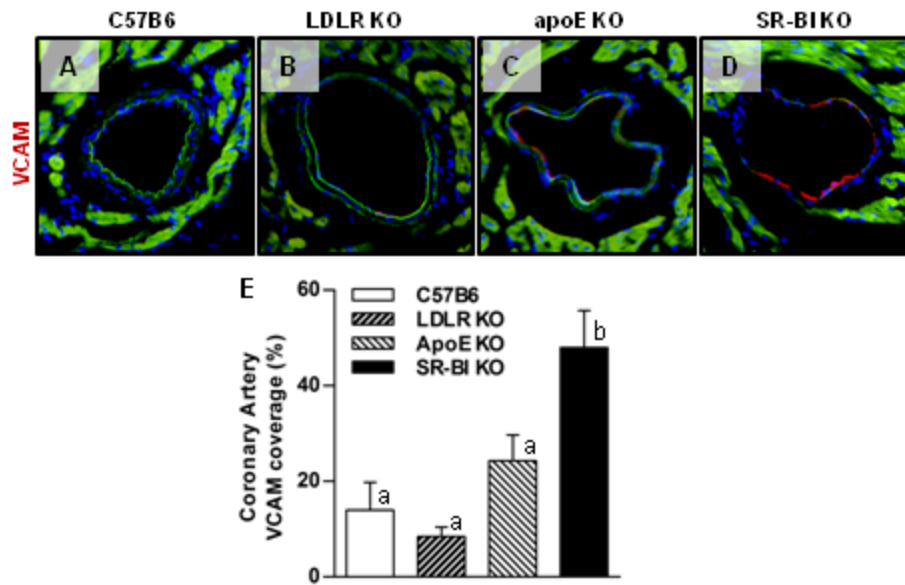
Figure 2.5 – Monocyte Subsets in HFCC-fed WT, LDLR KO, apoE KO and SR-B1 KO mice. Whole blood was collected from the tail veins of mice after 6 weeks of HFCC feeding and monocytes were analyzed by flow cytometry for levels of Ly6C expression. (A-D) Representative cytograms illustrating Ly6C expression patterns in monocytes from the indicated genotype groups are shown. Ly6C^{high} (E), Ly6C^{int} (F) and Ly6C^{low} (G) monocytes were counted using FloJo software. Graphs represent average proportions of each monocyte subset in blood + SEM of 8 mice per group. Bars with different letters are statistically significantly different from one another by one-way ANOVA with Tukey's post-hoc test (P<0.05).



2.4.5 Coronary Artery VCAM-1 Expression

We have previously shown that SR-B1/LDLR double KO mice that are susceptible to severe occlusive coronary artery atherosclerosis have high levels of adhesion molecule expression in their coronary arteries when compared to LDLR single KO controls. Since VCAM-1 expression is thought to precede the development of atherosclerosis and may be a major factor in determining where atherosclerotic plaques develop in the vasculature, we measured VCAM-1 expression in the coronary arteries of the mice in this study. Figure 2.6 (A-D) show representative images of VCAM-1 immunofluorescence in coronary arteries from WT, LDLR KO, apoE KO and SR-B1 KO mice. As a proportion of total endothelium analyzed, SR-B1 KO mice expressed significantly more VCAM-1 in coronary artery endothelium compared to all other groups (Figure 2.6E), suggesting that SR-B1 plays a major role in the suppression of VCAM-1 expression in coronary arteries, and possibly other arteries that are resistant to atherosclerosis in SR-B1 expressing mice.

Figure 2.6 – Expression of VCAM-1 in Coronary Artery Endothelial Cells in HFCC-fed WT, LDLR KO, apoE KO and SR-B1 KO mice. Coronary arteries in transverse cryosections of myocardium were stained for VCAM-1 expression by immunofluorescence. Representative images of VCAM-1-stained coronary arteries from mice from each indicated genotype group are shown in (A-D). The length VCAM-1 positive staining in coronary artery endothelium was measured using ImageJ software and expressed as a percentage of total artery endothelium length (the cumulative circumference of each artery counted). E) Average VCAM-1 coverage + SEM of 6-7 mice per group. Bars with different letters are statistically significantly different from one another by one-way ANOVA with Tukey's post-hoc test ($P < 0.05$).



2.5 Discussion

In mice that are genetically susceptible to experimental atherosclerosis, SR-B1 deficiency results in the development of severe occlusive coronary artery atherosclerosis, myocardial infarction and early death^{14, 15, 22}. This phenotype is associated with monocytosis, inflammation and elevated adhesion molecule expression in the coronary endothelium¹⁵. SR-B1 single KO mice develop extensive atherosclerosis in response to HFCC feeding¹⁹; however, HFCC-fed SR-B1 KO mice are not a commonly used model of experimental atherosclerosis and have not been comprehensively characterized. In this study, we compared SR-B1 KO mice fed the HFCC diet for 20 weeks to WT, LDLR KO and apoE KO mice fed the same diet for the same period of time. We show that SR-B1 KO mice developed large atherosclerotic plaques in the aortic sinus similar in size to equivalently treated LDLR KO mice and apoE KO mice. In the descending aorta and coronary arteries, SR-B1 KO mice developed more extensive atherosclerosis than LDLR KO and apoE KO mice. This was associated with leukocytosis, particularly monocytosis, and elevated VCAM-1 expression in coronary arteries and despite much lower plasma cholesterol levels in SR-B1 KO mice.

While hypercholesterolemia is a major risk factor for atherosclerosis, the results of this study highlight the requirement for other factors that facilitate atherosclerotic plaque development. The finding that total plasma cholesterol in HFCC fed SR-B1 KO mice, while elevated compared to chow fed SR-B1 KO

mice, is not significantly different from HFCC fed WT mice, indicates that disease development in these mice is more complicated than simply elevated cholesterol induced by the HFCC diet. SR-B1 KO mice have elevated free cholesterol: total cholesterol ratios compared to WT, LDLR KO and apoE KO mice. This indicates a compositional difference in lipoproteins in SR-B1 deficient mice that may lead to defects in normal lipoprotein function. SR-B1 KO mice also have a major defect in reverse cholesterol transport, leading to large HDL particles that are unable to off-load cholesterol to the liver²³. This may influence the ability of HDL to accept additional cholesterol from peripheral tissues, leading to retention of cholesterol in macrophages in the plaque, and may also influence the capacity of HDL in these mice to induce atheroprotective intracellular signaling pathways, especially those that are dependent on SR-B1.

In addition to elevated cholesterol, inflammation and the immune system also play a significant role in determining the progression of atherosclerosis². High levels of systemic pro-inflammatory cytokines can activate endothelial cells as well as immune cells in the atherosclerotic plaque and perpetuate atherosclerosis. Moreover, leukocytosis is a documented risk factor for atherosclerosis in humans and animal models²⁴. We measured IL-6 and TNF α levels in the plasma and found that TNF α levels were elevated in both apoE KO and SR-B1 KO mice compared to LDLR KO and WT mice. In addition, SR-B1 KO mice exhibited substantial leukocytosis, with monocytes elevated up to 6 fold compared to other groups in the study. Although the proportion of circulating

monocytes with high levels of Ly6C cell surface expression were not higher in SR-BI KO mice, the absolute numbers of Ly6C^{high} monocytes in circulation were higher by virtue of the overall increased numbers of circulating monocytes. This, combined with the increased VCAM-1 expression, at least in coronary arteries, might explain the increased susceptibility of some arteries (coronary arteries, abdominal aorta) to atherosclerosis in SR-BI KO mice compared to the LDLR and apoE KO mice. These data suggest that while cholesterol is not elevated to the same extent as in LDLR KO and apoE KO mice, it is sufficiently high in SR-B1 KO mice to facilitate atherosclerotic plaque formation under conditions of extreme monocytosis and elevated inflammation.

Elevated inflammatory markers in the plasma and leukocytosis are systemic risk factors that would be expected to influence overall atherosclerosis, but would not be expected to impact the distribution of atherosclerosis in different regions of the vasculature. One of the interesting findings in this study is the very different distribution of atherosclerosis observed in SR-B1 KO mice compared to the other groups. Like LDLR KO and apoE KO mice, SR-B1 KO mice developed extensive atherosclerosis in normally susceptible arterial sites such as the aortic sinus and aortic arch; however, SR-B1 KO mice also developed atherosclerosis along the entire length of their descending aortas as well as in coronary arteries. This observation suggests that SR-B1 expression in the arteries themselves may protect against the initiation of atherosclerosis. It is well documented that atherosclerosis in mice tends to develop at sites along the vasculature that

experience non-laminar blood flow^{25, 26}. Endothelial cells in these regions experience low shear stress and tend to be more permeable to components of the blood, including circulating lipoproteins³. These regions also have up-regulated expression of inflammatory genes including adhesion molecules, creating favorable sites for monocytes to attach to the artery wall^{4, 25, 26}. The expression of these adhesion molecules is thought to be a strong predictor of locations that are likely to develop atherosclerotic plaques⁴. HDL has been shown to protect endothelial cells against apoptosis induced by multiple stimuli²⁷⁻²⁹. HDL also enhances the activity of endothelial nitric oxide synthase (eNOS) in endothelial cells in an SR-B1 dependent manner^{30, 31}. This results in eNOS dependent suppression of TNF α -induced adhesion molecule expression⁸. HDL binding SR-B1 also induces eNOS independent EC migration³², which may influence endothelial repair. Here, we demonstrate that similar to SR-B1/LDLR dKO mice¹⁵, coronary arteries of SR-B1 single KO mice exhibit much higher levels of VCAM-1 compared to all other groups of mice analyzed in this study. These data support the notion that SR-B1 protects against the development of atherosclerosis in mouse arteries through its role in suppressing VCAM-1 expression in endothelial cells. Alternatively, it is possible that the abnormal HDL in SR-B1 KO mice is not capable of signalling, or that the abnormal HDL and/or other lipoproteins in SR-B1 KO mice actually induce VCAM-1 expression in endothelial cells. The influence of lipoproteins from SR-B1 KO mice on endothelial function requires further investigation.

In conclusion, HFCC fed SR-B1 KO mice develop widespread atherosclerosis in multiple arteries. We believe this phenotype is facilitated by slightly elevated cholesterol from the diet, but driven by a multitude of cholesterol independent factors such as inflammation, dysregulation of the haematopoietic system, and enhanced activation of vascular endothelial cells. Given that SR-B1 single KO mice possess intact mechanisms for LDL and VLDL clearance from the blood stream, they may prove a useful model of experimental atherosclerosis that is suitable for testing therapeutic agents, such as statins and PCSK9 inhibitors, which rely on the enhancement of this system as a mechanism for cholesterol lowering.

2.6 References

- [1] Fernandez ML, Webb D: The LDL to HDL cholesterol ratio as a valuable tool to evaluate coronary heart disease risk. *Journal of the American College of Nutrition* 2008, 27:1-5.
- [2] Libby P: Inflammation in atherosclerosis. *Nature* 2002, 420:868-74.
- [3] Chatzizisis YS, Coskun AU, Jonas M, Edelman ER, Feldman CL, Stone PH: Role of endothelial shear stress in the natural history of coronary atherosclerosis and vascular remodeling: molecular, cellular, and vascular behavior. *Journal of the American College of Cardiology* 2007, 49:2379-93.
- [4] Iiyama K, Hajra L, Iiyama M, Li H, DiChiara M, Medoff BD, Cybulsky MI: Patterns of vascular cell adhesion molecule-1 and intercellular adhesion

molecule-1 expression in rabbit and mouse atherosclerotic lesions and at sites predisposed to lesion formation. *Circ Res* 1999, 85:199-207.

[5] Yu XH, Fu YC, Zhang DW, Yin K, Tang CK: Foam cells in atherosclerosis. *Clinica chimica acta; international journal of clinical chemistry* 2013, 424:245-52.

[6] Castelli WP: Cholesterol and lipids in the risk of coronary artery disease--the Framingham Heart Study. *Can J Cardiol* 1988, 4 Suppl A:5A-10A.

[7] Linsel-Nitschke P, Tall AR: HDL as a target in the treatment of atherosclerotic cardiovascular disease. *Nature reviews Drug discovery* 2005, 4:193-205.

[8] Kimura T, Tomura H, Mogi C, Kuwabara A, Damirin A, Ishizuka T, Sekiguchi A, Ishiwara M, Im DS, Sato K, Murakami M, Okajima F: Role of scavenger receptor class B type I and sphingosine 1-phosphate receptors in high density lipoprotein-induced inhibition of adhesion molecule expression in endothelial cells. *J Biol Chem* 2006, 281:37457-67.

[9] Al-Jarallah A, Chen X, Gonzalez L, Trigatti BL: High density lipoprotein stimulated migration of macrophages depends on the scavenger receptor class B, type I, PDZK1 and Akt1 and is blocked by sphingosine 1 phosphate receptor antagonists. *PLoS One* 2014, 9:e106487.

[10] Llodra J, Angeli V, Liu J, Trogan E, Fisher EA, Randolph GJ: Emigration of monocyte-derived cells from atherosclerotic lesions characterizes regressive, but not progressive, plaques. *Proc Natl Acad Sci U S A* 2004, 101:11779-84.

- [11] Ishibashi S, Brown MS, Goldstein JL, Gerard RD, Hammer RE, Herz J: Hypercholesterolemia in low density lipoprotein receptor knockout mice and its reversal by adenovirus-mediated gene delivery. *J Clin Invest* 1993, 92:883-93.
- [12] Piedrahita JA, Zhang SH, Hagan JR, Oliver PM, Maeda N: Generation of mice carrying a mutant apolipoprotein E gene inactivated by gene targeting in embryonic stem cells. *Proc Natl Acad Sci U S A* 1992, 89:4471-5.
- [13] Whitman SC: A practical approach to using mice in atherosclerosis research. *The Clinical biochemist Reviews / Australian Association of Clinical Biochemists* 2004, 25:81-93.
- [14] Braun A, Trigatti BL, Post MJ, Sato K, Simons M, Edelberg JM, Rosenberg RD, Schrenzel M, Krieger M: Loss of SR-BI expression leads to the early onset of occlusive atherosclerotic coronary artery disease, spontaneous myocardial infarctions, severe cardiac dysfunction, and premature death in apolipoprotein E-deficient mice. *Circ Res* 2002, 90:270-6.
- [15] Fuller M, Dadoo O, Serkis V, Abutouk D, MacDonald M, Dhingani N, Macri J, Igdoura SA, Trigatti BL: The Effects of Diet on Occlusive Coronary Artery Atherosclerosis and Myocardial Infarction in Scavenger Receptor Class B, Type 1/Low-Density Lipoprotein Receptor Double Knockout Mice. *Arterioscler Thromb Vasc Biol* 2014.
- [16] Harder C, Lau P, Meng A, Whitman SC, McPherson R: Cholesteryl ester transfer protein (CETP) expression protects against diet induced atherosclerosis in SR-BI deficient mice. *Arterioscler Thromb Vasc Biol* 2007, 27:858-64.

[17] Hildebrand RB, Lammers B, Meurs I, Korporaal SJ, De Haan W, Zhao Y, Kruijt JK, Pratico D, Schimmel AW, Holleboom AG, Hoekstra M, Kuivenhoven JA, Van Berkel TJ, Rensen PC, Van Eck M: Restoration of high-density lipoprotein levels by cholesteryl ester transfer protein expression in scavenger receptor class B type I (SR-BI) knockout mice does not normalize pathologies associated with SR-BI deficiency. *Arterioscler Thromb Vasc Biol* 2010, 30:1439-45.

[18] Van Eck M, Twisk J, Hoekstra M, Van Rij BT, Van der Lans CA, Bos IS, Kruijt JK, Kuipers F, Van Berkel TJ: Differential effects of scavenger receptor BI deficiency on lipid metabolism in cells of the arterial wall and in the liver. *J Biol Chem* 2003, 278:23699-705.

[19] Huby T, Doucet C, Dacet C, Ouzilleau B, Ueda Y, Afzal V, Rubin E, Chapman MJ, Lesnik P: Knockdown expression and hepatic deficiency reveal an atheroprotective role for SR-BI in liver and peripheral tissues. *J Clin Invest* 2006, 116:2767-76.

[20] Covey SD, Krieger M, Wang W, Penman M, Trigatti BL: Scavenger receptor class B type I-mediated protection against atherosclerosis in LDL receptor-negative mice involves its expression in bone marrow-derived cells. *Arterioscler Thromb Vasc Biol* 2003, 23:1589-94.

[21] Rigotti A, Trigatti BL, Penman M, Rayburn H, Herz J, Krieger M: A targeted mutation in the murine gene encoding the high density lipoprotein (HDL) receptor

scavenger receptor class B type I reveals its key role in HDL metabolism. *Proc Natl Acad Sci U S A* 1997, 94:12610-5.

[22] Zhang S, Picard MH, Vasile E, Zhu Y, Raffai RL, Weisgraber KH, Krieger M: Diet-induced occlusive coronary atherosclerosis, myocardial infarction, cardiac dysfunction, and premature death in scavenger receptor class B type I-deficient, hypomorphic apolipoprotein ER61 mice. *Circulation* 2005, 111:3457-64.

[23] Trigatti B, Rayburn H, Vinals M, Braun A, Miettinen H, Penman M, Hertz M, Schrenzel M, Amigo L, Rigotti A, Krieger M: Influence of the high density lipoprotein receptor SR-BI on reproductive and cardiovascular pathophysiology. *Proc Natl Acad Sci U S A* 1999, 96:9322-7.

[24] Tall AR, Yvan-Charvet L, Westerterp M, Murphy AJ: Cholesterol efflux: a novel regulator of myelopoiesis and atherogenesis. *Arterioscler Thromb Vasc Biol* 2012, 32:2547-52.

[25] Hajra L, Evans AI, Chen M, Hyduk SJ, Collins T, Cybulsky MI: The NF-kappa B signal transduction pathway in aortic endothelial cells is primed for activation in regions predisposed to atherosclerotic lesion formation. *Proc Natl Acad Sci U S A* 2000, 97:9052-7.

[26] Won D, Zhu SN, Chen M, Teichert AM, Fish JE, Matouk CC, Bonert M, Ojha M, Marsden PA, Cybulsky MI: Relative reduction of endothelial nitric-oxide synthase expression and transcription in atherosclerosis-prone regions of the mouse aorta and in an in vitro model of disturbed flow. *Am J Pathol* 2007, 171:1691-704.

[27] Suc I, Escargueil-Blanc I, Trolly M, Salvayre R, Negre-Salvayre A: HDL and ApoA prevent cell death of endothelial cells induced by oxidized LDL. *Arterioscler Thromb Vasc Biol* 1997, 17:2158-66.

[28] Sugano M, Tsuchida K, Makino N: High-density lipoproteins protect endothelial cells from tumor necrosis factor-alpha-induced apoptosis. *Biochem Biophys Res Commun* 2000, 272:872-6.

[29] Nofer JR, Levkau B, Wolinska I, Junker R, Fobker M, von Eckardstein A, Seedorf U, Assmann G: Suppression of endothelial cell apoptosis by high density lipoproteins (HDL) and HDL-associated lysosphingolipids. *J Biol Chem* 2001, 276:34480-5.

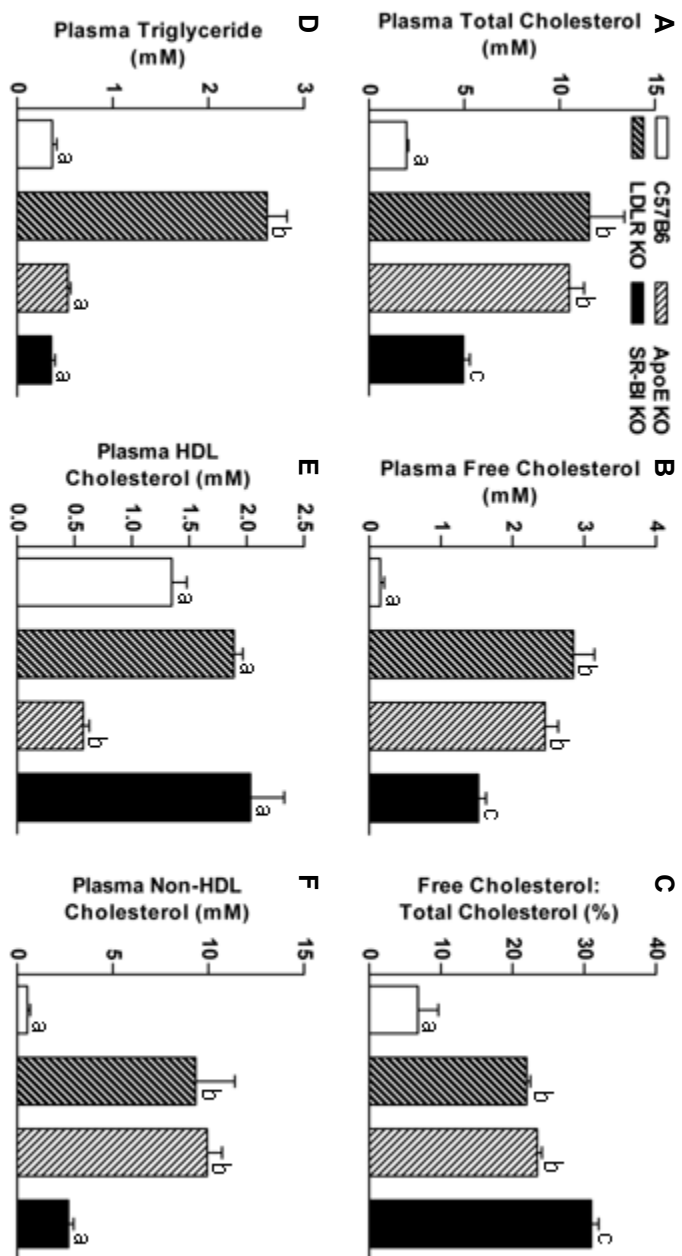
[30] Yuhanna IS, Zhu Y, Cox BE, Hahner LD, Osborne-Lawrence S, Lu P, Marcel YL, Anderson RG, Mendelsohn ME, Hobbs HH, Shaul PW: High-density lipoprotein binding to scavenger receptor-B1 activates endothelial nitric oxide synthase. *Nat Med* 2001, 7:853-7.

[31] Li XA, Titlow WB, Jackson BA, Giltiay N, Nikolova-Karakashian M, Uittenbogaard A, Smart EJ: High density lipoprotein binding to scavenger receptor, Class B, type I activates endothelial nitric-oxide synthase in a ceramide-dependent manner. *J Biol Chem* 2002, 277:11058-63.

[32] Seetharam D, Mineo C, Gormley AK, Gibson LL, Vongpatanasin W, Chambliss KL, Hahner LD, Cummings ML, Kitchens RL, Marcel YL, Rader DJ, Shaul PW: High-density lipoprotein promotes endothelial cell migration and reendothelialization via scavenger receptor-B type I. *Circ Res* 2006, 98:63-72.

2.7 Supplementary Materials

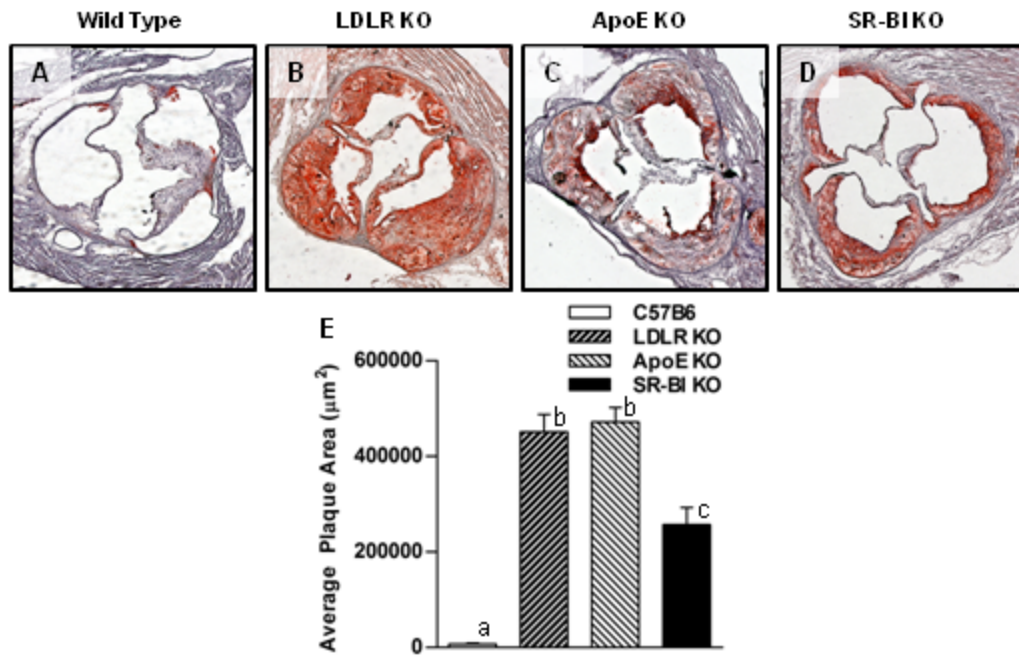
Supplementary Figure 2.7 – Plasma lipid parameters in chow-fed wild type, LDLR KO, apoE KO and SR-B1 KO mice. Plasma was prepared from blood collected from the tail vein of 10 week-old, normal chow-fed mice following a minimum of 4 hours of fasting. Average plasma lipid levels from WT (N=5-6), LDLR KO (N=7-8), apoE KO (N=10), and SR-B1 KO (N=8-9) mice are shown for A) total cholesterol, B) free cholesterol, C) free cholesterol: total cholesterol ratio, D) HDL cholesterol, E) non-HDL cholesterol, and F) triglyceride. Bars with different letters are statistically significantly different from one another by one-way ANOVA with Tukey's post-hoc test ($P < 0.05$).



Supplementary Figure 2.8 – Atherosclerosis in the aortic sinus of male wild type, LDLR KO, apoE KO and SR-B1 KO mice fed the HFCC for 20 weeks.

Male mice were fed the HFCC diet for 20 weeks starting at 10 weeks of age.

Representative oil red O stained transverse cryosections of that aortic sinus are shown in panels A-D, quantification of average plaque size in the aortic sinus is shown in E.



Supplementary Table 2.1. Hematology profiles for wild type, LDLR KO, apoE KO and SR-B1 KO mice fed either chow or HFCC diet for 20 weeks.

Whole blood was collected from tail or submandibular veins of 10-12 week old chow-fed mice or mice fed the HFCC diet for 20 weeks. Hematology profiles were generated using a Hemavet Multi-Species Hematology System (Drew Scientific). Results shown are mean \pm SEM for each output. Sample sizes are indicated in parentheses in the genotype column. Values with different letters are statistically significantly different from each other by one-way ANOVA with Tukey's post-hoc test within each diet group.

Genotype	Diet	RBC Count (M/ μ l)	Hematocrit (%)	Mean RBC Volume (fL)	RBC Dist. Width (%)	Platelet Count (K/ μ l)
Wild Type	Chow (6)	10.19 \pm 0.08 ^a	45.7 \pm 0.8 ^a	44.8 \pm 0.5 ^a	16.63 \pm 0.41 ^a	743 \pm 50 ^a
	HFCC (8)	9.92 \pm 0.41 ^a	44.2 \pm 2.1 ^a	44.5 \pm 0.5 ^{a,b}	17.3 \pm 0.4 ^a	754 \pm 97 ^a
LDLR KO	Chow (8)	10.81 \pm 0.16 ^{a,b}	44.5 \pm 0.7 ^a	45.4 \pm 0.1 ^a	15.94 \pm 0.13 ^a	730 \pm 48 ^a
	HFCC (10)	10.11 \pm 0.55 ^a	45.6 \pm 2.8 ^a	45.0 \pm 0.4 ^b	16.5 \pm 0.1 ^a	701 \pm 96 ^a
apoE KO	Chow (9)	9.40 \pm 0.13 ^b	43.6 \pm 1.0 ^a	46.4 \pm 0.6 ^{a,b}	16.78 \pm 0.22 ^a	625 \pm 67 ^{a,b}
	HFCC (10)	9.63 \pm 0.33 ^a	41.2 \pm 1.4 ^a	42.8 \pm 0.3 ^a	18.0 \pm 0.1 ^a	792 \pm 132 ^a
SR-B1 KO	Chow (9)	9.61 \pm 0.15 ^b	45.6 \pm 0.7 ^a	47.4 \pm 0.3 ^b	18.21 \pm 0.24 ^b	453 \pm 41 ^b
	HFCC (11)	5.10 \pm 0.33 ^b	41.0 \pm 2.7 ^a	80.5 \pm 0.6 ^d	22.1 \pm 0.6 ^b	570 \pm 46 ^a

**Chapter 3: The Effects of Diet on Occlusive Coronary Artery
Atherosclerosis and Myocardial Infarction in Scavenger Receptor Class B,
Type 1/Low-Density Lipoprotein Receptor Double Knockout Mice.**

Author List: Mark Fuller, Omid Dadoo, Viktoria Serkis, Dina Abutouk, Melissa MacDonald, Neel Dhingani, Joseph Macri, Suleiman A. Igdoura and Bernardo L. Trigatti

Foreword

In this manuscript, we demonstrate that mice lacking both SR-B1 and the LDLR develop diet-accelerated severe occlusive coronary artery atherosclerosis associated with myocardial infarction and reduced survival. This severity of this phenotype varied depending on the composition of the atherogenic diet employed. SR-B1/LDLR dKO mice also exhibited leukocytosis, diet-induced elevated systemic inflammation, and diet-induced elevated VCAM-1 and ICAM-1 expression in their coronary endothelium.

This paper was published in the November 2014 issue of *Arteriosclerosis, Thrombosis and Vascular Biology*. Permission is not required for the use of this manuscript in a dissertation/thesis. The full citation is:

Mark Fuller, Omid Dadoo, Viktoria Serkis, Dina Abutouk, Melissa MacDonald, Neel Dhingani, Joseph Macri, Suleiman A. Igdoura and Bernardo L. Trigatti. *Arteriosclerosis, Thrombosis, and Vascular Biology*. 2014; 34: 2394-2403.

The manuscript was written by Mark Fuller with input from Bernardo Trigatti. Experiments were designed by Mark Fuller and Bernardo Trigatti. All data was analyzed and interpreted by Mark Fuller under the guidance of Bernardo Trigatti. The majority of data was collected by Mark Fuller. Omid Dadoo assisted with sample collection, flow cytometry and cytokine measurement. Viktoria Serkis collected VCAM-1 and ICAM-1 immunofluorescence data and some coronary artery atherosclerosis data under the supervision of Mark Fuller. Dina Abutouk initiated the project and contributed to collection of some of the atherosclerosis data from HFCC fed animals. Melissa MacDonald assisted with animal care and sample collection. Neel Dhingani analyzed atherosclerosis, myocardial fibrosis and plasma lipids in normal chow-fed animals in the supplementary data under the supervision of Mark Fuller. Joseph Macri and Suleiman Igdoura contributed intellectually.

Note that SR-B1 is referred to as SR-BI in this chapter; this is because at the time of publication, SR-BI was the accepted nomenclature.

3.1 Abstract

Objective – Deficiency of the HDL receptor, SR-BI, in apolipoprotein E knockout or hypomorphic mice respectively results in spontaneous or diet-inducible occlusive coronary artery atherosclerosis, myocardial infarction, and early death. Here, we examine effects of SR-BI deficiency on cardiovascular phenotypes in LDLR knockout mice fed different atherogenic diets.

Approach and Results – SR-BI/LDLR double knockout and control LDLR knockout mice were fed atherogenic diets containing different amounts of fat, cholesterol and sodium cholate. Double knockout mice fed atherogenic diets high in cholesterol exhibited significantly reduced survival compared to LDLR knockout mice fed the same diets. In addition to increased diet accelerated aortic sinus atherosclerosis, we observed significant diet induced coronary artery atherosclerosis in double knockout mice, and diet dependent accumulation of platelets in coronary artery atherosclerotic plaques. This was accompanied by substantial myocardial fibrosis in double knockout mice fed high cholesterol diets. Atherogenic diet fed double knockout mice also exhibited higher circulating cytokine levels, monocytosis with increased proportions of Ly6Chi and Ly6Cint monocytes, and higher adhesion molecule expression in coronary artery endothelial cells compared to control LDLR knockout mice.

Conclusions – Diet accelerated atherosclerosis and occlusive, platelet rich coronary artery disease in SR-BI/LDLR dKO mice is affected by amounts of cholesterol and cholate in atherogenic diets, and is accompanied by increased expression of VCAM-1 and ICAM-1 in coronary arteries and increased Ly6Chi and Ly6Cint monocytes in circulation. The increased VCAM-1 and ICAM-1 in coronary artery endothelial cells in SR-BI-deficient mice likely explains their increased susceptibility to atherosclerosis in coronary arteries.

3.2 Introduction

Atherosclerosis is a chronic inflammatory disease driven by complex interactions between circulating lipoproteins, immune cells and the cells of the artery wall¹. Atherosclerotic coronary artery disease is a leading cause of death worldwide, and hypercholesterolemia is a major risk factor¹. High levels of cholesterol circulating in low and very low density lipoproteins (VLDL and LDL, respectively) are major risk factors for atherosclerosis, whereas high levels of high density lipoproteins (HDL) are considered to be atheroprotective². Traditional murine models of atherosclerosis are genetically predisposed to hypercholesterolemia and include the apolipoprotein E (apoE) knockout (KO) mouse^{3, 4}, and the fat fed LDL receptor (LDLR) KO mouse^{5, 6}. The aortic sinus, the lesser curvature of the aortic arch, and other regions of large arteries where blood flow is non-laminar are robustly susceptible to the development of atherosclerotic plaques in these mouse models⁷. However, coronary arteries, the arteries that supply blood to the

heart, remain largely resistant to atherosclerosis⁷. These mice therefore do not present with many of the clinical complications of atherosclerosis experienced by human CAD patients, including myocardial infarction and early death.

The HDL receptor, scavenger receptor class B type I (SR-BI), is expressed on the surface of multiple cell types and has been shown to mediate both HDL dependent atheroprotective signalling^{8,9}, and selective lipid transfer between HDL and cells, which is critical for functional reverse cholesterol transport, the major avenue for cholesterol removal from peripheral tissues^{8,10}. Deficiency of SR-BI not only accelerates atherosclerosis in the aortic sinus of apoE KO mice¹¹, but also renders these mice susceptible to spontaneous occlusive coronary artery (CA) atherosclerosis, myocardial infarction and ultimately early death¹². A related model, the SR-BI KO/apoE hypomorphic mouse, develops a similar phenotype when fed high fat, high cholesterol diets^{13,14}. We have previously shown that SR-BI deficiency increases atherosclerosis in the aortas of LDLR KO mice fed a high fat western type diet, however, reduced survival was not observed in these mice and CA atherosclerosis was not assessed¹⁵.

In the current study, we tested the effects of feeding SR-BI/LDLR double KO (dKO) mice four different atherogenic diets with varying concentrations of fat, cholesterol and sodium cholate. We found that dKO mice developed extensive occlusive CA atherosclerosis when fed any of the four diets that we tested; while CA's from control LDLR KO mice fed the same diets were virtually free of plaque.

This was accompanied by robust myocardial infarction and reduced survival in dKO mice fed diets with very high cholesterol content, but not in mice fed the high fat, low cholesterol western type diet. The severity of the survival phenotype appeared to correlate with the abundance of CA plaques that showed evidence of platelet accumulation. We also show that dKO mice exhibit monocytosis and increased diet-induced systemic inflammation compared to LDLR KO control mice, likely contributing to the increased overall atherosclerosis in dKO mice. Finally, we demonstrate that CA endothelium in atherogenic diet fed dKO mice express higher levels of VCAM-1 and ICAM-1 than that of control LDLR KO mice. This explains the relative susceptibility of SR-BI deficient mice to developing atherosclerosis in their CA's. The SR-BI/LDLR dKO mouse is therefore a novel model of diet-inducible CA atherothrombosis.

3.3 Results

3.3.1 Survival of SR-BI/LDLR dKO Mice Fed Different Atherogenic Diets

We studied the effects of four different atherogenic diets with varying levels of fat, cholesterol and sodium cholate on the progression of atherosclerosis in SR-BI/LDLR dKO and control LDLR KO mice. Mice were fed a high fat (HF) diet (Western type diet; 22% fat, 0.15% cholesterol), a high cholesterol (HC) diet (2% cholesterol), a high fat, high cholesterol (HFC) diet (15.8% fat, 1.25% cholesterol), or the same diet containing sodium cholate, (HFCC diet, commonly referred to as the Paigen diet)¹⁶. As controls, dKO and LDLR KO mice were also

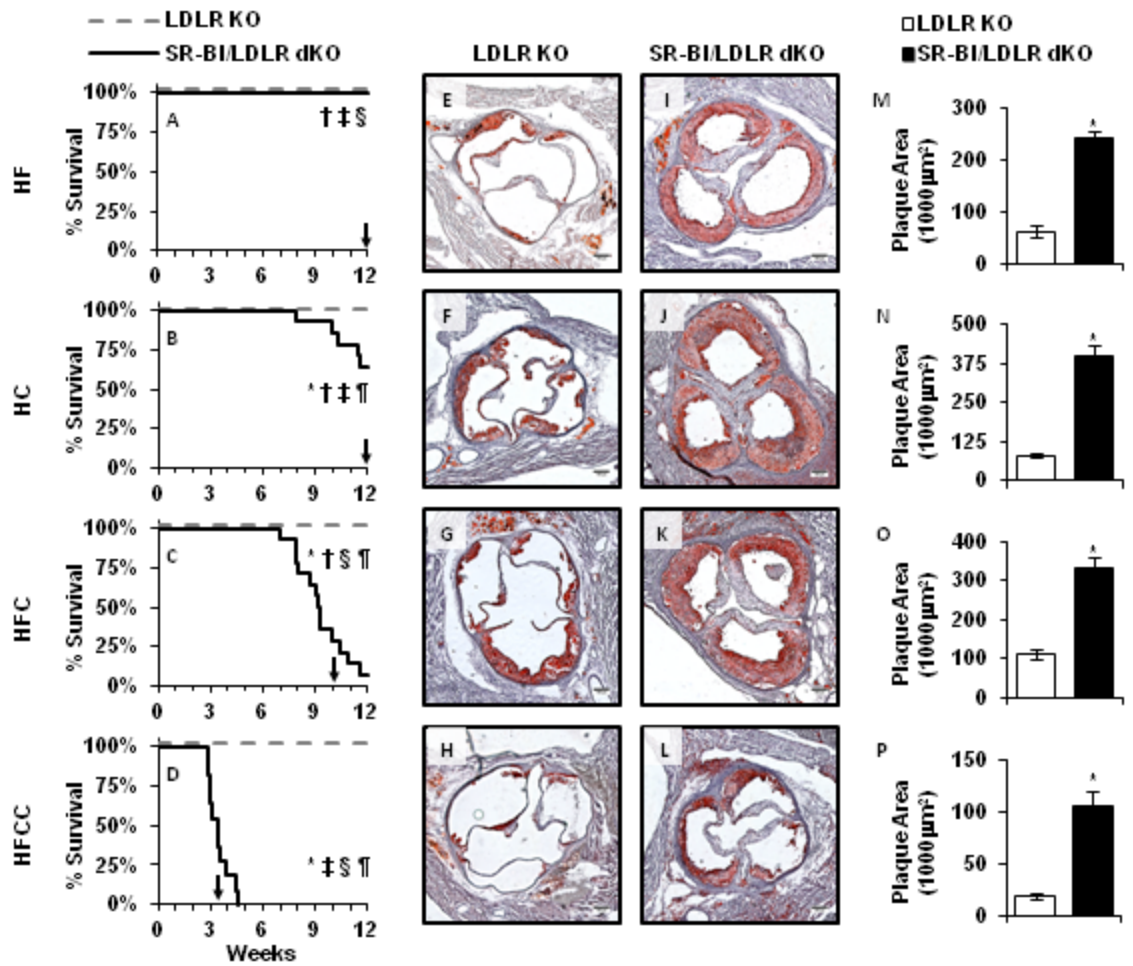
fed a normal chow diet. The dKO mice fed the HFCC, HFC and HC diets but not those fed the HF diet up to 12 weeks exhibited reduced survival compared to LDLR KO mice fed the same diets (Figure 3.1 A-D). Average survival for dKO mice fed the HFCC, HFC, and HC diets were 3.5, 9.4, and 11.4 weeks, respectively. No dKO mice fed the HFCC diet survived beyond 4.5 weeks of feeding, while ~7% of mice fed the HFC diet and ~64% mice fed the HC diet lived the full 12 weeks. Neither dKO mice nor LDLR KO control mice fed normal chow diets exhibited any reductions in survival during the course of our studies. These survival trends are similar to those reported by Nakagawa-Toyama et al. in SR-BI KO/apoE hypomorphic mice when fed the HFCC, HFC and HF diets¹⁴.

3.3.2 Atherosclerosis in the Aortic Sinus

Figure 3.1 (E-L) show images representing aortic sinus plaque burden in control LDLR KO mice (E-H) and dKO mice (I-L) fed each of the atherogenic diets. Aortic sinus plaque size was analyzed after 12 weeks of feeding the HF or HC diets, and at 10 weeks of feeding the HFC diet or 3.5 weeks of feeding the HFCC diet. These times were chosen to correspond to the length of time for ~50% survival of the dKO mice on the respective diets. Although longer feeding periods generally resulted in larger plaques, aortic sinus plaque area was dramatically and significantly increased in dKO mice fed any of the four diets that we tested compared to control LDLR KO mice fed the same diet for the same length of time (Figure 3.1 M-P). DKO mice fed a normal chow diet and age-matched to HF- and

HC-fed mice (22 weeks old) also developed substantially more atherosclerosis in their aortic sinuses than age matched LDLR KO mice (supplementary Figure 3.7 A-C). The extent of atherosclerosis in normal chow fed dKO mice was much less than similarly aged dKO mice that had been fed either the HF or HC diets for 12 weeks (compare supplementary Figure 3.7 B,C with Figure 3.1I,J and M,N), but was similar to the level of atherosclerosis in the aortic sinus of younger dKO mice that had been fed the HFCC diet for 3.5 weeks (Figure 3.1L,P).

Figure 3.1 – SR-BI/LDLR dKO mice exhibit diet dependent reduced survival and develop larger atherosclerotic plaques in their aortic sinuses compared to similarly treated LDLR KO control mice. Female SR-BI/LDLR dKO and control LDLR KO mice aged 10-12 weeks were fed atherogenic diets as indicated on the left and monitored until they reached cardiac endpoint for up to 12 weeks. (A-D) Kaplan Meier survival curves for SR-BI/LDLR dKO mice compared to control LDLR KO mice fed each diet. SR-BI/LDLR dKO mice were harvested and analyzed at cardiac endpoint or 12 weeks of feeding; the arrows indicate the feeding times for LDLR KO control mice used for all other comparisons. $P < 0.05$ by Kaplan Meier survival analysis versus: * Control LDLR KO mice fed the same diet, †HFCC fed dKO mice, ‡HFC fed dKO mice, §HC fed dKO mice, ¶HF fed dKO mice. (E-L) Representative oil red O stained cryosections of aortic sinuses from control LDLR KO (E-H) and SR-BI/LDLR dKO (I-L) mice fed different atherogenic diets for the time periods indicated in A-D. (M-P) Quantification of aortic sinus atherosclerosis in SR-BI/LDLR dKO and control LDLR KO mice fed the indicated diets for time periods shown in A. $*P < 10^{-4}$ by student's T-test between dKO and control mice.



3.3.3 *Atherosclerosis in CAs*

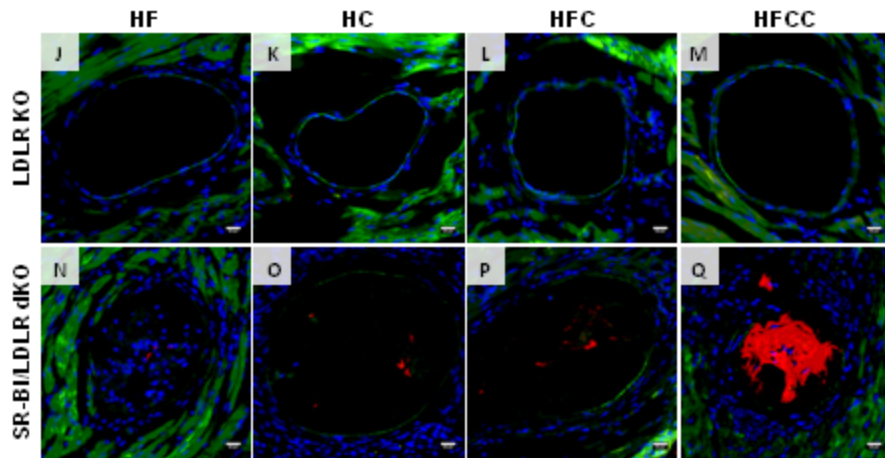
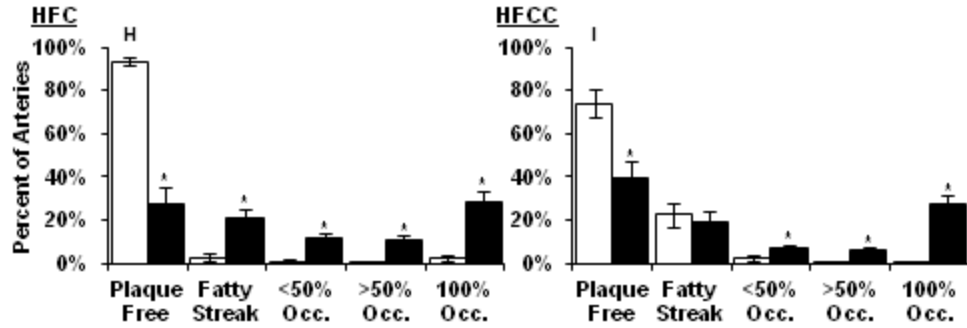
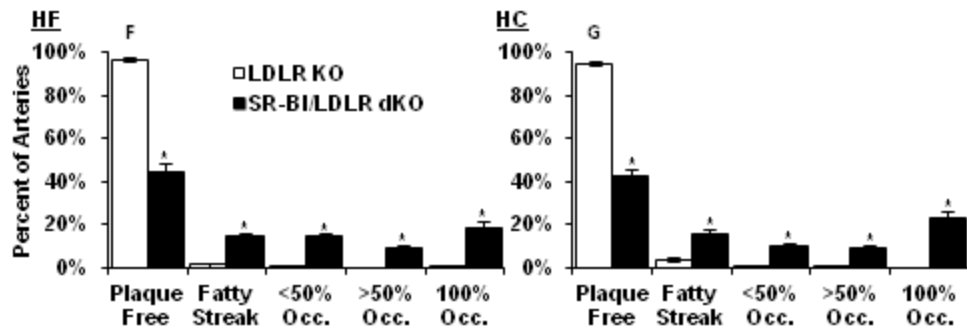
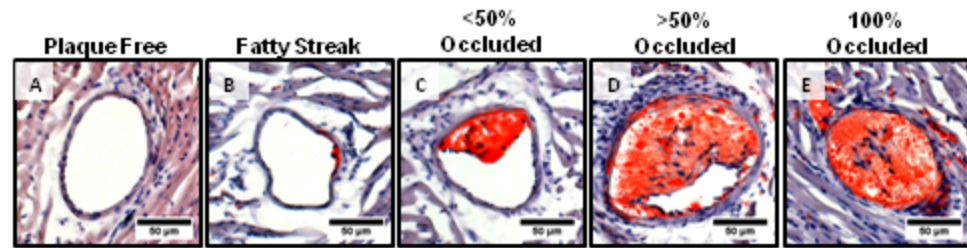
Coronary artery atherosclerosis was measured by scoring all CA's observed in at least 3 oil red O stained cross sections into 5 categories based on the level of occlusion. Representative images of CA's that were plaque free, which contained fatty streaks, or which were <50% occluded, >50% occluded and 100% occluded with raised atherosclerotic plaques are shown in Figure 3.2 (A-E). All SR-BI/LDLR dKO mice developed occlusive CA atherosclerosis when fed any of the four atherogenic diets (Figure 3.2 F-I). SR-BI/LDLR dKO mice had significantly greater proportions of CA's with all categories of atherosclerotic plaques, and correspondingly, significantly smaller proportions of CA's that were plaque free compared to control LDLR KO mice fed the same diets for similar time periods. In fact, more than 95% of CA's observed in all LDLR KO control groups, regardless of atherogenic diet, were either plaque free or contained only fatty streaks. In contrast less than 60% of CA's in from SR-BI/LDLR dKO mice were either plaque free or contained only fatty streaks, regardless of the atherogenic diet.

SR-BI/LDLR dKO mice fed the HF diet for 12 weeks exhibited the lowest proportion of completely occluded CA's (18%), whereas the SR-BI/LDLR dKO mice fed the HC diet (12 weeks), HFC diet (10 weeks) or HFCC diets (3.5 weeks) had similarly high proportions with approx. 30% of CA's completely occluded. Interestingly, the CA atherosclerosis burden did not appear to correlate directly with the atherosclerotic plaque sizes in the aortic sinus in SR-BI/LDLR dKO mice fed the four atherogenic diets. In particular, dKO mice fed the HFCC diet for 3.5

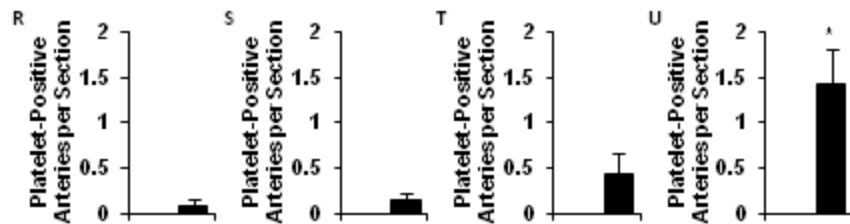
weeks had the lowest burden of aortic sinus atherosclerosis (Figure 3.1 P) but among the highest burden of CA atherosclerosis (Figure 3.2 I). In contrast, chow-fed dKO mice developed comparatively little coronary artery atherosclerosis by 22 weeks of age (supplementary Figure 3.7 E).

An important feature of human coronary heart disease is acute thrombosis on top of atherosclerotic plaques in CA's. We therefore looked for molecular evidence of thrombosis in dKO mice fed atherogenic diets. Thrombosis was detected in cryosections of CA's by immunofluorescence for CD41, a surface protein expressed by platelets. Figure 3.2 J-Q show representative images of CD41 stained (red) CA's in mice fed each of the four diets. No CA's from LDLR KO mice stained positively for platelets, consistent with the general absence of atherosclerotic plaques. On the other hand, platelet CD41 was detected in CA plaques from dKO mice fed each of the 4 atherogenic diets (Figure 3.2 R-U). Interestingly both the abundance of platelet staining (Figure 3.2 N-Q) and the number of CA's per section that stained positively for platelet CD41 (Figure 3.2 R-U) were substantially higher in the SR-BI/LDLR dKO mice fed the HFCC diet than for those fed the other atherogenic diets.

Figure 3.2 – SR-BI/LDLR dKO mice develop occlusive CA atherosclerosis with evidence of platelet accumulation. CA's in heart cryosections from SR-BI/LDLR dKO and control LDLR KO mice fed the indicated atherogenic diets were stained with oil red O and all observed arteries were scored as either plaque free, fatty streak, <50% occluded, >50% occluded, or 100% occluded. (A-E) Representative images of arteries for each category are shown. (F-I) Quantification of CA's in each category in heart sections from SR-BI/LDLR dKO and control LDLR KO mice fed the indicated diet. * $P < 0.01$ determined by student's T-test. (J-Q) Representative images of CA's from LDLR KO (J-M) and SR-BI/LDLR dKO (N-Q) mice fed each of the four diets, stained for platelet CD41 (red), and nuclei (blue DAPI staining). Autofluorescence of the artery wall appears green. (R-U) Graphs representing the numbers of platelet positive arteries per section. $P < 0.001$ for SR-BI/LDLR dKO vs control LDLR KO determined by 2 way ANOVA. † $P < 0.01$ v HFC-, HC- and HF-fed dKO mice determined by Holm-Sidak post hoc analysis.



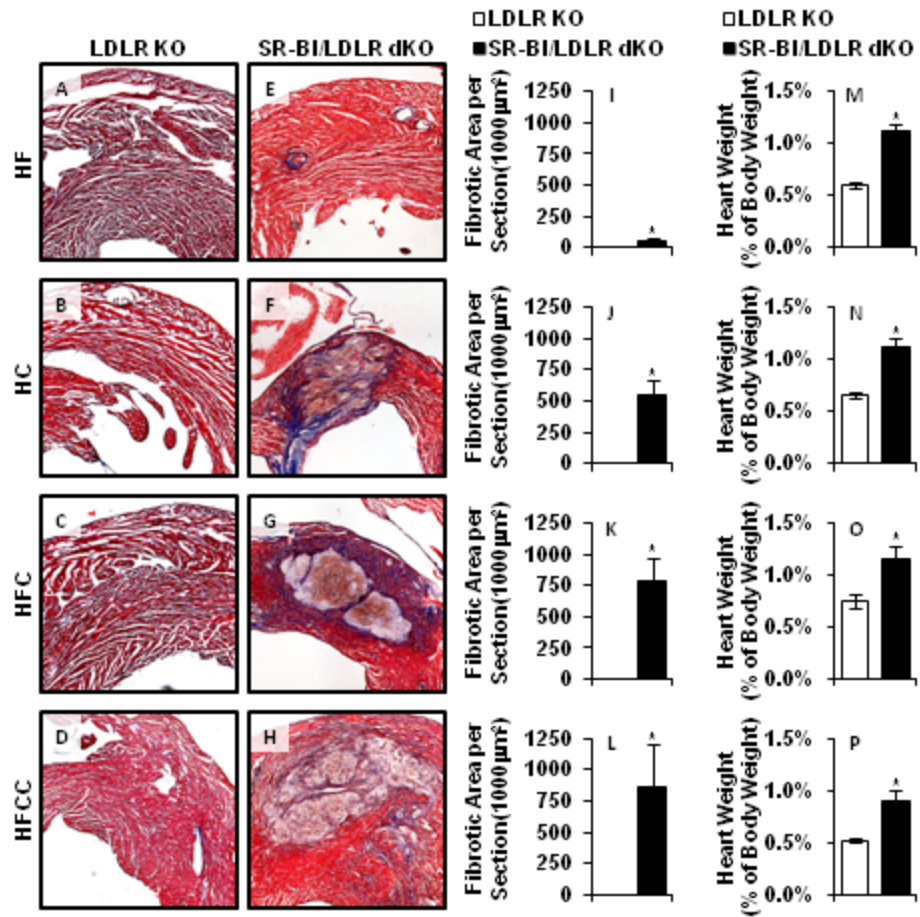
□ LDLR KO
 ■ SR-BI/LDLR dKO



3.3.4 Myocardial Infarction

Frozen cross sections of myocardial tissue were stained with Masson's Trichrome in order to detect collagen rich-fibrotic areas. Representative images are shown in Figure 3.3 A-H. SR-BI/LDLR dKO mice fed the HFCC, HFC, and HC diets had similar levels of myocardial fibrosis, which were substantially and significantly higher than levels observed in HF fed dKO mice (Figure 3.3 I-L). No fibrosis was detected in any LDLR KO control mice regardless of diet (Figure 3.3 I-L), or in dKO mice fed a normal chow diet up to 22 weeks of age (supplementary Figure 3.7 F,G). Similarly, we observed no differences in heart:body weights between dKO and LDLR KO mice fed the normal chow diets. Heart:body weight ratios were significantly increased to a similar extent in all atherogenic diet fed dKO groups compared to LDLR KO control mice fed the same diets for similar periods of time (Figure 3.3 M-P), suggesting that increased heart size is likely not a direct response to myocardial fibrosis.

Figure 3.3 – Large myocardial infarctions are observed in SR-BI/LDLR dKO mice fed diets that are very high in cholesterol. (A-H) Representative images of heart cryosections from SR-BI/LDLR dKO and control LDLR KO mice fed the indicated atherogenic diets stained with Masson's Trichrome. (I-L) Quantification of average infarct size in control LDLR KO and SR-BI LDLR dKO mice fed each of the diets. (M-P) Heart weights normalized to body weights for each group of mice.*P<0.05 by student's T-test.



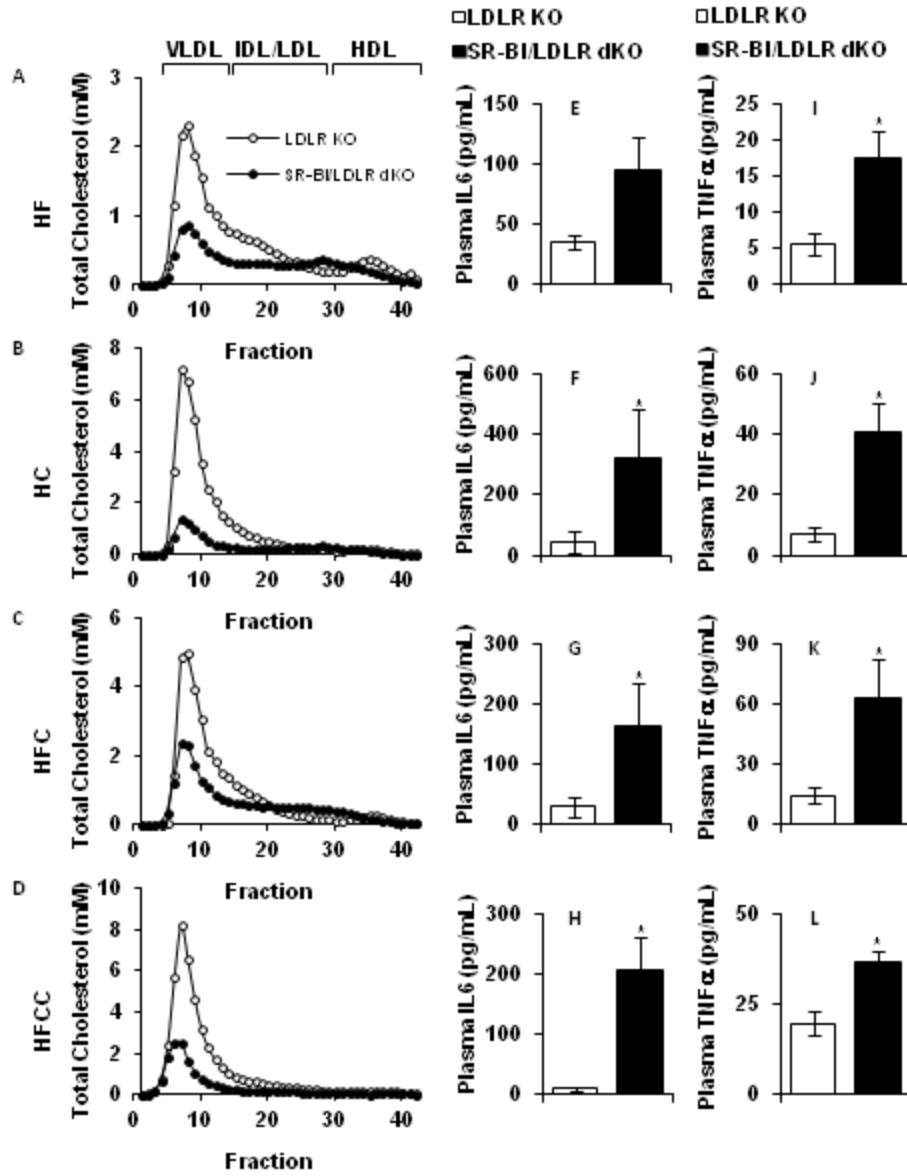
3.3.5 Plasma Lipoproteins and Cytokines

To investigate potential mechanisms underlying the increased susceptibility to atherosclerosis in the aortic sinus and CA's observed in dKO mice compared to control LDLR KO mice, we analyzed plasma lipid levels and lipoprotein cholesterol profiles from mice fed the four atherogenic diets and the normal chow diet. Consistent with previous reports¹⁵ plasma total cholesterol was 1.5 fold higher in the chow fed dKO than the chow fed LDLR KO mice (supplementary table 3.1), mainly due to increased cholesterol associated with enlarged HDL particles (supplementary Figure 3.7 D). As expected, plasma total cholesterol levels were substantially elevated in both dKO and in LDLR sKO mice when they were fed each of the four atherogenic diets (supplementary table 3.1). Consistent with our previous findings¹⁵, dKO mice fed atherogenic diets consistently had lower plasma total cholesterol levels than LDLR single KO mice fed the same diet (supplementary table 3.1). This appeared to be the result of lower total cholesterol associated with VLDL and LDL sized lipoproteins in the atherogenic diet fed dKO mouse plasma compared to plasma from LDLR KO control mice across all four atherogenic diets tested (Figure 3.4 A-D), indicating that plasma VLDL and LDL cholesterol levels are likely not responsible for the increased atherosclerosis observed in SR-BI/LDLR dKO mice. Lower steady state VLDL and LDL total cholesterol levels in atherogenic diet fed dKO compared to LDLR KO mice may be explained the lower rates of hepatic VLDL synthesis and triglyceride secretion, measured using standard methodologies in either HFCC or

HF fed dKO or LDLR KO mice that had been fasted and treated with either tyloxapol or poloxamer¹⁷ (supplementary Figure 3.8). This is consistent with our previous reports of reduced plasma apoB levels in HF fed SR-BI/LDLR dKO mice and in chow fed SR-BI/apoE dKO mice^{11, 15}. Despite the reduced levels of plasma total cholesterol in atherogenic diet fed dKO mice, we observed elevated levels of plasma free cholesterol in the dKO compared to the LDLR KO mice fed the control diet and each of the four atherogenic diets, such that the ratios of free:total cholesterol ratios were consistently 2-3 fold higher in the normal chow and atherogenic diet fed dKO mice than the LDLR KO controls. This is consistent with increased FC levels that have been described previously in SR-BI deficient mice^{13, 18, 19}.

Since inflammation is also a major driver of atherosclerosis, we measured IL-6 and TNF α in plasma from these mice. IL-6 and TNF α were undetectable in LDLR KO or dKO mice fed normal chow up to 22 weeks of age (data not shown). Each of the four atherogenic diets resulted in significantly increased levels of both IL-6 (Figure 3.4 E-H) and TNF α (Figure 3.4 I-L) in both the LDLR KO and the dKO mice, however plasma levels of each cytokine were consistently higher in dKO than in LDLR KO mice fed the same diet. We also noted that plasma levels of IL-6 and TNF α were higher in dKO mice fed the HFCC, HFC and HC diets compared to dKO mice fed the HF diet suggesting that they may have been influenced by dietary cholesterol and/or cholate.

Figure 3.4 – SR-BI/LDLR dKO mice fed atherogenic diets have lower plasma cholesterol levels but higher levels of circulating inflammatory cytokines than LDLR KO mice fed the same diets for the same length of time. (A-D) Plasma lipoprotein cholesterol profiles for SR-BI/LDLR dKO and control LDLR KO mice fed the indicated atherogenic diets were generated by size exclusion chromatography of plasma followed by cholesterol assay of the resulting fractions. Representative profiles derived from pooled plasma from 3 mice per group are shown. Levels of circulating IL-6 (D-H) and TNF- α (I-L) in plasma were measured by ELISA in SR-BI/LDLR dKO and control LDLR KO mice fed each of the atherogenic diets. dKO mice had significantly higher levels of both IL-6 and TNF- α than control LDLR KO mice, $P < 0.001$ by two way ANOVA for both markers. * $P < 0.05$ vs LDLR KO by Holm-Sidak post hoc test.



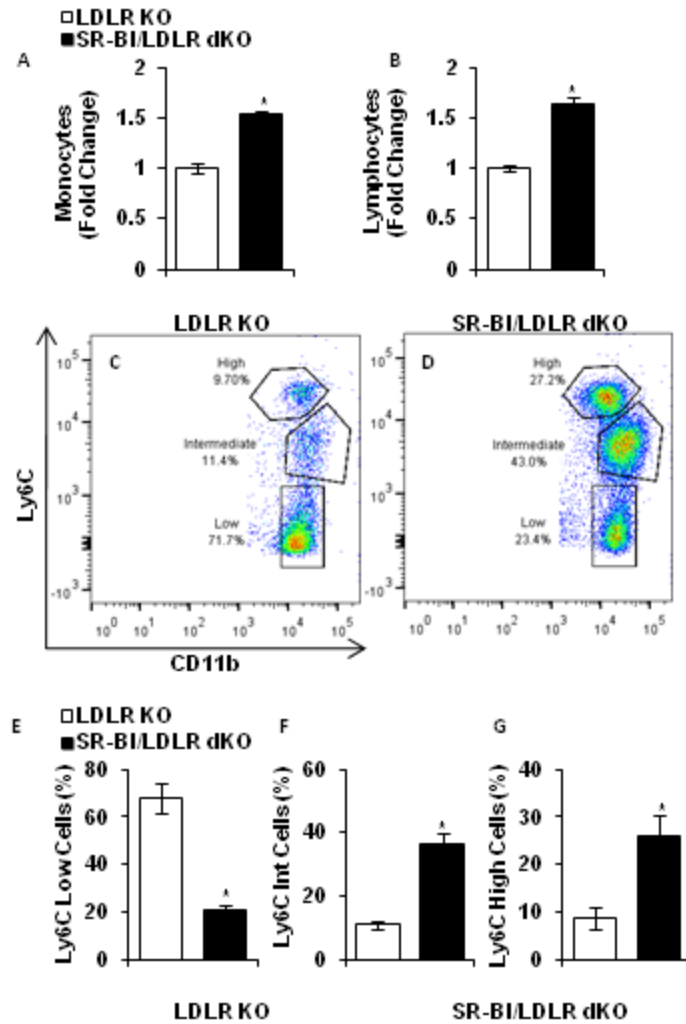
3.3.6 Blood Cells

Since immune cells are major components of atherosclerotic plaques, and can also influence levels of inflammatory cytokines in the plasma, we ran hematology profiles, including monocyte and lymphocyte counts, on the blood of HFCC fed mice. Circulating monocytes and lymphocytes were both significantly elevated in dKO mice compared to control LDLR KO mice fed either normal chow (supplementary Figure 3.7 H,I) or after 2 weeks of HFCC feeding (Figure 3.5 A,B). Monocytes (CD11b and CD115 double-positive cells) were analyzed for Ly6C expression using flow cytometry. Three distinct populations of monocytes were identified (Figure 3.5 C-D): Ly6C^{hi}, Ly6C^{lo} and a population that expressed intermediate levels of Ly6C (Ly6C^{int}). HFCC-fed dKO mice had significantly higher proportions of Ly6C^{hi} and Ly6C^{int} monocytes and concomitantly lower proportions of Ly6C^{lo} monocytes than did HFCC fed LDLR KO controls (Figure 3.5 E-G). No differences in the proportions of Ly6C^{hi}, Ly6C^{int} and Ly6C^{lo} monocytes were observed between LDLR KO and dKO mice fed normal chow (supplementary Figure 3.7 J-L). DKO mice also exhibited substantially and significantly larger spleens than control LDLR KO mice which were further increased in size upon atherogenic diet feeding (supplementary table 3.2). HFCC diet fed dKO mice also exhibited significantly fewer red blood cells, accompanied by lower hematocrits and a higher mean cell volume compared to control LDLR KO mice fed the same diet (supplementary table 3.3), consistent with published findings in high cholesterol fed SR-BI KO mice and in SR-BI/apoE dKO mice²⁰.

No significant differences in platelet numbers were observed between the two groups of mice (supplementary table 3.3).

Figure 3.5 – SR-BI/LDLR dKO mice exhibit increased circulating monocyte and lymphocyte numbers and proportionally larger populations of Ly6Chi monocytes compared to control LDLR KO mice when fed the HFCC diet.

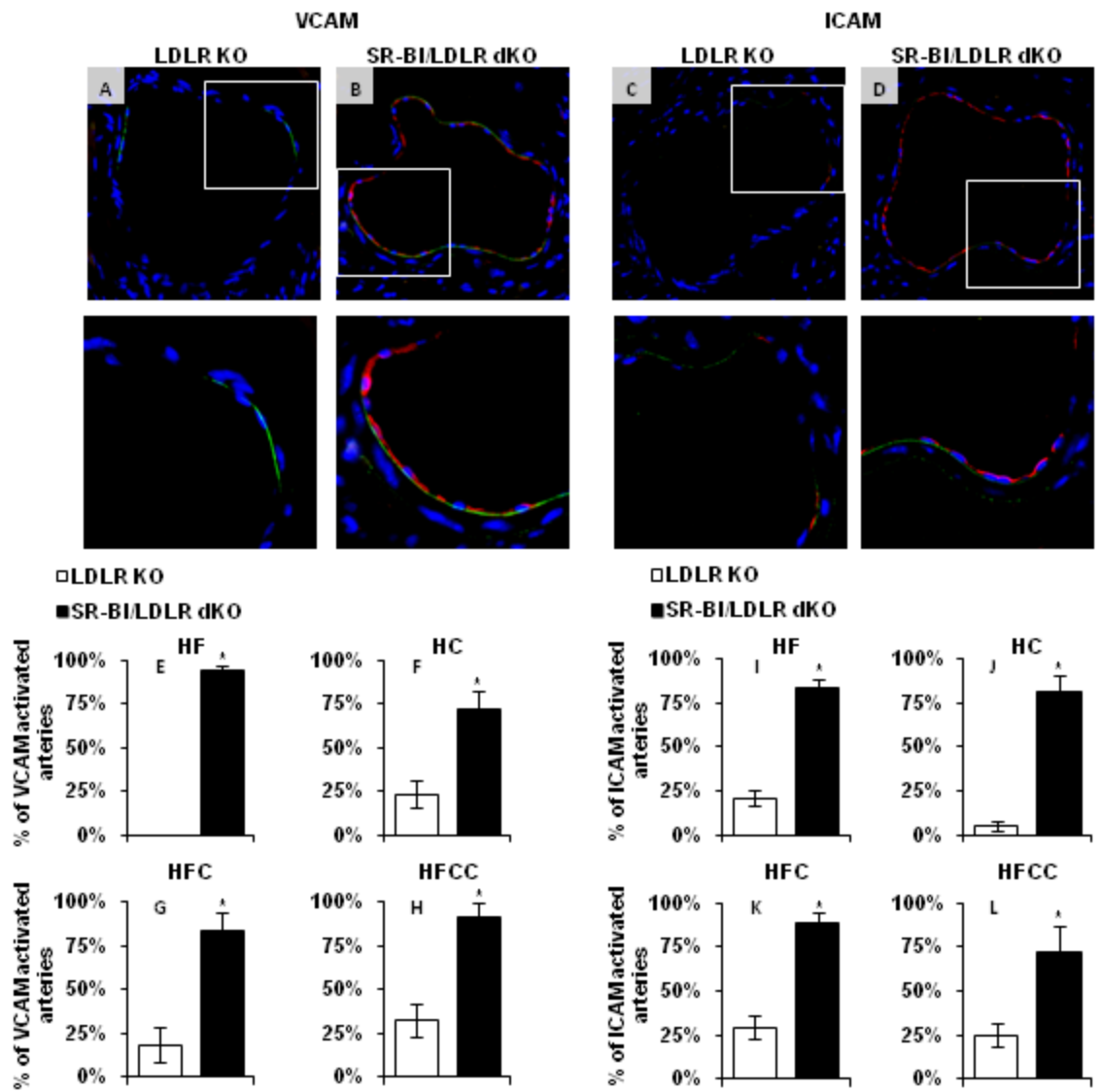
Blood was collected from the tail vein of SR-BI/LDLR dKO and control LDLR KO mice fed the HFCC diet for 2 weeks. Monocytes (A) and Lymphocytes (B) were counted using a Hemavet Multi-Species Hematology System. (C) Ly6C was detected on monocytes (CD11b+ CD145+) by flow cytometry and proportions of Ly6Chi(E), Ly6Cint(F) and Ly6Clo(G) monocytes were measured using FloJo software. *P<0.05 vs LDLR KO mice fed the same diet by Student's T-test.



3.3.7 CA Endothelial Cell Activation

To further investigate the robust susceptibility of SR-BI/LDLR dKO mice to CA atherosclerosis, we investigated the expression of VCAM-1 and ICAM-1 in the CA's of both control LDLR KO and dKO by immunofluorescence. Figure 3.6 A-D depict representative images of VCAM-1 (A-B) and ICAM-1 (C-D) staining in non-atherosclerotic CA's from HFCC fed LDLR KO and dKO mice. Quantification of VCAM-1 and ICAM-1 immunostaining in non atherosclerotic CA's from mice fed each of the four atherogenic diets revealed that atherogenic diet fed dKO mice had significantly greater proportions of non-atherosclerotic CA's exhibiting immunodetectable VCAM-1 (Figure 3.6 E-H) and ICAM-1 (Figure 3.6 I-L) compared to control LDLR KO mice fed the same diets for similar times. In contrast, no differences were seen in VCAM-1 or ICAM-1 levels in LDLR KO mice fed either the atherogenic diets or fed a normal diet up to 22 weeks of age, and no differences were seen between the chow fed 22 week old dKO and LDLR KO mice (supplementary Figure 3.7 M-R). These data demonstrate that each of the 4 atherogenic diets tested induces significant VCAM-1 and ICAM-1 expression in non-atherosclerotic CA's only in the dKO mice.

Figure 3.6 – Larger proportions of CA's stain positively for endothelial activation markers VCAM-1 and ICAM-1 in SR-BI/LDLR dKO mice compared to control LDLR KO mice fed each of the atherogenic diets. VCAM-1 and ICAM-1 expression in CA's was detected by immunofluorescence in cryosections. A-D show images of CA's stained for VCAM-1 (A-B) or ICAM-1 (C-D), represented in red, from HFCC fed LDLR KO (A,C) and SR-BI/LDLR dKO (B,D) mice. Autofluorescence of the artery wall is shown in green, DAPI counterstained nuclei are shown in blue. VCAM-1- and ICAM-1-activated CA's, as defined in the materials and methods, were counted and expressed as a proportion of the total arteries counted (E-L). Overall, $P < 0.001$ for dKO vs LDLR KO for both markers by two way ANOVA. * $P < 0.05$ by Holm-Sidak post hoc test.



3.4 Discussion

In this study, we demonstrated that SR-BI/LDLR dKO mice develop diet accelerated occlusive coronary artery atherosclerosis and myocardial infarction, in which the severity of the disease can be modulated by altering different components of the diet. We have previously shown that dKO mice develop increased aortic atherosclerosis compared to control LDLR KO mice when fed a HF diet, however, there was no difference in survival and the study did not examine atherosclerosis in CA's¹⁵. Consistent with our previous findings, dKO mice fed the HF diet for 12 weeks did not exhibit reduced survival but had significantly increased aortic sinus atherosclerosis compared to LDLR KO controls (Figure 3.1). Occlusive CA atherosclerosis was observed in these mice (Figure 3.2), however, only small myocardial infarctions were detected (Figure 3.3). In contrast, higher levels of occlusive CA atherosclerosis developed in dKO mice fed diets much higher in cholesterol (Figure 3.2). This was accompanied by large myocardial infarctions (Figure 3.3) and significantly reduced survival (Figure 3.1) compared to similarly fed LDLR KO mice. Control LDLR KO mice fed any of the four atherogenic diets that we tested developed virtually no CAD up to 12 weeks of feeding. We also show that aggregated platelets are present in a subset of the occluded CA's in the dKO mice, and that platelet staining is most prominent in CA's of dKO mice fed the HFCC diet (Figure 3.2), which led to the most rapid development of myocardial infarction (Figure 3.3) and the earliest death of the dKO mice (Figure 3.1). These data suggest that the nature of the

atherogenic diet affects not only the extent and time course of development of CA atherosclerosis but also affects the severity of platelet accumulation within plaques, possibly reflecting plaque rupture and thrombosis.

Deficiency of SR-BI increases cholesterol associated with enlarged HDL particles in otherwise wild type mice and in LDLR KO mice fed normal chow (supplementary Figure 3.1 D)^{21, 22}, and in VLDL and IDL/LDL sized lipoproteins in apoE KO mice fed normal chow and apoE hypomorphic mice fed the HFCC diet^{11, 13}. In contrast, SR-BI/LDLR dKO mice have lower cholesterol levels associated with VLDL- and LDL-sized lipoproteins compared to LDLR KO mice on all four of the atherogenic diets. This is consistent with our previous reports of reduced cholesterol associated with VLDL-sized lipoproteins and reduced plasma apoB in SR-BI/LDLR dKO mice compared to LDLR KO mice when both were fed the HF diet¹⁵, and with the reduced apoB levels observed in SR-BI/apoE dKO mice compared to apoE single KO controls¹¹. In the high fat and/or high cholesterol fed SR-BI/LDLR dKO mice, this appears to be a consequence of reduced VLDL production as compared to similarly fed LDLR KO control mice (supplementary Figure 3.8). The mechanism of reduced VLDL production in dKO mice is not clear, however, SR-BI over-expression has been shown to enhanced apoB trafficking and apoB secretion²³ in Caco-2 cells, while loss of SR-BI function and knockdown of SR-BI²³ blunts apoB trafficking and secretion respectively. SR-BI may have an equivalent role in hepatocytes. A similar reduction in VLDL levels has also been reported in LDLR KO mice that

lack apolipoprotein A1²⁴, the major apolipoprotein of HDL. Additionally, apolipoprotein A1 deficiency has been linked with reduced hepatic VLDL production in mice²⁵, suggesting that interaction between SR-BI and its major ligand may be responsible for influencing the production of VLDL; further experiments are required to confirm this. It is possible this effect of a lack SR-BI on VLDL production is an anti-atherogenic effect that is masked by more severe pro-atherogenic forces, yet it is also possible that this represents a consequence of a fundamental disruption in VLDL metabolism, resulting in promotion of atherosclerosis. Nevertheless, in this context, increased atherosclerosis is associated with lower overall and VLDL cholesterol levels, and this observation suggests that the susceptibility of SR-BI/LDLR dKO mice to CAD cannot be explained by exacerbated hypercholesterolemia, although the disproportionately large ratio of free cholesterol to total cholesterol (supplementary table 3.7) indicates there is likely a major effect on lipoprotein composition which could, in turn, affect CAD susceptibility. The influence of a lack of SR-BI on the composition and function of different lipoproteins in these mice requires further investigation.

There is mounting evidence that SR-BI may play an atheroprotective role in immune cells. Bone marrow specific deficiency of SR-BI in both apoE KO and LDLR KO mice increases atherosclerosis in the aorta^{15, 26, 27} Conversely, we have recently shown that restoring SR-BI expression in the bone marrow of SR-BI KO/apoE hypomorphic mice reduces diet induced occlusive CA

atherosclerosis, while others have shown that transplanting SR-BI/apoE dKO mice with wild type bone marrow has a similar effect^{28, 29}. SR-BI in macrophages reduces the inflammatory response to lipopolysaccharide treatment *in vitro*³⁰, and SR-BI deficiency is associated with higher serum cytokine levels in naïve, septic and lipopolysaccharide challenged mice³¹⁻³³. Results from the current study show that SR-BI/LDLR dKO mice challenged with atherogenic diets have increased levels of both IL-6 and TNF α in plasma, accompanied by increased numbers of both monocytes and lymphocytes in blood compared to LDLR KO mice fed the same diets. We have previously demonstrated that monocyte recruitment into atherosclerotic plaques is attenuated by restoration of SR-BI expression in the bone marrow of SR-BI KO/apoE hypomorphic mice, and that SR-BI deficient monocytes bind VCAM-1 and ICAM-1 more readily than SR-BI expressing monocytes²⁹. Monocytes can be divided into subsets based on their level of Ly6C expression. Ly6C^{hi} monocytes are considered to be more inflammatory, adhere more efficiently to activated endothelium, migrate more efficiently into established atherosclerotic plaques and selectively accumulate in atherosclerotic plaques compared to Ly6C^{lo} monocytes^{34, 35}. We observed a large shift in the monocyte populations with HFCC diet fed dKO mice exhibiting significantly higher proportions of Ly6C^{hi} and Ly6C^{int} monocytes and correspondingly lower proportions Ly6C^{lo} monocytes compared to LDLR KO control mice fed similar diets.

While increased inflammation and altered lipoprotein metabolism may explain an increase in susceptibility to atherosclerosis in general, the robust dichotomy between the SR-BI/LDLR dKO mice and the LDLR KO controls in terms of CA atherosclerosis suggests that SR-BI may influence the susceptibility of the vessels themselves. A major factor that dictates the regions of the vascular system that are prone to atherosclerosis is the activation of endothelial cells³⁶. Endothelial cells from arterial regions that experience laminar flow conditions express very low levels of VCAM-1 and ICAM-1 and these arteries tend to be resistant to atherosclerosis^{37, 38}. Alternatively, endothelial cells from arterial regions that experience non-laminar blood flow and low shear stress exhibit reduced eNOS expression and activation³⁹, and increased expression of adhesion molecules VCAM-1 and ICAM-1^{37, 38}. This provides favourable sites for monocyte adhesion and initiation of atherosclerosis³⁶. SR-BI mediates HDL induced up-regulation and activation of eNOS in vivo and concomitant suppression of VCAM-1 and ICAM-1 expression by endothelial cells in vitro⁴⁰⁻⁴². Our results provide in vivo evidence that endothelial cells in non-atherosclerotic CAs of dKO mice fed atherogenic diets express more VCAM-1 and ICAM-1 than CA endothelial cells in LDLR KO control mice. This may at least in part explain why SR-BI deficiency in LDLR KO mice gives rise to diet induced CA atherosclerosis, while LDLR single KO mice appear to be largely resistant. A limitation of study is that it is difficult to determine if the Ly6C^{hi} monocytosis, inflammation and up-regulated VCAM-1 and ICAM-1 expression in coronary

artery endothelial cells precede development of CAD, or if they are consequences of enhanced lesion development. Further investigation will be required to conclude that these are causative factors of CAD in these mice.

In summary, SR-BI/LDLR dKO mice are a robust and flexible mouse model of diet accelerated occlusive CA atherothrombosis and myocardial infarction which could prove to be a useful tool in understanding the mechanisms of and exploring new treatments for human coronary heart disease. We believe that mouse CAD resulting from SR-BI deficiency is a multi-factorial phenomenon that may be influenced by a lack of SR-BI function in multiple cell types including hepatocytes, immune cells and endothelial cells. In particular the increased expression of endothelial cell adhesion molecules in CA's, together with the increased proportions of circulating Ly6C^{hi} monocytes may conspire to trigger diet induced occlusive CA atherosclerosis in these mice, which, depending on the atherogenic diet employed, leads to substantial platelet accumulation in occluded CA's, myocardial infarction and early death. The importance of specific protective roles of SR-BI in each of these cell types and characterization of the molecular pathways involved requires further investigation and may lead to the identification of new therapeutic targets in the treatments of cardiovascular diseases.

- a) Acknowledgements: We thank Michael Kim for technical assistance and Robin Roberts for advice on statistical analyses.

- b) Sources of Funding: This research was supported by a grant (MOP74765) to BLT, and in part from a Team Grant in Thromboembolism (FRN-79846) from the Canadian Institutes of Health Research and a Program Grant (PRG 6502) from the Heart and Stroke Foundation of Ontario. MF was supported by graduate scholarships from the Heart and Stroke Foundation of Ontario and the Canadian Institutes of Health Research. OD was the recipient of an International Excellence graduate scholarship from McMaster University. DA was the recipient of a Natural Sciences and Engineering Research Council undergraduate student research award.
- c) Disclosures: None.

3.5 References

1. Libby P. Inflammation in atherosclerosis. *Nature*. 2002;420:868-874.
2. Libby P, Aikawa M, Schonbeck U. Cholesterol and atherosclerosis. *Biochim Biophys Acta*. 2000;1529:299-309.
3. Zhang SH, Reddick RL, Piedrahita JA, Maeda N. Spontaneous hypercholesterolemia and arterial lesions in mice lacking apolipoprotein E. *Science*. 1992;258:468-471.
4. Plump AS, Smith JD, Hayek T, Aalto-Setälä K, Walsh A, Verstuyft JG, Rubin EM, Breslow JL. Severe hypercholesterolemia and atherosclerosis in apolipoprotein E-deficient mice created by homologous recombination in ES cells. *Cell*. 1992;71:343-353.

5. Ishibashi S, Brown MS, Goldstein JL, Gerard RD, Hammer RE, Herz J. Hypercholesterolemia in low density lipoprotein receptor knockout mice and its reversal by adenovirus-mediated gene delivery. *J Clin Invest.* 1993;92:883-893.
6. Ishibashi S, Goldstein JL, Brown MS, Herz J, Burns DK. Massive xanthomatosis and atherosclerosis in cholesterol-fed low density lipoprotein receptor-negative mice. *J Clin Invest.* 1994;93:1885-1893.
7. VanderLaan PA, Reardon CA, Getz GS. Site specificity of atherosclerosis: site-selective responses to atherosclerotic modulators. *Arterioscler Thromb Vasc Biol.* 2004;24:12-22.
8. Al-Jarallah A, Trigatti BL. A role for the scavenger receptor, class B type I in high density lipoprotein dependent activation of cellular signaling pathways. *Biochim Biophys Acta*;1801:1239-1248.
9. Saddar S, Mineo C, Shaul PW. Signaling by the high-affinity HDL receptor scavenger receptor B type I. *Arterioscler Thromb Vasc Biol.* 2010;30:144-150.
10. Krieger M. Charting the fate of the "good cholesterol": identification and characterization of the high-density lipoprotein receptor SR-BI. *Annu Rev Biochem.* 1999;68:523-558.
11. Trigatti B, Rayburn H, Vinals M, Braun A, Miettinen H, Penman M, Hertz M, Schrenzel M, Amigo L, Rigotti A, Krieger M. Influence of the high

- density lipoprotein receptor SR-BI on reproductive and cardiovascular pathophysiology. *Proc Natl Acad Sci U S A*. 1999;96:9322-9327.
12. Braun A, Trigatti BL, Post MJ, Sato K, Simons M, Edelberg JM, Rosenberg RD, Schrenzel M, Krieger M. Loss of SR-BI expression leads to the early onset of occlusive atherosclerotic coronary artery disease, spontaneous myocardial infarctions, severe cardiac dysfunction, and premature death in apolipoprotein E-deficient mice. *Circ Res*. 2002;90:270-276.
 13. Zhang S, Picard MH, Vasile E, Zhu Y, Raffai RL, Weisgraber KH, Krieger M. Diet-induced occlusive coronary atherosclerosis, myocardial infarction, cardiac dysfunction, and premature death in scavenger receptor class B type I-deficient, hypomorphic apolipoprotein ER61 mice. *Circulation*. 2005;111:3457-3464.
 14. Nakagawa-Toyama Y, Zhang S, Krieger M. Dietary manipulation and social isolation alter disease progression in a murine model of coronary heart disease. *PLoS One*. 2012;7:e47965.
 15. Covey SD, Krieger M, Wang W, Penman M, Trigatti BL. Scavenger receptor class B type I-mediated protection against atherosclerosis in LDL receptor-negative mice involves its expression in bone marrow-derived cells. *Arterioscler Thromb Vasc Biol*. 2003;23:1589-1594.

16. Paigen B, Morrow A, Brandon C, Mitchell D, Holmes P. Variation in susceptibility to atherosclerosis among inbred strains of mice. *Atherosclerosis*. 1985;57:65-73.
17. Millar JS, Cromley DA, McCoy MG, Rader DJ, Billheimer JT. Determining hepatic triglyceride production in mice: comparison of poloxamer 407 with Triton WR-1339. *J Lipid Res*. 2005;46:2023-2028.
18. Braun A, Zhang S, Miettinen HE, Ebrahim S, Holm TM, Vasile E, Post MJ, Yoerger DM, Picard MH, Krieger JL, Andrews NC, Simons M, Krieger M. Probucol prevents early coronary heart disease and death in the high-density lipoprotein receptor SR-BI/apolipoprotein E double knockout mouse. *Proc Natl Acad Sci U S A*. 2003;100:7283-7288.
19. Van Eck M, Twisk J, Hoekstra M, Van Rij BT, Van der Lans CA, Bos IS, Kruijt JK, Kuipers F, Van Berkel TJ. Differential effects of scavenger receptor BI deficiency on lipid metabolism in cells of the arterial wall and in the liver. *J Biol Chem*. 2003;278:23699-23705.
20. Holm TM, Braun A, Trigatti BL, Brugnara C, Sakamoto M, Krieger M, Andrews NC. Failure of red blood cell maturation in mice with defects in the high-density lipoprotein receptor SR-BI. *Blood*. 2002;99:1817-1824.
21. Rigotti A, Trigatti BL, Penman M, Rayburn H, Herz J, Krieger M. A targeted mutation in the murine gene encoding the high density lipoprotein (HDL) receptor scavenger receptor class B type I reveals its key role in HDL metabolism. *Proc Natl Acad Sci U S A*. 1997;94:12610-12615.

22. Varban ML, Rinninger F, Wang N, Fairchild-Huntress V, Dunmore JH, Fang Q, Gosselin ML, Dixon KL, Deeds JD, Acton SL, Tall AR, Huszar D. Targeted mutation reveals a central role for SR-BI in hepatic selective uptake of high density lipoprotein cholesterol. *Proc Natl Acad Sci U S A*. 1998;95:4619-4624.
23. Hayashi AA, Webb J, Choi J, Baker C, Lino M, Trigatti B, Trajcevski KE, Hawke TJ, Adeli K. Intestinal SR-BI is upregulated in insulin-resistant states and is associated with overproduction of intestinal apoB48-containing lipoproteins. *Am J Physiol Gastrointest Liver Physiol*;301:G326-337.
24. Zabalawi M, Bhat S, Loughlin T, Thomas MJ, Alexander E, Cline M, Bullock B, Willingham M, Sorci-Thomas MG. Induction of fatal inflammation in LDL receptor and ApoA-I double-knockout mice fed dietary fat and cholesterol. *Am J Pathol*. 2003;163:1201-1213.
25. Karavia EA, Papachristou DJ, Liopeta K, Triantaphyllidou IE, Dimitrakopoulos O, Kypreos KE. Apolipoprotein A-I modulates processes associated with diet-induced nonalcoholic fatty liver disease in mice. *Mol Med*;18:901-912.
26. Van Eck M, Bos IS, Hildebrand RB, Van Rij BT, Van Berkel TJ. Dual role for scavenger receptor class B, type I on bone marrow-derived cells in atherosclerotic lesion development. *Am J Pathol*. 2004;165:785-794.

27. Zhang W, Yancey PG, Su YR, Babaev VR, Zhang Y, Fazio S, Linton MF. Inactivation of macrophage scavenger receptor class B type I promotes atherosclerotic lesion development in apolipoprotein E-deficient mice. *Circulation*. 2003;108:2258-2263.
28. Yu H, Zhang W, Yancey PG, Koury MJ, Zhang Y, Fazio S, Linton MF. Macrophage apolipoprotein E reduces atherosclerosis and prevents premature death in apolipoprotein E and scavenger receptor-class BI double-knockout mice. *Arterioscler Thromb Vasc Biol*. 2006;26:150-156.
29. Pei Y, Chen X, Aboutouk D, Fuller MT, Dadoo O, Yu P, White EJ, Igdoura SA, Trigatti BL. SR-BI in Bone Marrow Derived Cells Protects Mice from Diet Induced Coronary Artery Atherosclerosis and Myocardial Infarction. *PLoS One*. 2013;8:e72492.
30. Cai L, Wang Z, Meyer JM, Ji A, van der Westhuyzen DR. Macrophage SR-BI regulates LPS-induced pro-inflammatory signaling in mice and isolated macrophages. *J Lipid Res*. 2012;53:1472-1481.
31. Feng H, Guo L, Wang D, Gao H, Hou G, Zheng Z, Ai J, Foreman O, Daugherty A, Li XA. Deficiency of scavenger receptor BI leads to impaired lymphocyte homeostasis and autoimmune disorders in mice. *Arterioscler Thromb Vasc Biol*. 2011;31:2543-2551.
32. Cai L, Ji A, de Beer FC, Tannock LR, van der Westhuyzen DR. SR-BI protects against endotoxemia in mice through its roles in glucocorticoid production and hepatic clearance. *J Clin Invest*. 2008;118:364-375.

33. Guo L, Song Z, Li M, Wu Q, Wang D, Feng H, Bernard P, Daugherty A, Huang B, Li XA. Scavenger Receptor BI Protects against Septic Death through Its Role in Modulating Inflammatory Response. *J Biol Chem*. 2009;284:19826-19834.
34. Tacke F, Alvarez D, Kaplan TJ, Jakubzick C, Spanbroek R, Llodra J, Garin A, Liu J, Mack M, van Rooijen N, Lira SA, Habenicht AJ, Randolph GJ. Monocyte subsets differentially employ CCR2, CCR5, and CX3CR1 to accumulate within atherosclerotic plaques. *J Clin Invest*. 2007;117:185-194.
35. Swirski FK, Libby P, Aikawa E, Alcaide P, Luscinskas FW, Weissleder R, Pittet MJ. Ly-6Chi monocytes dominate hypercholesterolemia-associated monocytosis and give rise to macrophages in atheromata. *J Clin Invest*. 2007;117:195-205.
36. Galkina E, Ley K. Vascular adhesion molecules in atherosclerosis. *Arterioscler Thromb Vasc Biol*. 2007;27:2292-2301.
37. Hajra L, Evans AI, Chen M, Hyduk SJ, Collins T, Cybulsky MI. The NF-kappa B signal transduction pathway in aortic endothelial cells is primed for activation in regions predisposed to atherosclerotic lesion formation. *Proc Natl Acad Sci U S A*. 2000;97:9052-9057.
38. Iiyama K, Hajra L, Iiyama M, Li H, DiChiara M, Medoff BD, Cybulsky MI. Patterns of vascular cell adhesion molecule-1 and intercellular adhesion

- molecule-1 expression in rabbit and mouse atherosclerotic lesions and at sites predisposed to lesion formation. *Circ Res.* 1999;85:199-207.
39. Won D, Zhu SN, Chen M, Teichert AM, Fish JE, Matouk CC, Bonert M, Ojha M, Marsden PA, Cybulsky MI. Relative reduction of endothelial nitric-oxide synthase expression and transcription in atherosclerosis-prone regions of the mouse aorta and in an in vitro model of disturbed flow. *Am J Pathol.* 2007;171:1691-1704.
40. Yuhanna IS, Zhu Y, Cox BE, Hahner LD, Osborne-Lawrence S, Lu P, Marcel YL, Anderson RG, Mendelsohn ME, Hobbs HH, Shaul PW. High-density lipoprotein binding to scavenger receptor-BI activates endothelial nitric oxide synthase. *Nat Med.* 2001;7:853-857.
41. Li XA, Titlow WB, Jackson BA, Giltiay N, Nikolova-Karakashian M, Uittenbogaard A, Smart EJ. High density lipoprotein binding to scavenger receptor, Class B, type I activates endothelial nitric-oxide synthase in a ceramide-dependent manner. *J Biol Chem.* 2002;277:11058-11063.
42. Kimura T, Tomura H, Mogi C, Kuwabara A, Damirin A, Ishizuka T, Sekiguchi A, Ishiwara M, Im DS, Sato K, Murakami M, Okajima F. Role of scavenger receptor class B type I and sphingosine 1-phosphate receptors in high density lipoprotein-induced inhibition of adhesion molecule expression in endothelial cells. *J Biol Chem.* 2006;281:37457-37467.

3.6 Supplementary Materials and Methods

3.6.1 Animals

All procedures involving animals were approved by the Animal Research Ethics Board of McMaster University and are in accordance with the guidelines of the Canadian Council on Animal Care. All mice are on mixed C57BL/6:129 backgrounds. SR-BI^{+/-}/LDLR KO mice were bred together to generate littermate SR-BI/LDLR dKO mice and LDLR KO control mice. Only female mice were used in this study.

3.6.2 Diet Induction of Atherosclerosis

The following atherogenic diets were used in this study: The high fat, high cholesterol, cholate containing (HFCC or “Paigen”) diet (Harlan Teklad TD88051) contains 15% fat (7.5% from cocoa butter), 1.25% cholesterol and 0.5% sodium cholate (Paigen et al., 1985). The high fat, high cholesterol (HFC) diet (Harlan Teklad TD90221) is identical to the HFCC diet except that it lacks sodium cholate. The high cholesterol (HC) diet is a normal chow diet supplemented with 2% cholesterol (Harlan Teklad TD01383). The high fat (HF) or Western type diet contains 21% butter fat and 0.15% cholesterol (Dyets Inc. 112286). SR-BI/LDLR dKO and control LDLR KO mice were fed one of the above diets starting at 10-12 weeks of age and monitored daily. Mice were fed until they reached cardiac endpoint or for up to twelve weeks. Cardiac endpoint was identified as exhibiting one or more of the following symptoms: hunched posture, laboured breathing,

unsteady gate and ruffled coat. For HFCC and HFC fed groups, separate control LDLR KO groups in which the length of feeding equaled the mean survival of the corresponding SR-BI/LDLR dKO groups were generated. Separate cohorts of control dKO and LDLR KO mice were also fed the normal chow diet until they were 22 weeks of age (age matched to the 12 week atherogenic diet fed mice).

3.6.3 Histology

Hearts were perfused in situ through the left ventricle with 10 U/mL heparinised saline followed by 10% formalin. Hearts were then excised, fixed overnight in 10% formalin, cryoprotected in 30% sucrose for 24 hours and embedded in OCT. 10 μ m transverse cryosections were cut from the middle of the heart to the aortic sinus in 0.5mm intervals; the aortic sinus was sampled in 0.1mm intervals from the base of the valve leaflets to the coronary ostia.

Atherosclerosis was detected in the aortic sinus and CA's by oil red O staining. Atherosclerotic plaque cross-sectional area in the aortic sinus was measured manually using ImageJ software in the section that best represented three full and intact valve leaflets. CA atherosclerosis was assessed in transverse sections from the middle of the heart up to the sinus in 0.5mm intervals. CA's were scored as either lacking atherosclerosis (no plaque), containing fatty streaks, or which were <50% occluded, >50% occluded or 100% occluded by atherosclerotic plaques.

Myocardial fibrosis was detected by Masson's trichrome stain (Sigma), which stains collagen-rich fibrotic tissue blue, and healthy myocardium red. Total infarcted area was measured manually using the outline function in ImageJ software in images taken with a 10X objective lens on an Axiovert 200M microscope (Zeiss). Fibrotic area was measured in non-overlapping images of two transverse sections from each mouse near the top of the heart spaced 0.5mm apart and expressed as average cross-sectional area per section.

3.6.4 Immunofluorescence

Platelets in CA's were detected using a rat anti-mouse CD41 antibody (BD Pharmingen, 553847, Mississauga, Canada). CA's staining positive for platelets were counted and normalized to the total number of sections stained. Endothelial adhesion molecule expression was detected using cell-culture supernatants from rat B-lymphocyte hybridoma cells that produce antibodies against mouse VCAM-1 or ICAM-1 (CRL-1909 and CRL 1878, respectively, ATCC, Manassas, VA, USA)(Iiyama et al., 1999). We defined an ICAM-1-activated artery as containing a continuous line of at least 4 cells staining positive for ICAM-1, while VCAM-1 activated arteries were defined as arteries with detectable VCAM-1 expression. Using these criteria, all CA's observed in at least 4 sections per mouse were counted and classified as either activated or not activated for each marker. All antigens were visualized using a goat anti-rat IgG

secondary antibody conjugated to AlexaFluor 594 (Molecular Probes, Burlington, ON, Canada).

3.6.5 Plasma Lipid and Lipoprotein Analysis

Plasma was prepared from blood collected via cardiac puncture at the time of harvest. Total cholesterol, free cholesterol and triglyceride were measured by enzymatic assays following manufacturers' protocols (total cholesterol: Cholesterol Infinity, Thermo Scientific, Ottawa, ON, Canada, free cholesterol: Free Cholesterol E, Wako Diagnostics, Mountain View, CA, USA, triglyceride: L-Type Triglyceride M, Wako Chemicals, Richmond, VA, USA). Plasma lipoproteins were fractionated by size exclusion chromatography over a Superose 6 column using an AKTA Fast Protein Liquid Chromatography System (GE Biosciences, Baie d'Urfe, QC, Canada). Total cholesterol in the resulting fractions was measured by enzymatic assay as described above.

3.6.5 Triglyceride Production

10 week old mice were fed the HF or HFCC diet for 2 weeks. Mice were fasted overnight before lipoprotein lipase (LPL) was inhibited by intraperitoneal poloxamer 500mg/kg (HF) or intravenous tyloxapol 500mg/kg (HFCC). Blood was collected hourly following LPL inhibition, and triglyceride concentration in plasma was measured as described above.

3.6.6 Plasma Cytokine Measurements

Interleukin 6 and tumor necrosis factor (TNF-) α levels in plasma were measured by ELISA (BioLegend, San Diego, CA) following the manufacturer's instructions.

3.6.7 Blood Cell Analysis

Blood was collected via the tail vein from a subset of HFCC or control diet fed mice prior to harvest. Blood cells were counted using a Hemavet Multi-Species Hematology System (Drew Scientific). Ly6C expression was assessed by flow cytometry on a BD LSR II flow cytometer. Briefly, red blood cells and dead cells were excluded from analysis based on forward scatter and side scatter plots. Monocytes were defined as blood cells expressing both CD11b and CD115 and detected with FITC- and PE- conjugated antibodies, respectively (BD Pharmingen). Ly6C expression was then analyzed in this sub-population using an APC-conjugated antibody (BD Pharmingen).

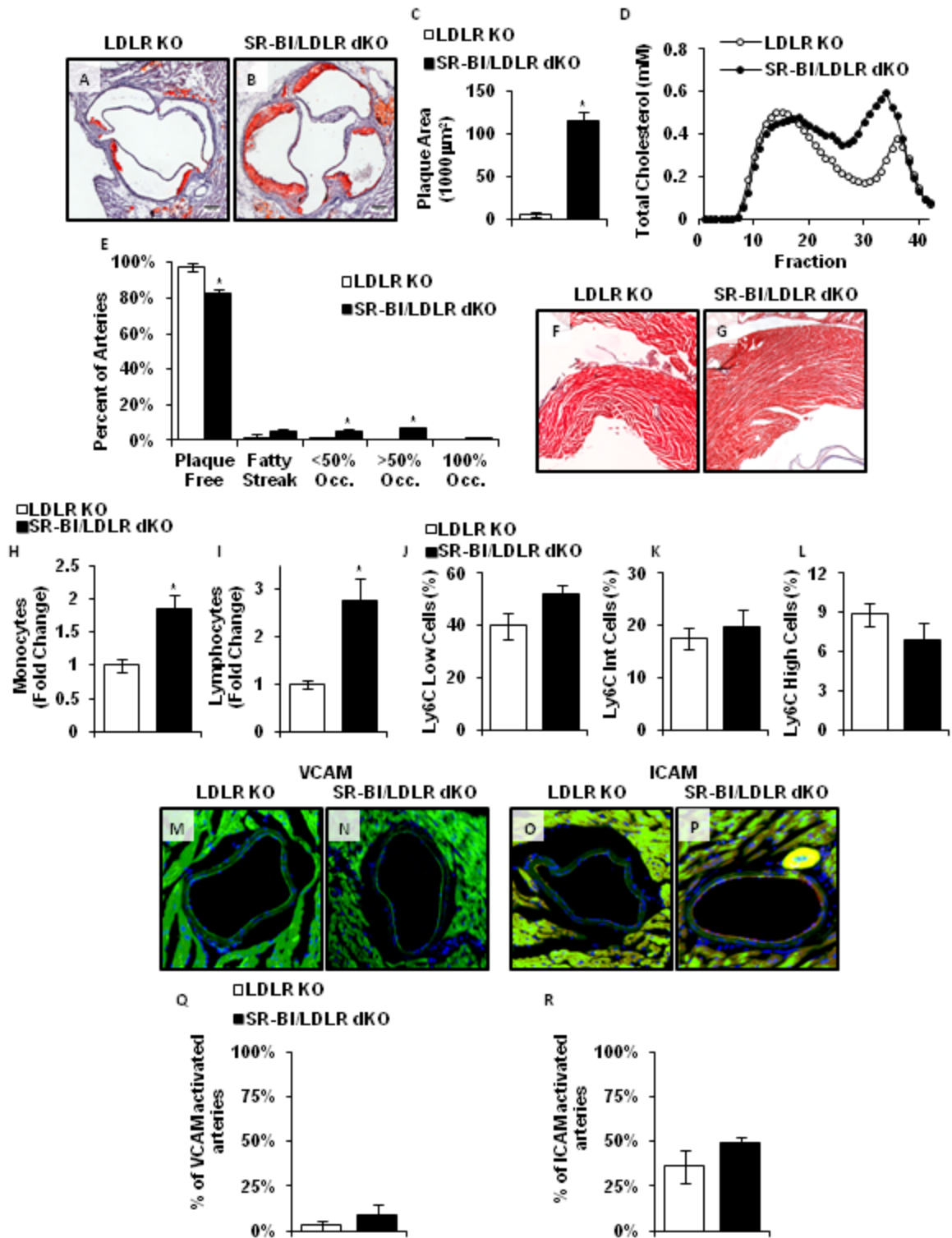
3.6.8 Statistical Analysis

For comparisons between two groups, data was first analyzed for Normality using the Shapiro-Wilk test. Data that passed this test for Normality were analyzed using Student's t-test and considered significant if $P < 0.05$.

Comparisons between multiple groups were made using one-way or two-way ANOVA where appropriate coupled with Dunn's and Holm-Sidak post-hoc tests, respectively.

3.7 Supplementary Data

Supplementary Figure 3.7 – Atherosclerosis and associated phenotypes in normal chow fed SR-BI/LDLR dKO and control LDLR KO mice. Female mice were fed a normal chow diet and were analyzed at 22 weeks of age to match the longest period of atherogenic diet feeding. (A,B) Representative oil red O-stained sections of aortic sinuses from LDLR KO and SR-BI/LDLR dKO mice, respectively. (C) Quantification of average plaque area in the aortic sinuses of each group. (D) Representative FPLC lipoprotein cholesterol profiles for each group. (E) Quantification of coronary artery atherosclerosis in each group. (F,G) Representative Masson's Trichrome stained sections of myocardium illustrating absence of fibrosis in both groups of mice. (H,I) Relative monocyte and lymphocyte levels in each group as measured on a Hemavet Multi Species Hematology System. (J-L) Proportions of circulating Ly6C^{hi}, Ly6C^{int} and Ly6C^{lo} monocytes in each group as measured by flow cytometry. (M-P) Representative immunofluorescent images of coronary arteries stained for VCAM-1 (M,N) and ICAM-1 (O,P), represented in red, from each group of mice. (Q,R) Quantification of VCAM-1 (Q) and ICAM-1 (R) activated coronary arteries as outlined in the materials and methods.

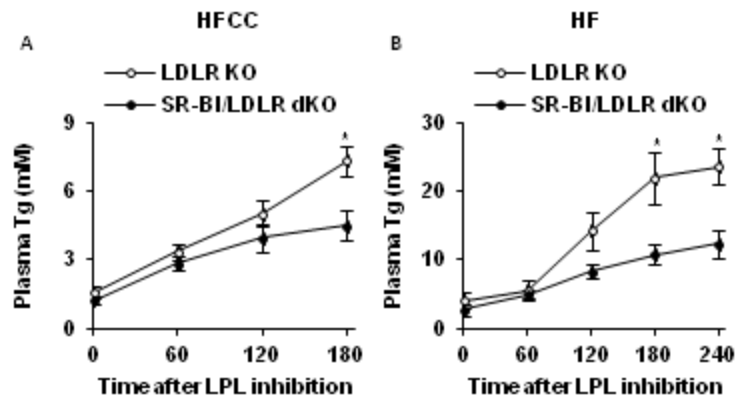


Supplementary Table 3.1 – Plasma lipid parameters in LDLR KO and SR-

BI/LDLR dKO mice fed different diets. Total cholesterol, free cholesterol, and triglycerides were measured using commercial assays. Cholesterol ester levels were calculated as total cholesterol - free cholesterol. Results are presented as mean \pm SEM for each measurement. Sample sizes are indicated in parentheses in the genotype column.

Diet	Genotype	Total Cholesterol (TC) (mM)	Free Cholesterol (FC) (mM)	FC:TC Ratio (%)	Cholesterol Ester (mM)	Triglycerides (mM)
Chow	LDLR KO (7)	12.2 \pm 1.0	3.2 \pm 0.3	26.3 \pm 0.9%	9.0 \pm 0.5	2.3 \pm 0.3
	SR-BI/LDLR dKO (11)	17.8 \pm 0.6*	9.0 \pm 0.5*	50.4 \pm 1.6%*	8.8 \pm 0.4	2.9 \pm 0.3
HF	LDLR KO (7)	36.0 \pm 3.2	11.1 \pm 1.2	30.9 \pm 2.2%	24.9 \pm 2.4	2.6 \pm 0.3
	SR-BI/LDLR dKO (9)	27.0 \pm 2.0*	19.7 \pm 1.4*	74.1 \pm 4.1%*	7.3 \pm 1.3*	1.7 \pm 0.3*
HC	LDLR KO (8)	57.1 \pm 5.4	15.1 \pm 1.7	27.1 \pm 2.3%	42.0 \pm 4.5	1.0 \pm 0.1
	SR-BI/LDLR dKO (8)	32.7 \pm 3.3*	17.8 \pm 2.1	55.0 \pm 4.2%*	15.0 \pm 2.3*	1.6 \pm 0.4
HFC	LDLR KO (12)	50.0 \pm 3.8	13.5 \pm 0.9	27.6 \pm 1.1%	36.5 \pm 3.3	0.7 \pm 0.1
	SR-BI/LDLR dKO (10)	38.7 \pm 3.7	26.5 \pm 2.0*	70.3 \pm 2.9%*	12.2 \pm 2.0*	1.2 \pm 0.1*
HFCC	LDLR KO (14)	106.0 \pm 5.2	27.1 \pm 1.4	25.7 \pm 0.8%	78.9 \pm 4.1	2.1 \pm 0.5
	SR-BI/LDLR dKO (8)	49.9 \pm 5.0*	41.5 \pm 3.5*	81.3 \pm 5.4%*	10.1 \pm 2.9*	1.3 \pm 0.3

Supplementary Figure 3.8 – Hepatic VLDL triglyceride secretion is reduced in SR-BI/LDLR dKO mice compared to LDLR KO control mice fed HF and HFCC diets. 10 week old mice were fed HF or HFCC diet for 2 weeks. Mice were fasted over night and lipoprotein lipase was inhibited by a single injection of tyloxapol (A) or poloxamer (B) at time 0. Blood was collected hourly for 4 (A) or 3 (B) hours. (A) HF diet fed mice. (B) HFCC diet fed mice. * $P < 0.05$ vs. LDLR KO for a given time point by student's T-test.



Supplementary Table 3.2 – Spleen weights. ND: Not determined. *P<0.01 by student's T-test. Sample sizes are indicated in parentheses in the genotype column.

Diet	Genotype	Spleen Weight (g)
Chow	LDLR KO (3)	0.11 ± 0.01
	SR-BI/LDLR dKO (5)	0.31 ± 0.04*
HF	LDLR KO (10)	0.19 ± 0.02
	SR-BI/LDLR dKO (7)	0.95 ± 0.05*
HC	LDLR KO	ND
	SR-BI/LDLR dKO (3)	1.09 ± 0.21
HFC	LDLR KO (12)	0.12 ± 0.01
	SR-BI/LDLR dKO (6)	1.03 ± 0.05*
HFCC	LDLR KO (7)	0.13 ± 0.01
	SR-BI/LDLR dKO (7)	1.63 ± 0.07*

Supplementary Table 3.3 – Hematology profiles of Chow- and HFCC-fed SR-BI/LDLR dKO and control LDLR KO mice. Whole blood was collected from tail or submandibular veins of 22 week old chow-fed mice or 12 week old mice fed the HFCC diet for 2 weeks. Hematology profiles were generated using a Hemavet Multi-Species Hematology System (Drew Scientific). Results shown are mean ± SEM for each output. Sample sizes are indicated in parentheses in the genotype column. *P<0.01 vs LDLR KO.

Diet	Genotype	RBC Count (M/μl)	Hematocrit (%)	Mean RBC Volume (fL)	RBC Dist. Width (%)	Platelet Count (Fold Change)
Chow	LDLR KO (6)	9.42 ± 0.50	51.9 ± 2.8	55.0 ± 0.2	14.1 ± 0.1	1 ± 0.05
	SR-BI/LDLR dKO (5)	7.66 ± 0.62	49.5 ± 4.1	64.1 ± 1.6*	22.7 ± 1.0*	0.82 ± 0.10
HFCC	LDLR KO (5)	10.42 ± 0.27	59.6 ± 1.6	57.2 ± 0.6	21.0 ± 0.9	1 ± 0.06
	SR-BI/LDLR dKO (6)	5.24 ± 0.21*	45.3 ± 1.4*	86.6 ± 1.1*	28.2 ± 0.4*	0.88 ± 0.05

**Chapter 4: Splenectomy has no Influence on the Development of Occlusive
Coronary Artery Atherosclerosis in High Fat, High Cholesterol Diet Fed
Scavenger Receptor Class B Type 1/Low Density Lipoprotein Receptor
Double Knockout Mice.**

Author List: Mark Fuller, Omid Dadoo, Neel Dhingani, Melissa MacDonald and
Bernardo Trigatti.

Foreword

In this manuscript we aimed to determine if, and to what extent, the abnormally large spleens in HFC diet-fed SR-B1/LDLR dKO mice contribute to leukocytosis and the development of atherosclerosis and occlusive coronary artery disease. Mice were subjected to either splenectomy or a sham surgery and fed a HFC diet for 5 weeks. No difference was observed in blood leukocyte counts; atherosclerosis in the aortic sinus and coronary arteries; or myocardial fibrosis between sham operated and splenectomized mice. We conclude that splenectomy has no effect on atherosclerosis in SR-B1/LDLR dKO mice.

This manuscript will be submitted for publication in early 2015. The project was initiated by Mark Fuller. Experiments were designed by Mark Fuller with guidance from Bernardo Trigatti. The manuscript was written by Mark Fuller with guidance from Bernardo Trigatti. All data was interpreted by Mark Fuller with guidance from Bernardo Trigatti. Animals were set up and all specimens were collected and prepared collaboratively by Mark Fuller and Omid Dadoo. Cytokine,

blood cell and organ data were collected collaboratively by Mark Fuller and Omid Dadoo. Neel Dhingani collected most of the aortic sinus atherosclerosis, coronary artery atherosclerosis, myocardial fibrosis and plasma lipid data under the supervision of Mark Fuller. Mark Fuller collected the remaining aortic sinus atherosclerosis, coronary artery atherosclerosis, myocardial fibrosis and plasma lipid data. Melissa MacDonald assisted with animal care and carried out en face analysis of atherosclerosis in the aortas under the guidance of Mark Fuller.

4.1 Abstract

Mice that lack the HDL receptor, SR-B1, on a variety of atherosclerosis susceptible backgrounds develop accelerated aortic atherosclerosis and severe occlusive coronary artery disease. This phenotype is associated with leukocytosis in SR-B1/LDL receptor (LDLR) double knockout mice and enlargement of the spleen in SR-B1/LDLR dKO and other SR-B1 deficient mice. The spleen is a major source of myeloid cells that contribute to atherosclerotic plaque formation. In this study, we tested the influence of the spleen on diet-accelerated atherosclerosis and coronary artery disease in SR-B1/LDLR double knockout mice.

SR-B1/LDLR double knockout mice underwent splenectomy or sham surgery and were subsequently fed a high fat high cholesterol diet for 5 weeks. Splenectomy had no effect on the size of atherosclerotic plaques or the degree of coronary atherosclerosis in SR-B1/LDLR double knockout mice. Additionally, splenectomy did not impact circulating cytokine levels or monocyte and lymphocyte counts. Splenectomized mice had enlarged livers, possibly reflecting compensatory extramedullary hematopoiesis, which may explain the absence of an effect of splenectomy on circulating leukocytes.

Therefore, the spleen is not essential to leukocytosis and diet-accelerated atherosclerosis and occlusive coronary artery disease in SR-B1/LDLR double knockout mice.

4.2 Introduction

Atherosclerosis is a chronic inflammatory disease characterized by the accumulation of cholesterol, macrophages and other immune cells in the artery wall. Hyperlipidemia[1], vascular inflammation[2] and dysregulation of the immune system, particularly leukocytosis[3], are three major drivers of atherosclerosis in both human patients and common mouse models of the disease. The number and phenotypic characterization of circulating monocytes has been a focus of several recent studies leading to the conclusion that monocytosis, with increased proportions of monocytes that express high levels of Ly6C (Ly6C^{high}), is a risk factor for increased atherosclerotic lesion development in mice[4-7]. Extramedullary hematopoiesis in the spleen is known to give rise to Ly6C^{high} monocytes that are subsequently incorporated into atherosclerotic lesions[4]. Additionally, after experimental myocardial infarction (MI), extramedullary hematopoiesis in the spleen is increased, and spleen-derived monocytes contribute to acceleration of atherosclerosis in apolipoprotein E deficient mice[8].

High density lipoprotein (HDL) has been shown to suppress hematopoietic stem cell proliferation[9,10]. Mice that lack the ATP binding cassette transporters ABCA1 and ABCG1, which are responsible for cholesterol efflux from tissues to HDL, have expanded myeloid progenitor populations, leukocytosis and enlarged spleens[9]. Bone marrow specific deficiency of ABCA1 and ABCG1 in low density

lipoprotein receptor (LDLR) heterozygous mice results in leukocytosis and accelerated atherogenesis[9].

Scavenger receptor class b type 1 (SR-BI) is another major receptor for HDL that is expressed on the surface of multiple cell types. Our lab recently established SR-B1/ LDLR double knockout (dKO) mice as a novel murine model of diet inducible occlusive coronary artery atherosclerosis and spontaneous MI[11]. When fed a variety of atherogenic diets, SR-B1/LDLR dKO mice develop increased atherosclerosis in the aortic sinus and descending aorta[11,12] as well as severe occlusive coronary artery atherosclerosis, MI, and significantly reduced survival compared to conventional LDLR single KO mice fed the same diets[11]. This unique phenotype is shared by a small number of related mouse models[13-15]. Along with other pro-atherogenic phenotypes, atherogenic diet fed SR-B1/LDLR dKO mice exhibit substantial leukocytosis with elevated proportions of Ly6C^{high} monocytes, accompanied by drastically enlarged spleens[11].

Because SR-B1/LDLR d KO mice exhibit splenomegaly and monocytosis when fed high fat diets, and because they develop MI that appears to be secondary to CA atherosclerosis, we tested if the spleen was essential for monocytosis and whether its removal affected the degree of atherosclerosis in the aortic sinus, descending aorta, or coronary arteries and the degree of MI in SR-B1/LDLR dKO mice fed a high fat, high cholesterol (HFC) diet. We demonstrate that splenectomised SR-B1/LDLR dKO mice exhibit no change in blood monocyte, lymphocyte or cytokine levels. Similar levels of atherosclerosis

in the aortic sinus, descending aorta and coronary arteries as well as similar levels of myocardial fibrosis were observed between splenectomised and sham operated mice. We note that splenectomised SR-B1/LDLR dKO mice exhibited significantly enlarged livers compared to sham operated mice, suggesting that extramedullary hematopoiesis in these mice is compensated for by the liver upon splenectomy.

4.3 Materials and Methods

4.3.1 Mice, Diet and Splenectomy

All procedures on mice were approved by the internal ethics committee at McMaster University and meet the requirements of the Canadian Council on Animal Care. LDLR KO and SR-B1/LDLR dKO mice were bred in house on a mixed C57BL/6:129Sv background. Both genotypes were generated by breeding SR-B1^{+/-} LDLR KO mice together such that littermates were used in each comparison. All mice used in this study were female.

Splenectomy was performed on mice at 9-11 weeks of age following a previously published procedure[16]. Mice were anaesthetized with ketamine/xylazine and the surgical site was shaved and swabbed with iodine. A small incision was made on the left side of the peritoneum, through which the spleen was exposed. The splenic vasculature was ligated with sutures and the spleen was removed. The abdominal wall and skin was then closed with sutures. Sham operation was performed in the same manner, excluding exteriorization

and removal of the spleen, instead, the spleen was gently manipulated with blunt forceps prior to closure of the incision. Mice recovered for one week following surgery.

Mice were fed a HFC diet (15% fat (7.5% from cocoa butter) and 1.25% cholesterol; Harlan Teklad TD90221)[11] for 5 weeks starting one week after surgery or at 10-12 weeks of age (non-surgical control mice). At the end of the feeding period, mice were euthanized and blood and tissues were collected for analysis.

4.3.2 Blood Cell Analysis

Blood was collected by cardiac puncture at the time of harvest. Hematology profiles, including monocyte and lymphocyte counts, were generated using a Hemavet Multi-Species Hematology System.

4.3.3 Assessment of Atherosclerosis in the Aortic Sinus and Coronary Arteries

Hearts were prepared and sectioned as described previously[11,12,14,17].

Briefly, fixed, frozen hearts were mounted in OCT and 10 μ m transverse cryosections were collected from the middle of the heart upwards in 0.5mm intervals until the aortic sinus was visible. 10 μ m sections of the aortic sinus were collected every 100 μ m until valve leaflets were no longer visible. Atherosclerosis was detected by oil red O/Meyer's hematoxylin staining. Plaque cross-sectional area in the aortic sinus was measured in the section in which all three full valve

leaflets were clearly visible. Coronary arteries in each section before the aortic sinus were categorized as either atherosclerotic (arteries with raised atherosclerotic plaque) or non-atherosclerotic (arteries with no plaque or thin fatty streaks).

4.3.4 Assessment of Atherosclerosis in the Descending Aorta

En face analysis of aortas was performed as described previously[12]. Aortas were excised and fixed in 10% formalin. Extra-vascular tissue was trimmed away and full aortas were stained with sudan IV. Aortas were then opened longitudinally, mounted and cover slipped en face on a slide, and imaged with a digital SLR camera. Plaque coverage was measured using ImageJ software and expressed as the area of sudan IV positive (red) staining as a proportion of total vessel area.

4.3.5 Myocardial Infarction

Fibrosis in the myocardium was detected by Masson's Trichrome staining of 10 μ m cryosections as described previously[11,14,18,19]. Cardiac fibrosis is expressed as the average area of blue staining (collagen-rich tissue) in two sections of myocardium from each mouse within 1.5mm of the aortic sinus.

4.3.6 Plasma Lipid Analysis

Plasma was prepared from blood collected after a 4 hour fast at the time of harvest. Total cholesterol (Cholesterol Infinity, Thermo Scientific), HDL cholesterol (HDL Cholesterol E, WAKO), free cholesterol (Free Cholesterol E, WAKO) and triglycerides (L-Type Triglyceride M, WAKO) were measured using the commercially available kits indicated in parentheses following manufacturers' protocols.

4.3.7 Plasma Cytokine Analysis

Levels of interleukin 6 (IL-6) and tumor necrosis factor alpha (TNF α) were measured by ELISA using commercially available kits (BioLegend, San Diego, CA, USA) following the manufacturer's protocol.

4.3.8 Statistical Analysis

All data passed tests for normality and equal variance. Comparisons were made by students T-test.

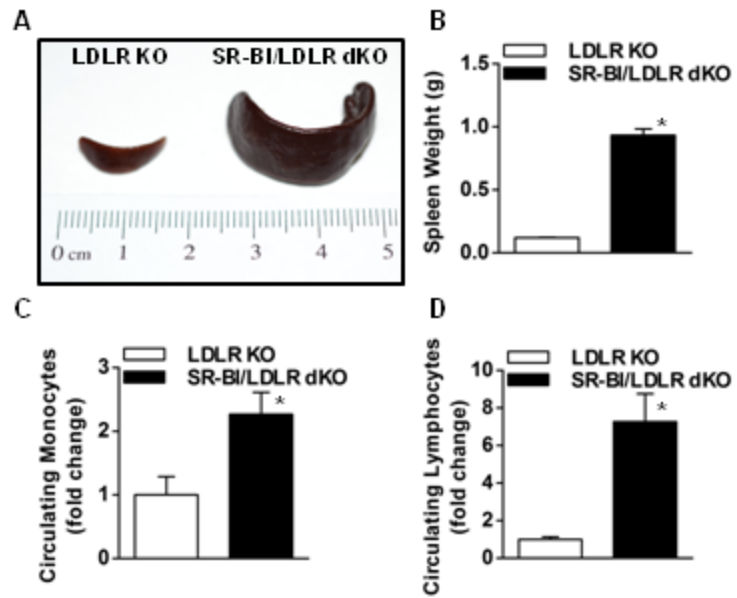
4.4 Results

4.4.1 Spleen Size and Leukocytosis in HFC-fed SR-B1/LDLR dKO Mice

We studied the effects of spleen removal on HFC diet induced monocytosis and associated inflammation, atherosclerosis, coronary artery disease and MI in SR-B1/LDLR dKO mice. To establish an overall phenotype of HFC diet-exacerbated splenomegaly and monocytosis in SR-B1/LDLR dKO mice, female SR-B1/LDLR dKO mice and LDLR single KO control mice were fed a HFC diet

for 5 weeks, starting at 10-12 weeks of age. Consistent with our previous findings[11], spleens from SR-B1/LDLR dKO mice were approximately 8-fold larger in dKO than in control LDLR sKO mice fed the HFCC diet (Figure 4.1A&B) (we previously reported that on chow diet, spleens from dKO mice were 2.5-3x larger than those from LDLR sKO mice and that spleens from LDLR sKO mice were not affected by diet[11]). Blood cell counts were measured on a Hemavet multi-species hematology system. Circulating monocyte numbers in dKO mice were double those of LDLR KO controls (Figure 4.1C), and lymphocyte numbers were increased by approximately 7-fold (Figure 4.1D). Furthermore, dKO mice exhibited reduced red blood cell counts and hematocrits, and increased red blood cell sized compared to LDLR single KO control mice (supplementary table 4.1).

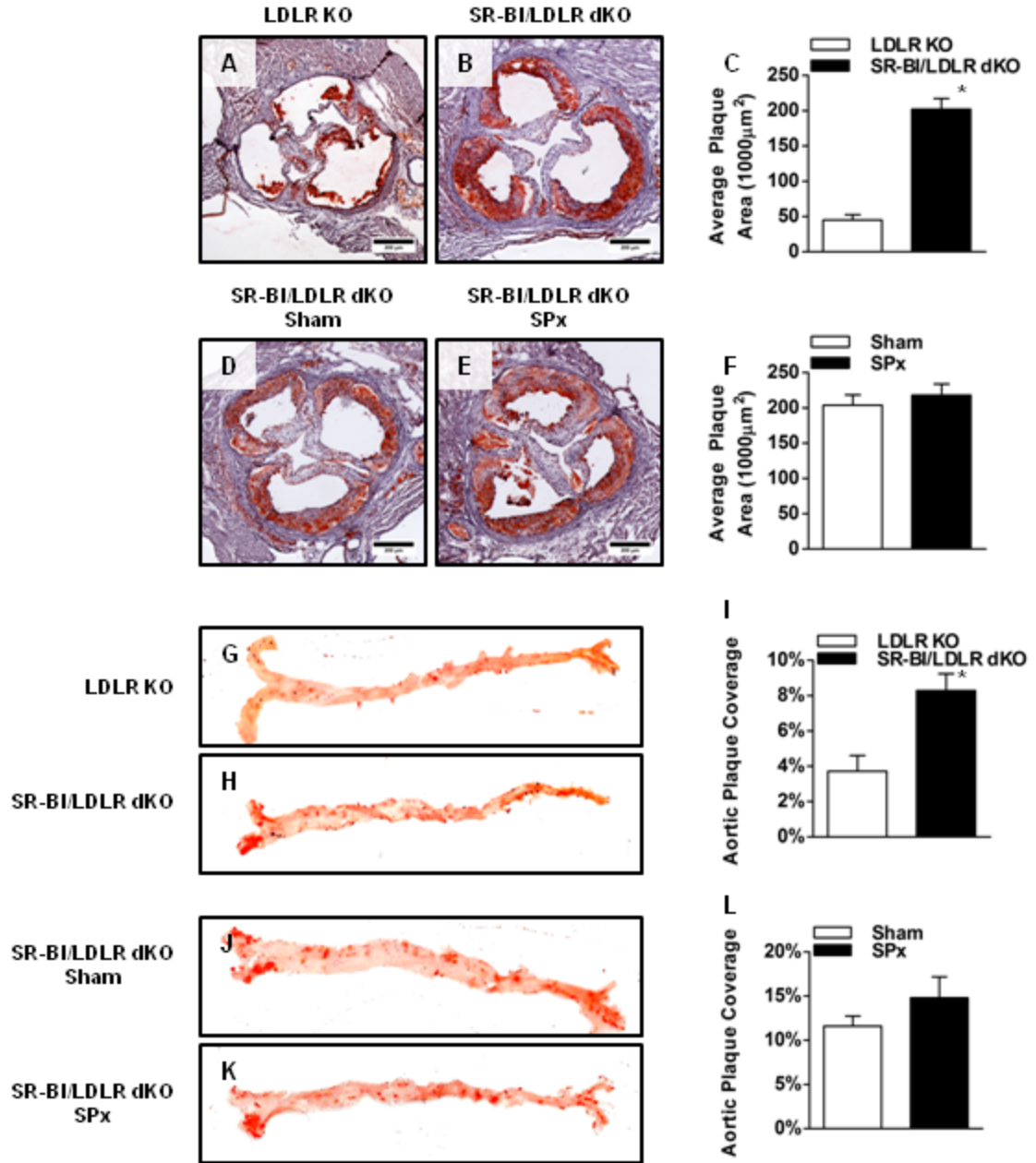
Figure 4.1 – SR-B1/LDLR dKO mice have enlarged spleens and elevated monocyte and lymphocyte counts in circulation compared to LDLR KO mice when fed a high fat, high cholesterol diet. Female mice were fed a HFC diet for 5 weeks starting at 10-12 weeks of age. Images representative of spleens from LDLR KO and SR-B1/LDLR dKO mice are shown in panel A. B: Spleen weights for each group of mice (n=12 mice per group). C&D: Blood monocyte and lymphocyte counts respectively from both groups of mice (n=7-8 mice per group). *P<0.05 by student's t-test.



4.4.2 The Effect of Splenectomy on Atherosclerosis in the Aortic Sinus and Descending Aorta

To determine if removal of the spleen from SR-B1/LDLR dKO mice affected HFC diet accelerated atherosclerosis, female SR-B1/LDLR dKO mice were subjected to splenectomy or sham surgery at 9-11 weeks of age. After a one week recovery period, mice were fed a HFC diet for 5 weeks and blood and tissues were collected for analysis. In parallel, SR-B1/LDLR dKO mice and LDLR single KO mice that had not undergone surgery were analyzed as controls to establish the overall phenotype of SR-B1/LDLR dKO mice. Figure 4.2 (A&B) show representative images of oil red O stained aortic sinuses from SR-B1/LDLR dKO and LDLR single KO control mice fed a HFC diet for 5 weeks. As reported previously[11], aortic sinus plaque size was ~3-fold larger in dKO mice compared to LDLR KO control mice (Figure 4.2 C). Figure 4.2 (D&E) depict representative images of oil red O stained aortic sinuses from dKO mice that were subjected to either, sham surgery or splenectomy, followed by 5 weeks of HFC feeding. No difference was observed in aortic plaque size between splenectomised and sham operated mice (Figure 4.2 E). Similarly, while HFC feeding induced significantly greater plaque development, measured en face, in the descending aortas of dKO mice compared to LDLR KO controls (Figure 4.2 F-H), splenectomy had no effect on HFC diet-induced atherosclerosis in the descending aortas of dKO mice (Figure 4.2 J-L).

Figure 4.2 – Splenectomy does not reduce HFC diet accelerated atherosclerosis in the aortic sinus or descending aorta of SR-B1/LDLR dKO mice. Female SR-B1/LDLR dKO mice aged 9-11 weeks were subjected to splenectomy or sham surgery and fed a HFC diet starting one week after surgery for five weeks. Female LDLR KO and SR-B1/LDLR dKO mice that did not undergo surgery were fed a HFC diet from 10-12 weeks of age as controls. A&B: Representative images of oil red O stained aortic sinuses from LDLR KO (A) and SR-B1/LDLR dKO (B) mice after 5 weeks of HFC feeding. C: Quantification of aortic sinus plaque cross-sectional area in non-surgical control mice (n=9-10 mice per group). D&E: Representative images of oil red O stained aortic sinuses from SR-B1/LDLR dKO mice that underwent sham (D) or splenectomy (E) surgeries prior to HFC feeding. F: Quantification of plaque area in mice in surgical groups (n=11-13 mice per group). G&H: Representative en face sudan IV stained aortas from HFC fed LDLR KO (G) and SR-B1/LDLR dKO (H) mice. I: Quantification of aortic plaque coverage in non-surgical control mice (n=13 mice per group). J&K: Representative en face sudan IV stained aortas from sham (J) or splenectomy (K) operated mice. L: Quantification of aortic plaque coverage in mice in surgical groups (n=9-14 mice per group).

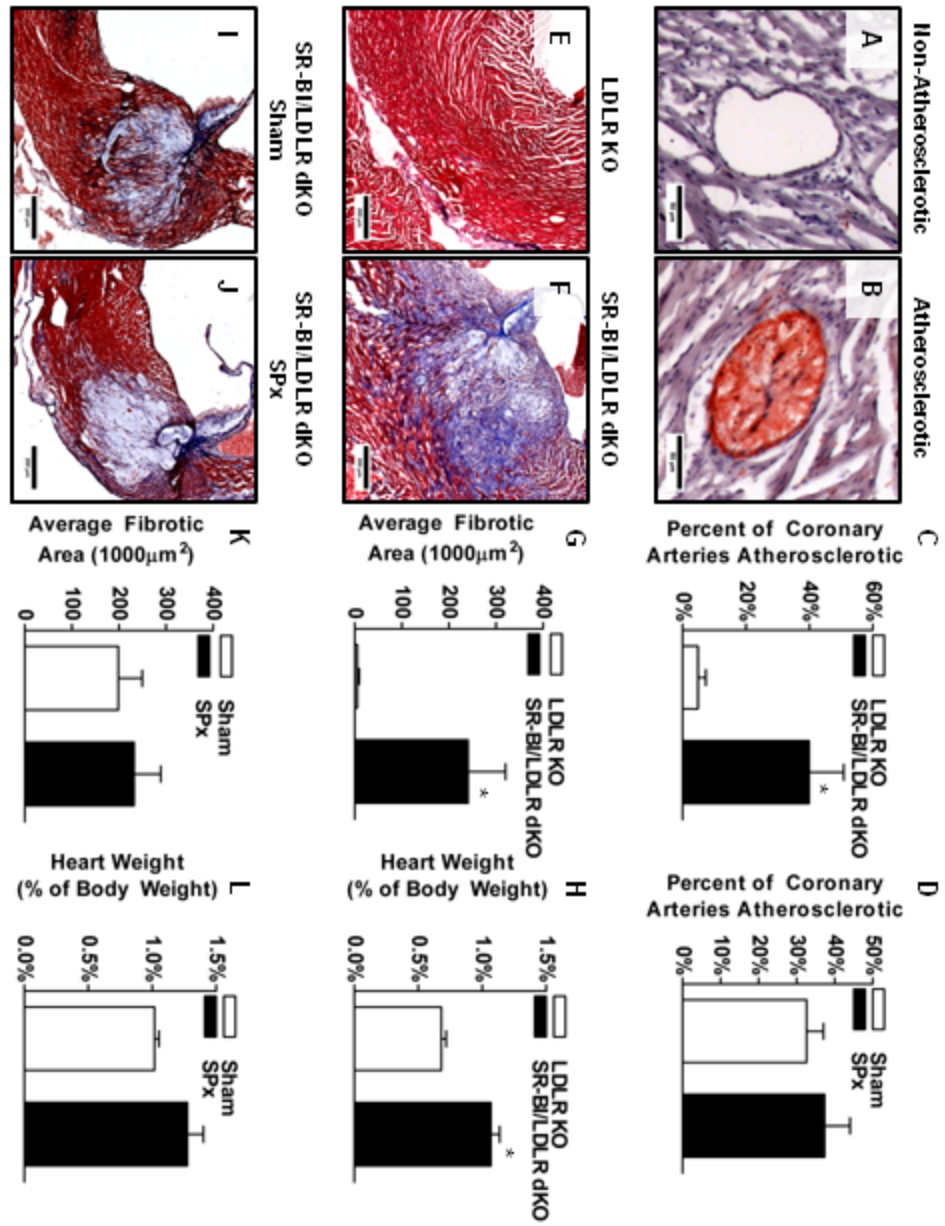


4.4.3 The Effect of Splenectomy on Coronary Artery Atherosclerosis and Myocardial Infarction

To measure the effects of splenectomy on coronary artery atherosclerosis and MI, coronary arteries in at least 3 oil red O stained transverse cryosections of the heart spaced a minimum of 0.5mm apart from the middle of the heart to the aortic sinus were counted and classified as either non-atherosclerotic (containing no raised plaque) (Figure 4.3 A) or atherosclerotic (containing raised plaque) (Figure 4.3 B). As previously reported, HFC feeding induced significant coronary atherosclerosis in SR-B1/LDLR dKO mice while negligible coronary atherosclerosis was observed in LDLR KO control mice (Figure 4.3 C). Both sham operated and splenectomised mice exhibited substantial coronary atherosclerosis to a similar extent as observed in non-surgical dKO mice. There was no significant difference in coronary atherosclerosis between sham and splenectomised mice (Figure 4.3 D). MI was analyzed in two Masson's trichrome stained cryosections spaced a minimum of .5mm apart near the top of the heart for each mouse. Collagen rich fibrotic tissue, represented in blue, was measured in each section. Figure 4.3 (E&F) show representative images of Masson's trichrome stained heart sections from non-surgical LDLR single KO and SR-B1/LDLR dKO mice fed the HFC diet for 5 weeks. While very little myocardial fibrosis was observed in LDLR KO control mice, SR-B1/LDLR dKO mice exhibited substantial myocardial fibrosis (Figure 4.3 G), consistent with our previous findings[11]. Hearts from SR-B1/LDLR dKO mice were also significantly

larger than those of LDLR KO control mice (Figure 4.3 H). The extent of myocardial fibrosis and heart:body weight ratios in splenectomised dKO mice were similar to those of non-surgical dKO mice and not significantly different from those in sham-operated mice (Figure 4.3 I-L).

Figure 4.3 – Splenectomy does not influence the development of HFC diet induced coronary artery atherosclerosis or myocardial infarction in SR-B1/LDLR dKO mice. A&B: Representative images depicting non-atherosclerotic (A) and atherosclerotic (B) coronary artery categories. C&D: Quantification of coronary artery atherosclerosis in non-surgical LDLR KO and SR-B1/LDLR dKO mice (n=4-9 mice per group) (C) and sham and splenectomy operated SR-B1/LDLR dKO mice (n=10-13 mice per group) (D). E&F: Representative Masson's trichrome stained heart images from HFC fed LDLR KO (E) and SR-B1/LDLR dKO (F) non-surgical control mice. G: Quantification of myocardial fibrosis in non-surgical control groups (n=9 mice per group). H: Heart:body weight ratios of non-surgical control mice (n=12-16 mice per group). I&J: Representative Masson's trichrome stained heart images from HFC fed SR-B1/LDLR dKO mice that were either sham operated (I) or splenectomised (J). K: Quantification of myocardial fibrosis in mice from surgical groups (n=13 mice per group). L: Heart:body weight ratios of mice from surgical groups (n=9 mice per group).



4.4.4 The Effect of Splenectomy on Plasma Lipids

Since the concentration of lipids in plasma can have a profound effect on atherosclerotic plaque development, we measured plasma lipid concentrations to rule out splenectomy induced lipid changes as a possible confounding variable in our study. Consistent with our previous findings[11], total cholesterol levels in HFC-fed SR-B1/LDLR dKO mice were significantly lower than in LDLR KO control mice fed the same diet (Figure 4.4 A) while free cholesterol levels were significantly higher in dKO mice (Figure 4.4 C). Also consistent with our previous findings[11], free cholesterol represented approximately 50% of total plasma cholesterol in SR-B1/LDLR dKO mice, compared to approximately 25% in LDLR KO control mice (Figure 4.4 E). Plasma HDL cholesterol levels and plasma triglyceride levels were not significantly different between SR-B1/LDLR dKO mice and LDLR KO control mice (Figure 4.4 G&I). Splenectomy did not significantly alter the plasma total cholesterol (Figure 4.4 B), HDL cholesterol (Figure 4.4 H) or triglyceride levels (Figure 4.4 F) in HFC-fed SR-B1/LDLR dKO mice; however, free cholesterol levels were slightly but significantly higher in splenectomised mice than in sham-operated mice (Figure 4.4 D), the reason for this is unclear.

Figure 4.4 – Splenectomy has little effect on plasma lipid levels in HFC fed

SR-B1/LDLR dKO mice. A&B: Total cholesterol levels in LDLR KO and SR-

B1/LDLR dKO non-surgical control mice (A; n=12-15 mice per group) and sham operated and splenectomised SR-B1/LDLR dKO mice (B; n=9 mice per group).

C&D: Free cholesterol levels in non-surgical control groups (C; n=12-15 mice per group) and surgical groups (D; n=9 mice per group). E&F: Free cholesterol: total

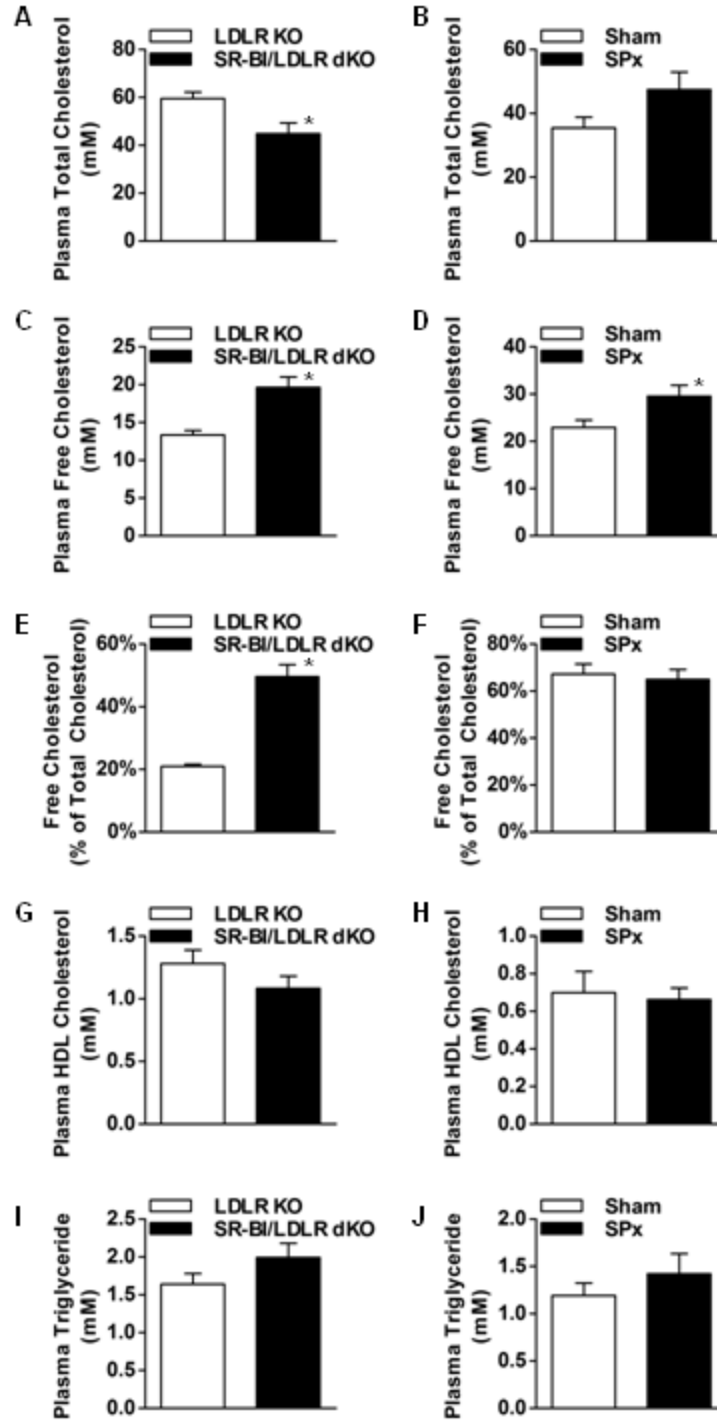
cholesterol ratios in non-surgical control groups (E; n=12-15 mice per group) and

surgical groups (F; n=9 mice per group). G&H: HDL cholesterol levels in non-

surgical control groups (G; n=12-16 mice per group) and surgical groups (H; n=8-

10 mice per group). I&J: Triglyceride levels in non-surgical control groups (I;

n=12-14 mice per group) and surgical groups (J; n=9 mice per group).



4.4.5 The Effect of Splenectomy on Leukocytosis

To determine if splenectomy was able to ameliorate monocytosis and lymphocytosis in HFC fed SR-B1/LDLR dKO mice, we generated hematology profiles for both splenectomised and sham operated mice. No differences were observed in monocyte or lymphocyte numbers between splenectomised and sham-operated mice (Figure 4.5 A&B). However, red blood cell counts and hematocrits were significantly reduced to an even greater extent in splenectomised mice than in sham operated mice, and red blood cell size was significantly increased in splenectomised mice compared to sham operated mice. This is consistent with the role of the spleen in removal of damaged red blood cells.

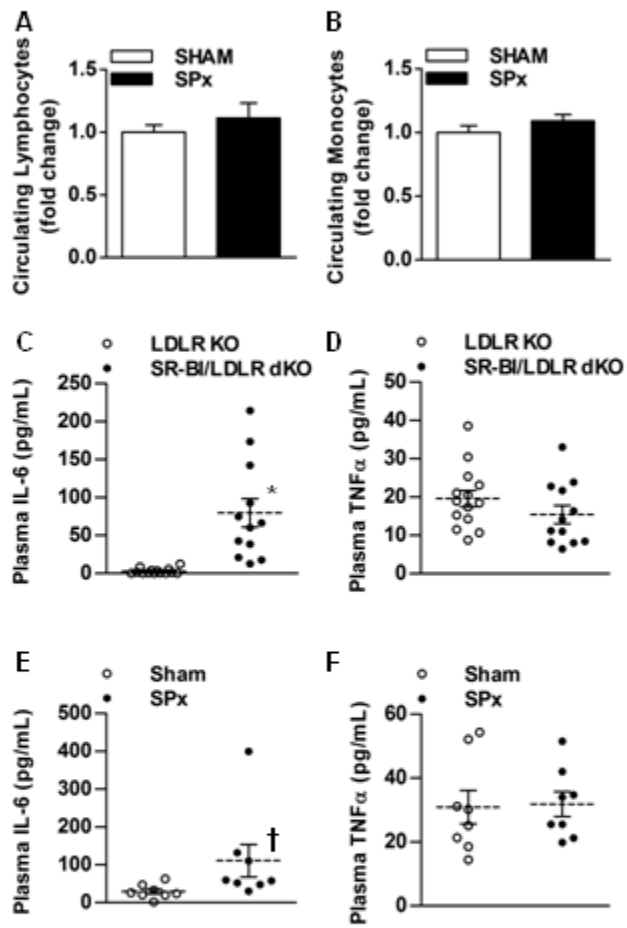
4.4.6 The Effect of Splenectomy on Systemic Inflammation

To measure the effects of splenectomy on HFC diet induced inflammation in SR-B1/LDLR dKO mice, we measured plasma levels of inflammatory cytokines IL-6 and TNF α . Consistent with our previous work[11], we observed a substantial and significant increase in plasma IL-6 levels in HFC fed dKO mice compared to LDLR KO controls (Figure 4.5 C). However, no difference was observed in TNF α levels between LDLR KO and dKO mice (Figure 4.5 D) fed the HFC diet for 5 weeks. Levels of IL-6 in the plasma of splenectomised SR-B1/LDLR dKO mice were slightly higher than those in sham-operated mice (Figure 4.5 E); however, plasma IL-6 levels in splenectomised mice were similar to those measured in

non-surgical SR-B1/LDLR dKO mice (compare panels C and E in Figure 4.5).

Plasma TNF α levels were not significantly different between splenectomised and sham-operated mice (Figure 4.5 E&F). Therefore, the data suggests that sham operation suppressed plasma IL-6 levels but that splenectomy itself did not increase levels above those seen in naive dKO mice but did increase levels above those in sham operated mice. Overall, these results suggest that splenectomy does not meaningfully influence HFC diet induced inflammation in SR-B1/LDLR dKO mice.

Figure 4.5 – Splenectomy does not alter circulating monocyte, lymphocyte or cytokine levels in HFC fed SR-B1/LDLR dKO mice. A&B: Circulating monocyte (A) and lymphocyte (B) levels in HFC fed sham operated and splenectomised SR-B1/LDLR dKO mice (n=8-9 mice per group). C&D: Plasma IL-6 (C) and TNF α (D) levels in HFC fed LDLR KO and SR-B1/LDLR dKO non-surgical control mice (n=12-14 mice per group). D&E: Plasma IL-6 (E) and TNF α (F) levels in HFC fed sham operated and splenectomised SR-B1/LDLR dKO mice (n=8 mice per group).

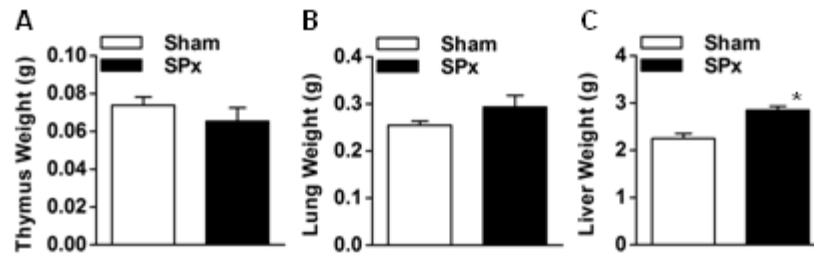


4.4.7 The Effect of Splenectomy on the Liver

Since removal of the massively enlarged spleen, theoretically a large source of leukocytes, did not reverse the leukocytosis phenotypes in SR-B1/LDLR dKO mice, we looked for changes in the weights of other organs, which may indicate compensatory extramedullary haematopoiesis in the absence of the spleen.

While the thymus or lung weights did not differ between splenectomised and sham-operated mice (Figure 4.6 A&B), there was a significant increase in liver weight in splenectomised mice compared to sham-operated mice (Figure 4.6 C&D). These data suggest that extramedullary haematopoiesis may take up in other organs, including the liver, upon removal of the spleen. This has been reported in splenectomized mice after experimental MI[8].

Figure 4.6 – Splenectomy results in enlargement of the liver in HFC fed SR-B1/LDLR dKO mice. A-C: Thymus (A; n=8-9 mice per group), lung (B; n=9 mice per group) and liver (C; n=9 mice per group) weights in HFC fed sham operated and splenectomised SR-B1/LDLR dKO mice. D: Representative images of livers from HFC fed sham operated and splenectomised SR-B1/LDLR dKO mice.



4.5 Discussion

SR-B1/LDLR dKO mice develop accelerated atherosclerosis in their aortas, and occlusive coronary artery atherosclerosis accompanied by myocardial infarction when fed a variety of atherogenic diets[11]. This unique phenotype is accompanied by leukocytosis including monocytosis and lymphocytosis, elevated systemic inflammation, and severely enlarged spleens[11]. Given that the spleen is a major source of extramedullary haematopoiesis that gives rise to Ly6C^{high} “inflammatory” monocytes which are incorporated into atherosclerotic plaques[4], we tested the hypothesis that removal of the enlarged spleens in HFC fed SR-B1/LDLR dKO mice would reduce HFC diet-induced leukocytosis, aortic and coronary atherosclerosis, and MI.

As previously demonstrated[11,12], compared to LDLR single KO control mice, SR-B1/LDLR dKO mice fed the HFC diet for 5 weeks developed significantly larger plaques in their aortic sinuses, more extensive plaque coverage in their descending aortas, and severe occlusive coronary artery atherosclerosis with associated myocardial infarction. This was accompanied by increased blood monocyte and lymphocyte counts, elevated circulating IL-6 levels and extremely large spleens. However, we found that splenectomy before the onset of atherogenic HFC diet feeding had no effect on any of the parameters listed above. These findings suggest that despite the obvious abnormalities observed in spleens of these animals, the spleens are either not contributing to leukocytosis, or removal of the spleens leads to compensatory haematopoiesis in

other organs. The enlargement of the liver in splenectomised mice suggests that extramedullary hematopoiesis may take place in the liver in the absence of a spleen. This is consistent with previous reports of increased progenitor cells in the liver of C57BL6/J mice after myocardial infarction and splenectomy[8].

Alternatively, livers of splenectomized mice may be more inflamed, or accumulate more lipid than those of sham-operated mice and this may explain the increase in liver size. Additional experiments are required to determine the cause of the observed increase in liver size in splenectomized mice.

Past studies have demonstrated that splenectomy actually accelerates atherosclerosis in both apolipoprotein E deficient mice[20-22] and LDLR KO mice[23]. This is due to a reduction in atheroprotective B1a lymphocytes that produce IgM antibodies[22]. While these conventional mouse models do not typically exhibit major splenic pathology, an alternative expectation for the outcome of the current study is that splenectomy will increase HFC diet-induced atherosclerosis and coronary artery disease in SR-B1/LDLR dKO mice. The absence of an effect of splenectomy on atherosclerosis in this study suggests that either B1a lymphocytes do not afford protection against atherosclerosis in this particularly severe model of disease, or that the spleens of these mice do not produce adequate amounts of B1a lymphocytes to be protective such that removal of the spleen has no impact on B1a lymphocyte levels or atherosclerosis. In SR-B1/apolipoprotein E dKO mice, a related mouse model of spontaneous occlusive coronary artery atherosclerosis and MI, complete

deficiency of all lymphocytes achieved by deletion of the RAG2 gene had no impact on the development of coronary artery atherosclerosis or reduced survival[24]. These mice lack both atheroprotective and atherogenic subclasses of lymphocytes; however this study lends credence to the notion that lymphocytes do not play a major role in the development of occlusive coronary artery atherosclerosis in SR-B1 deficient mice.

In conclusion, we have demonstrated that the spleens of SR-B1/LDLR dKO mice are not required for leukocytosis or the development of HFC diet-accelerated atherosclerosis and occlusive coronary artery disease. Moreover, the removal of the spleen neither increases nor decreases the severity of this disease in these mice, suggesting that while the enlarged spleens are not driving the disease progression, the spleens in these mice are also not functioning in their usual protective role against atherosclerosis.

4.6 References

1. Hegele RA (2009) Plasma lipoproteins: genetic influences and clinical implications. *Nat Rev Genet* 10: 109-121.
2. Libby P, Ridker PM, Maseri A (2002) Inflammation and atherosclerosis. *Circulation* 105: 1135-1143.
3. Tall AR, Yvan-Charvet L, Westerterp M, Murphy AJ (2012) Cholesterol efflux: a novel regulator of myelopoiesis and atherogenesis. *Arterioscler Thromb Vasc Biol* 32: 2547-2552.

4. Robbins CS, Chudnovskiy A, Rauch PJ, Figueiredo JL, Iwamoto Y, et al. (2012) Extramedullary hematopoiesis generates Ly-6C(high) monocytes that infiltrate atherosclerotic lesions. *Circulation* 125: 364-374.
5. Swirski FK, Libby P, Aikawa E, Alcaide P, Luscinskas FW, et al. (2007) Ly-6Chi monocytes dominate hypercholesterolemia-associated monocytosis and give rise to macrophages in atheromata. *J Clin Invest* 117: 195-205.
6. Tacke F, Alvarez D, Kaplan TJ, Jakubzick C, Spanbroek R, et al. (2007) Monocyte subsets differentially employ CCR2, CCR5, and CX3CR1 to accumulate within atherosclerotic plaques. *J Clin Invest* 117: 185-194.
7. Combadiere C, Potteaux S, Rodero M, Simon T, Pezard A, et al. (2008) Combined inhibition of CCL2, CX3CR1, and CCR5 abrogates Ly6C(hi) and Ly6C(lo) monocytosis and almost abolishes atherosclerosis in hypercholesterolemic mice. *Circulation* 117: 1649-1657.
8. Dutta P, Courties G, Wei Y, Leuschner F, Gorbato R, et al. (2012) Myocardial infarction accelerates atherosclerosis. *Nature* 487: 325-329.
9. Yvan-Charvet L, Pagler T, Gautier EL, Avagyan S, Siry RL, et al. (2010) ATP-binding cassette transporters and HDL suppress hematopoietic stem cell proliferation. *Science* 328: 1689-1693.
10. Feng Y, Schouteden S, Geenens R, Van Duppen V, Herijgers P, et al. (2012) Hematopoietic stem/progenitor cell proliferation and differentiation is differentially regulated by high-density and low-density lipoproteins in mice. *PLoS One* 7: e47286.

11. Fuller M, Dadoo O, Serkis V, Abutouk D, MacDonald M, et al. (2014) The effects of diet on occlusive coronary artery atherosclerosis and myocardial infarction in scavenger receptor class B, type 1/low-density lipoprotein receptor double knockout mice. *Arterioscler Thromb Vasc Biol* 34: 2394-2403.
12. Covey SD, Krieger M, Wang W, Penman M, Trigatti BL (2003) Scavenger receptor class B type I-mediated protection against atherosclerosis in LDL receptor-negative mice involves its expression in bone marrow-derived cells. *Arterioscler Thromb Vasc Biol* 23: 1589-1594.
13. Zhang S, Picard MH, Vasile E, Zhu Y, Raffai RL, et al. (2005) Diet-induced occlusive coronary atherosclerosis, myocardial infarction, cardiac dysfunction, and premature death in scavenger receptor class B type I-deficient, hypomorphic apolipoprotein ER61 mice. *Circulation* 111: 3457-3464.
14. Braun A, Trigatti BL, Post MJ, Sato K, Simons M, et al. (2002) Loss of SR-BI expression leads to the early onset of occlusive atherosclerotic coronary artery disease, spontaneous myocardial infarctions, severe cardiac dysfunction, and premature death in apolipoprotein E-deficient mice. *Circ Res* 90: 270-276.
15. Yesilaltay A, Daniels K, Pal R, Krieger M, Kocher O (2009) Loss of PDZK1 causes coronary artery occlusion and myocardial infarction in Paigen diet-fed apolipoprotein E deficient mice. *PLoS One* 4: e8103.

16. Reeves JP, Reeves PA, Chin LT (2001) Survival surgery: removal of the spleen or thymus. *Curr Protoc Immunol* Chapter 1: Unit 1 10.
17. Trigatti B, Rayburn H, Vinals M, Braun A, Miettinen H, et al. (1999) Influence of the high density lipoprotein receptor SR-BI on reproductive and cardiovascular pathophysiology. *Proc Natl Acad Sci U S A* 96: 9322-9327.
18. Al-Jarallah A, Igdoura F, Zhang Y, Tenedero CB, White EJ, et al. (2013) The effect of pomegranate extract on coronary artery atherosclerosis in SR-BI/APOE double knockout mice. *Atherosclerosis* 228: 80-89.
19. Pei Y, Chen X, Aboutouk D, Fuller MT, Dadoo O, et al. (2013) SR-BI in Bone Marrow Derived Cells Protects Mice from Diet Induced Coronary Artery Atherosclerosis and Myocardial Infarction. *PLoS One* 8: e72492.
20. Rezende AB, Neto NN, Fernandes LR, Ribeiro AC, Alvarez-Leite JI, et al. (2011) Splenectomy increases atherosclerotic lesions in apolipoprotein E deficient mice. *J Surg Res* 171: e231-236.
21. Caligiuri G, Nicoletti A, Poirier B, Hansson GK (2002) Protective immunity against atherosclerosis carried by B cells of hypercholesterolemic mice. *J Clin Invest* 109: 745-753.
22. Kyaw T, Tay C, Krishnamurthi S, Kanellakis P, Agrotis A, et al. (2011) B1a B lymphocytes are atheroprotective by secreting natural IgM that increases IgM deposits and reduces necrotic cores in atherosclerotic lesions. *Circ Res* 109: 830-840.

23. Lammers B, Zhao Y, Foks AC, Hildebrand RB, Kuiper J, et al. (2012)
Leukocyte ABCA1 remains atheroprotective in splenectomized LDL
receptor knockout mice. *PLoS One* 7: e48080.
24. Karackattu SL, Picard MH, Krieger M (2005) Lymphocytes are not required
for the rapid onset of coronary heart disease in scavenger receptor class
B type I/apolipoprotein E double knockout mice. *Arterioscler Thromb Vasc
Biol* 25: 803-808.

4.7 Supplementary Materials

Supplementary Table 4.1 – Hematology profiles of HFC-fed non-surgical LDLR KO and SR-B1/LDLR dKO mice, and sham operated or splenectomized SR-B1/LDLR dKO mice. Whole blood was collected from tail or submandibular veins of mice fed HFC diet for 5 weeks. Hematology profiles were generated using a Hemavet Multi-Species Hematology System (Drew Scientific). Results shown are mean \pm SEM for each output. Sample sizes are indicated in parentheses in the genotype column. *P<0.01 vs LDLR KO / NS or SR-B1/LDLR dKO / Sham.

Genotype / Treatment	RBC Count (M/ μ l)	Hematocrit (%)	Mean RBC Volume (fL)	RBC Dist. Width (%)	Platelet Count (Fold Change)
LDLR KO / NS (8)	8.42 \pm 0.40	43.3 \pm 0.6	51.4 \pm .4	15.0 \pm 0.2	1.00 \pm 0.03
SR-B1/LDLR dKO / NS (7)	4.38 \pm 0.33*	35.2 \pm 2.4*	80.9 \pm 2.3*	25.1 \pm 0.6*	1.02 \pm 0.08
SR-B1/LDLR dKO / Sham (9)	5.50 \pm 0.32	44.5 \pm 2.6	80.9 \pm 1.0	26.2 \pm 0.6	1.00 \pm 0.04
SR-B1/LDLR dKO / SPx (8)	3.80 \pm 0.22*	36.9 \pm 2.0*	97.4 \pm 1.9*	34.3 \pm 1.0*	1.27 \pm 0.40

Chapter 5: Discussion

This thesis centers around the roles of the HDL receptor, SR-B1, in multiple cell types and their impact on the development of atherosclerosis *in vivo* in the mouse. Particular attention is given to the effect of a lack of SR-B1 on the development of occlusive coronary artery atherosclerosis, a major clinically relevant manifestation of atherosclerosis in humans which conventional mouse models of atherosclerosis are generally resistant to. Chapters 2 and 3 characterize the effects of SR-B1 deficiency on the development of atherosclerosis and the cellular and systemic factors that may influence it in different murine model systems. In chapter 2, diet-induced atherosclerosis is evaluated in the context of genetic deficiency of SR-B1 alone. In this study, wild type mice are used to establish baseline atherosclerosis, while LDLR KO and apoE KO mice are used to compare SR-B1 KO mice against conventional mouse models of atherosclerosis. In chapter 3, coronary atherosclerosis and associated outcomes such as MI are evaluated in the context of dual deficiency of SR-B1 and the LDLR in mice fed a variety of atherogenic diets. Chapter 4 is aimed at testing the involvement of the spleen, which is substantially enlarged in SR-B1 KO mice, in the exacerbation of atherosclerosis in the model system described in chapter 3. This chapter serves as both an example of an application of this model, as well an attempt to understand the unique pathology of SR-B1/LDLR dKO mice on a deeper level. As a whole, these studies provide insight into the cellular and molecular mechanisms by which SR-B1 protects against the

development of atherosclerosis in the mouse, and in particular, in the coronary vasculature.

5.1 Summary of Results in Chapters 2-4

Chapter 2 of this thesis describes the cardiovascular phenotype of SR-B1 single KO mice compared to those of LDLR KO and apoE KO mice after being fed a cholate-containing atherogenic diet for an extended period of time. SR-B1 deficient mice developed substantial atherosclerotic plaques in their aortic sinuses, comparable in size to those of LDLR KO and apoE KO mice when fed equivalently. Additionally, SR-B1 KO mice developed plaques in regions of the vasculature, including the coronary arteries and the entire length of the descending aorta, where other mouse models developed little atherosclerosis. This phenotype was accompanied by dramatic elevations in circulating monocytes and lymphocytes, and increased expression of VCAM-1 in the coronary endothelium. Interestingly, this severe phenotype exists in the absence of elevated plasma total cholesterol compared to HFCC-fed wild type mice, which develop minimal atherosclerosis even after extended HFCC feeding. These results support atheroprotective roles of SR-B1 in multiple relevant cell types and are consistent with the notion that local and systemic inflammatory and immune responses play critical roles in the development of atherosclerosis and can drive plaque development in context of diet-induced hyperlipidemia. Alternatively, it is possible that the nature of the lipoproteins carrying the cholesterol is critical to

the development of atherosclerosis, and that the lipoproteins in SR-B1 deficient mice have particularly atherogenic properties.

Chapter 3 describes SR-B1/LDLR dKO mice as a novel model of diet-accelerated occlusive coronary artery atherosclerosis and MI. We fed SR-B1/LDLR dKO mice several atherogenic diets varying in their contents of fat, cholesterol and sodium cholate. When fed diets containing very high cholesterol, SR-B1/LDLR dKO mice exhibited significantly reduced survival compared LDLR KO control mice, accompanied by cardiac enlargement and extensive myocardial fibrosis. Severe coronary artery atherosclerosis was observed in these mice, in which up to 40% of coronary arteries were completely occluded with atherosclerotic plaque, and often in HFCC-fed mice, platelet-rich thrombi. Similar to HFCC-fed SR-B1 single KO mice, atherogenic diet fed SR-B1/LDLR dKO mice exhibited reduced plasma cholesterol levels, as well as monocytosis and lymphocytosis compared to LDLR KO mice, and expressed higher levels of adhesion molecules in their coronary endothelium. The results of this study are consistent with those of previous studies in which SR-B1 deficiency results in spontaneous or diet-inducible coronary artery atherosclerosis, MI and early death in apoE KO mice (Braun et al., 2002) and apoE hypomorphic mice (Nakagawa-Toyama et al., 2012; S. Zhang et al., 2005), respectively, however, the current model offers several advantages which will be discussed later.

In chapters 2 and 3, SR-B1 deficient mice were shown to have abnormally large spleens, an effect that is exacerbated by atherogenic diet feeding.

Considering that the spleen is a major site of extramedullary haematopoiesis and a reservoir for Ly6C^{high} monocytes (Robbins et al., 2012), in chapter 4, we tested the effect of splenectomy on the development of diet-accelerated CA atherosclerosis and MI in SR-B1/LDLR dKO mice. Surprisingly, splenectomy did not affect the numbers of circulating monocytes or lymphocytes in the blood of SR-B1/LDLR dKO mice fed a HFC diet; and failed to influence myocardial fibrosis or atherosclerosis in any arteries. Splenectomised SR-B1/LDLR dKO mice had significantly larger livers than sham-operated controls, suggesting that the liver may be an alternative site for extramedullary haematopoiesis in the absence of a spleen. These results suggest that the splenomegaly observed in SR-B1/LDLR dKO mice does not directly impact the atherosclerosis phenotype of these mice.

5.2 Implications from the Studies Detailed in Chapters 2-4

5.2.1 The Role of SR-B1 in the Liver and in Lipoprotein Metabolism

In apoE KO and HFCC-fed apoE hypomorphic mice, SR-B1 deficiency significantly increases VLDL/LDL cholesterol levels in plasma, which may explain some of the effects of SR-B1 deficiency on atherosclerosis in these mice (B. Trigatti et al., 1999; S. Zhang et al., 2005). In contrast, in wild type mice fed a HFCC diet SR-B1 deficiency had no effect on total plasma cholesterol levels, HDL cholesterol levels or non-HDL cholesterol levels, while in LDLR KO mice, SR-B1 deficiency lowered total cholesterol, cholesterol associated with VLDL and

LDL-sized lipoproteins, and VLDL secretion. In both of these mouse models, SR-B1 deficiency drastically increased atherosclerosis at multiple arterial sites.

These results indicate that the increased susceptibility to atherosclerosis in SR-B1 KO mice is not simply a result of elevated cholesterol. However, the effect of SR-B1 deficiency on the structure and function of different lipoproteins needs to be considered.

SR-B1 mediates selective cholesterol uptake from HDL by the liver and steroidogenic tissues (Krieger, 1999). Consistent with this function, mice that lack SR-B1 have a much higher concentration of HDL cholesterol in their plasma than wild type mice, and this cholesterol is associated with much larger HDL particles (Rigotti et al., 1997). The results from chow-fed SR-B1 deficient mice in chapters 2 and 3 are consistent with these observations. However, atherogenic diet feeding reduces HDL cholesterol levels in both SR-B1KO and SR-B1/LDLR dKO mice to lower than SR-B1 expressing controls fed the same diet, as shown both in FPLC lipoprotein profiles and by enzymatic assay for HDL associated cholesterol. A possible explanation for these observations is that SR-B1 deficiency combined with diet-induced hypercholesterolemia alters both the size of HDL particles such that they migrate with VLDL and LDL-sized lipoproteins over a size exclusion column; and the composition of HDL particles such that they are no longer measurable by conventional laboratory assays for HDL cholesterol. In support of the first statement, apoA1 western blots of FPLC fractions show that apoA1 in the plasma of B1/E dKO mice is limited to VLDL and

LDL- sized particles (B. Trigatti et al., 1999). In support of the notion that HDL morphology and composition is altered in SR-B1 KO mice, lipid parameters presented in chapters 2-4 as well as those published by others indicate that SR-B1 deficient mice have elevated plasma free cholesterol:total cholesterol ratios, and this ratio increases with atherogenic diet feeding (S. Zhang et al., 2005). Therefore, it is possible that HDL particles in SR-B1 KO mice at least partially lose some or all of their atheroprotective functions, and may even become pathogenic. The functionality of this HDL can be tested *in vitro* by isolating HDL from SR-B1 KO mice and testing its ability to suppress EC adhesion molecule expression, and induce EC migration; as well its ability to suppress macrophage apoptosis and induce macrophage migration. Because these potentially dysfunctional and/or pathogenic HDL particles may have secondary consequences on other cell types, it is difficult to separate the influence of SR-B1 in the liver from the influence of SR-B1 in other tissues on the development of atherosclerosis *in vivo*. The most direct way to accomplish this would be to transgenically re-introduce SR-B1 expression in the livers of SR-B1 deficient mice and measure diet-induced atherosclerosis in the aortic sinus, descending aorta and CAs. Assuming that liver-specific expression of SR-B1 fully corrects the lipoprotein abnormalities in SR-B1 KO mice; which is expected given that free cholesterol:total cholesterol ratios in PDZK1/apoE dKO mice, which express only ~5% of WT SR-B1 levels in the liver, are only mildly elevated in comparison to those of B1/E dKO mice (Kocher et al., 2008); this experiment would broadly have

four conceivable outcomes: 1) Liver-specific expression of SR-B1 is sufficient to prevent increased atherosclerosis and reverse endothelial, haematopoietic and inflammatory phenotypes. This would suggest that SR-B1 deficient phenotypes in other cells are secondary to the effect of SR-B1 deficiency on lipoproteins. 2) Liver SR-B1 prevents increased atherosclerosis but does not correct SR-B1 deficient phenotypes in other cells. This would indicate that lipoprotein abnormalities are the major driver of increased atherosclerosis in these mice, but do not account for the phenotypes observed in other cells. 3) Liver SR-B1 partially reduces atherosclerosis but does not correct SR-B1 deficient phenotypes in other cells. This would indicate that both lipoprotein and non-lipoprotein factors contribute to increased atherosclerosis in these mice. 4) Liver SR-B1 has no effect on atherosclerosis and fails to correct SR-B1 deficient phenotypes in other cells. This would suggest that the increased susceptibility to atherosclerosis in SR-B1 KO mice is a result of a lack of SR-B1 in peripheral cells. Given that bone marrow-specific deficiency of SR-B1 augments (Covey et al., 2003; Van Eck, Bos, Hildebrand, Van Rij, & Van Berkel, 2004), while restoration of SR-B1 in BM of SR-B1 KO mice reduces atherosclerosis (Pei et al., 2013; H. Yu et al., 2006), the most likely outcome of the experiment proposed above is outcome 3. This is further supported by the observation that liver specific deletion of SR-B1 reproduces the SR-B1 KO lipoprotein profile and increases atherosclerosis, but not to the same extent as full body SR-B1 deficiency (Huby et al., 2006). It would be interesting to measure the extent of CA

atherosclerosis in mice with liver specific SR-B1 deficiency to assess the impact of SR-B1's role in the liver in protection of the coronary vasculature against atherosclerosis.

5.2.2 The Role of SR-B1 in Immune Cells and Inflammation

We found substantial leukocytosis and elevated systemic inflammation in SR-B1 KO mice and SR-B1/LDLR dKO mice fed atherogenic diets. The elevated inflammation can be partially explained by adrenal insufficiency in SR-B1 deficient mice. Others have described elevated IL-6 and TNF α levels in SR-B1 KO mice treated with LPS and experimental sepsis, and have attributed much of this phenotype to an inability to produce sufficient corticosterone to mitigate the inflammatory response (Cai et al., 2008; Gilibert et al., 2014; Guo et al., 2009). However, others have also reported increased circulating cytokine levels in mice with BM-specific SR-B1 deficiency (Cai et al., 2012), and we have reported a reduction in circulating IL-6 levels when SR-B1 is restored in the BM of SR-B1 KO/ apoE Hypomorphic mice (Pei et al., 2013). Thus, it is likely that SR-B1 deficiency in both the BM and the adrenal glands contributes to diet-induced elevated inflammation in SR-B1 KO and SR-B1/LDLR dKO mice. The leukocytosis phenotype may be a direct result of a deficiency of SR-B1 in the leukocytes or leukocyte progenitor cells, an indirect result of abnormal HDL, or a combination of the above. Two groups have reported that HDL suppresses haematopoietic stem cell (HSC) proliferation (Y. Feng et al., 2012; Yvan-Charvet

et al., 2010), and combined deficiency of ABCA1 and ABCG1 in the BM is associated with monocytosis and splenomegaly (Yvan-Charvet et al., 2010). The myeloproliferative phenotype in these mice appears to be dependent on reduced cholesterol efflux to HDL (Westerterp et al., 2012). It is not known whether HDL particles in SR-B1 KO mice are effective cholesterol efflux acceptors, and it is therefore possible that monocytosis in SR-B1 KO mice is a result of impaired HDL-driven cholesterol efflux from progenitor cells. It has also recently been reported that apoA1 infusion can reduce Lin-Sca1+Kit+ HSCs in the BM of LDLR KO mice transplanted with SR-B1 expressing BM, but not in LDLR KO mice transplanted with SR-B1 KO BM (Gao et al., 2014), suggesting there may be a direct role of SR-B1 in HSCs in regulating proliferation. In agreement with this, lymphocytes from SR-B1 deficient mice exhibit increased proliferation under basal conditions in culture (H. Feng et al., 2011), suggesting that SR-B1 has an intrinsic effect on lymphocyte proliferation. However, HDL isolated from SR-B1 KO mice had a reduced capacity to suppress the proliferation of stimulated wild type lymphocytes in culture (H. Feng et al., 2011). Taken together, the above studies suggest both a direct role of SR-B1 expression and an indirect role of SR-B1 through maintenance of HDL function on regulating circulating leukocyte numbers in the mouse. Correction of the lipoprotein abnormalities by transgenic expression of SR-B1 in the liver, as well as BMT studies can be carried out to address these two issues separately. It has been suggested that the enlarged spleens found in SR-B1 KO and ABCA1/ABCG1 BM dKO mice is due to the

myeloproliferative disorders in these mice and a reflection of increased extramedullary haematopoiesis (Yvan-Charvet et al., 2010). Removal of the spleens in SR-B1/LDLR dKO mice failed to reverse the leukocytosis phenotypes in those mice and did not affect atherosclerosis in any arterial locations that we looked in. These results suggest that the spleen is not essential for leukocytosis and accelerated atherosclerosis in SR-B1/LDLR dKO mice. Additional experiments are needed to determine whether or not other organs such as the liver, lungs or thymus are compensating as sites of extramedullary haematopoiesis in the absence of the spleen. This can be accomplished by measuring numbers of haematopoietic progenitor cells in these organs in splenectomised and sham-operated mice by flow cytometry.

In addition to affecting the proliferation of HSCs and the numbers of undifferentiated immune cells, SR-B1 also exerts atheroprotective functions in macrophages. HDL induces migration of macrophages in culture in an SR-B1 dependent manner. This process is dependent on activation of a complicated intracellular signaling that appears to be activated by SR-B1, and involves among other components, sphingosine-1-phosphate receptor-1 (S1P1), PDZK1, PI3K/AKT1 activation, and ERK/MAPK activation (Al-Jarallah et al., 2014). Macrophage migration may be important in atherosclerotic plaque regression (Llodra et al., 2004).

Unpublished work from our lab has also uncovered a role of SR-B1 in suppression of apoptosis in macrophages. Macrophage apoptosis can influence

both the development and complexity of an atherosclerotic plaque, limiting the progression of early stage atherosclerotic lesions, but contributing to necrotic core formation in more advanced plaques (Tabas, 2010). HDL protects cultured macrophages against apoptosis in response to free cholesterol loading, oxLDL and chemical inducers of ER stress in a manner that requires SR-B1. Similar to HDL-stimulated macrophage migration, HDL-dependent protection against apoptosis in macrophages requires PI3K activity and AKT1. *In vivo*, elimination of SR-B1 expression in the bone marrow of apoE KO mice leads to the development of larger necrotic cores associated with increased apoptosis of macrophages in atherosclerotic plaques as detected by TUNEL staining after 12 weeks of western diet feeding (B. Trigatti, unpublished, personal communication). Although necrotic cores were not analyzed in SR-B1/LDLR dKO mice, based on the role of SR-B1 in preventing macrophage apoptosis and limiting necrotic core development in apoE KO mice it is conceivable that plaques in SR-B1/LDLR dKO mice have large necrotic cores and are therefore vulnerable to rupture. This is consistent with the presence platelets in the coronary artery plaques of SR-B1/LDLR dKO mice fed the HFCC diet.

Restoration of SR-B1 expression in the BM of SR-B1 KO/ apoE hypomorphic mice reduces coronary artery atherosclerosis without altering lipoprotein cholesterol levels (Pei et al., 2013). Similarly, transplantation of B1/E dKO mice with wild type BM delays early onset CA atherosclerosis significantly in that model system (H. Yu et al., 2006). It is likely that these results are

reproducible in the SR-B1/LDLR dKO mice described here, however these experiments have not yet been carried out. Assuming that BM SR-B1 also protects SR-B1/LDLR dKO mice from diet-induced occlusive CA atherosclerosis, this model could serve as a convenient tool to test the importance of other aspects of the proposed SR-B1 signaling cascade to BMT-mediated atheroprotection. LDLR KO mice are routinely used in BMT studies because unlike BM-derived apoE, BM-derived LDLR has minimal impact on lipoprotein cholesterol profiles and plaque development in LDLR KO mice (Van Eck et al., 2004). This eliminates the requirement of crossing BM donor mice to apoE KO or apoE Hypomorphic backgrounds when carrying out BMT experiments. Therefore, it would be relatively straightforward to test the requirement for proteins such as PDZK1, S1P1, and AKT1 in the protection afforded by SR-B1 expressed in BM, using singly deficient mice as donors and SR-B1/LDLR dKO mice as recipients.

5.2.3 The Role of SR-B1 in Platelets

SR-B1 appears to effect platelet function both directly and indirectly, in opposing manners. SR-B1 KO platelets have a blunted response to most platelet activators in culture (Ma et al., 2010); however SR-B1 KO mice are more susceptible to thrombosis, presumably due to the effects of SR-B1 deficiency on the plasma lipid environment (Korporaal et al., 2011). SR-B1/LDLR dKO mice develop platelet-rich thrombi in atherosclerotic CAs when fed a HFCC diet. This observation gives rise to two important questions: 1) Are these thrombi

developing as a result of plaque rupture? And 2) Are these thrombi responsible for the severely reduced mortality in these mice? The first question can be addressed by histological examination of the CA plaques in these mice for markers of plaque instability such as large necrotic cores, thin fibrous caps and the presence of extracellular proteases (MMPs, elastases, cathepsins) and tissue factor. The second question can be addressed using interventions that block thrombosis. We have carried out preliminary studies using clopidogrel and a combination of both clopidogrel and acetylsalicylic acid administered in the drinking water and as components of the diet. Neither of these treatments extended the survival of SR-B1/LDLR dKO mice (Fuller and Trigatti, unpublished), however it is difficult to determine whether these treatments were effective in blocking thrombosis. Antibody mediated platelet depletion in these mice resulted in rapid death within two days of the initial treatment (Fuller and Trigatti, unpublished). Therefore, other methods of platelet inhibition would need to be explored in order to address this question. In addition to other established antithrombotic therapies such as glycoprotein IIb/IIIa inhibitors, different dosing and administration protocols for acetylsalicylic acid and clopidogrel treatments can be tested. Alternatively, SR-B1/LDLR dKO mice could be crossed to one of a variety of mutant mice with defective platelet activation.

5.2.4 The Role of SR-B1 in Endothelial and Endothelial Progenitor Cells

The effects of SR-B1 deficiency on immune cells, inflammation and lipoprotein metabolism are systemic effects and would be expected to impact the development of atherosclerosis throughout the arterial system. As expected, we show in chapters 2-4 and others have reported (B. Trigatti et al., 1999; S. Zhang et al., 2005) that SR-B1 deficiency exacerbates atherosclerosis in the aortic sinus compared to SR-B1-expressing controls. However, it is interesting that equivalent levels of atherosclerosis can develop in the aortic sinus of LDLR KO and apoE KO mice without the associated increase in coronary artery atherosclerosis or widespread atherosclerosis along the entire descending aorta observed in SR-B1 deficient animals (compare SR-B1 KO to LDLR KO and apoE KO mice in chapter 2, and chow fed SR-B1/LDLR dKO mice to atherogenic diet-fed LDLR KO mice in chapter 3). These observations suggest that SR-B1 plays an important atheroprotective role in the vessels themselves. Since endothelial dysfunction is thought to play a major role in initiation of atherosclerosis, and patterns of endothelial cell activation and adhesion molecule expression correlate with patterns of atherosclerotic plaque development (Iiyama et al., 1999), the role of SR-B1 in endothelial cells is likely responsible for this protection.

In cultured endothelial cells, HDL stimulates the activation of intracellular signaling in an SR-B1 dependent manner that leads to the downstream activation of eNOS and production of NO (X. A. Li et al., 2002; Yuhanna et al., 2001). This leads to induction of endothelial cell migration (Seetharam et al., 2006) and suppression of adhesion molecule expression *in vitro* (Kimura et al., 2006),

increased NO-mediated vaso-relaxation in cultured aortic rings (Yuhanna et al., 2001), and enhanced endothelial repair after vascular injury *in vivo* (Seetharam et al., 2006). In chapters 2 and 3, we showed that when fed atherogenic diets, SR-B1 deficient mice express significantly elevated levels of adhesion molecules in their coronary artery endothelial cells compared to SR-B1-expressing mice fed the same diets. This provides *in vivo* evidence that SR-B1 affects the expression of VCAM-1 and ICAM-1 in mouse coronary arteries. Given that the expression of VCAM-1 and ICAM-1 is elevated in arterial regions that are prone to atherosclerosis (Iiyama et al., 1999), these results provide a plausible explanation for the unique phenotype of coronary artery atherosclerosis that is observed in SR-B1 deficient mice. If the same differential expression pattern of VCAM-1 and ICAM-1 is also observable in the descending aortas, this would also explain the widespread atherosclerosis observed in the descending aortas of SR-B1 KO mice in chapter 2; however VCAM-1 and ICAM-1 were not measured in the aortas of those mice.

Transgenic expression of SR-B1 in endothelial cells of SR-B1 deficient mice would facilitate direct assessment of SR-B1's endothelial cell-specific role in protection against diet-induced CA atherosclerosis. If restoration of SR-B1 expression in endothelial cells alone is sufficient to prevent CA atherosclerosis, then it can be concluded that SR-B1's role(s) in endothelial cells suppress the development of atherosclerosis in mouse CAs. However, if restoration of SR-B1 in endothelial cells fails to protect SR-B1 KO mice from CA atherosclerosis, the

situation becomes more complicated. Since HDL appears to initiate most SR-B1-mediated signaling in endothelial cells, and SR-B1 KO mice have impaired HDL metabolism, the functional ability of HDL from SR-B1 KO mice to induce endothelial cell signaling would need to be considered. This could be addressed *in vitro* by measuring NO production and phosphorylation of various signaling proteins in cultured endothelial cells in response to HDL isolated from both wild type and SR-B1 KO mice.

The protective role(s) of SR-B1 in endothelial cells could also explain the observation that restoring SR-B1 expression in bone marrow protected SR-B1 KO/ HypoE mice from diet-induced occlusive CA atherosclerosis (Pei et al., 2013). If SR-B1 expression in EPCs increases circulating EPC numbers and enhances BM-mediated endothelial repair, it is possible that SR-B1-expressing EPCs from the BM are incorporated into damaged CA endothelium and restore normal endothelial function in those vessels. This hypothesis could be tested by performing BMTs using marked donor BM, and measuring the incorporation of BM-derived cells into the CA endothelium.

5.3 Conclusions

The results presented in this thesis demonstrate the importance of SR-B1 as an HDL receptor with multiple atheroprotective functions that can be attributed to both its effects on HDL metabolism and its role in HDL-mediated intracellular signaling. SR-B1 KO mice develop exacerbated atherosclerosis in their aortic

sinuses compared to SR-BI expressing control mice, and are uniquely susceptible to the development of CA atherosclerosis. Deficiency of SR-B1 is associated with a number of atherogenic phenotypes including dysregulated lipoprotein metabolism, leukocytosis, elevated systemic inflammation, and elevated local inflammation in the vascular endothelium. Future studies should focus on isolating the specific role(s) of SR-B1 in different cell types in vivo and evaluating their importance in protection against atherosclerosis in mice, particularly in their CAs.

References

- Acton, S., Rigotti, A., Landschulz, K. T., Xu, S., Hobbs, H. H., & Krieger, M. (1996). Identification of scavenger receptor SR-BI as a high density lipoprotein receptor. *Science*, *271*(5248), 518-520.
- Al-Jarallah, A., Chen, X., Gonzalez, L., & Trigatti, B. L. (2014). High density lipoprotein stimulated migration of macrophages depends on the scavenger receptor class B, type I, PDZK1 and Akt1 and is blocked by sphingosine 1 phosphate receptor antagonists. *PLoS One*, *9*(9), e106487. doi: 10.1371/journal.pone.0106487
- Al-Jarallah, A., Igdoura, F., Zhang, Y., Tenedero, C. B., White, E. J., MacDonald, M. E., . . . Trigatti, B. L. (2013). The effect of pomegranate extract on coronary artery atherosclerosis in SR-BI/APOE double knockout mice. *Atherosclerosis*, *228*(1), 80-89. doi: 10.1016/j.atherosclerosis.2013.02.025
- Al-Jarallah, A., & Trigatti, B. L. (2010). A role for the scavenger receptor, class B type I in high density lipoprotein dependent activation of cellular signaling pathways. *Biochim Biophys Acta*, *1801*(12), 1239-1248. doi: 10.1016/j.bbalip.2010.08.006
- Arai, T., Wang, N., Bezouevski, M., Welch, C., & Tall, A. R. (1999). Decreased atherosclerosis in heterozygous low density lipoprotein receptor-deficient mice expressing the scavenger receptor BI transgene. *J Biol Chem*, *274*(4), 2366-2371.

- Assanasen, C., Mineo, C., Seetharam, D., Yuhanna, I. S., Marcel, Y. L., Connelly, M. A., . . . Silver, D. L. (2005). Cholesterol binding, efflux, and a PDZ-interacting domain of scavenger receptor-BI mediate HDL-initiated signaling. *Journal of Clinical Investigation*, *115*(4), 969-977.
- Asztalos, B. F., Tani, M., & Schaefer, E. J. (2011). Metabolic and functional relevance of HDL subspecies. *Curr Opin Lipidol*, *22*(3), 176-185. doi: 10.1097/MOL.0b013e3283468061
- Babitt, J., Trigatti, B., Rigotti, A., Smart, E. J., Anderson, R. G., Xu, S., & Krieger, M. (1997). Murine SR-BI, a high density lipoprotein receptor that mediates selective lipid uptake, is N-glycosylated and fatty acylated and colocalizes with plasma membrane caveolae. *J Biol Chem*, *272*(20), 13242-13249.
- Bourdillon, M. C., Poston, R. N., Covacho, C., Chignier, E., Bricca, G., & McGregor, J. L. (2000). ICAM-1 deficiency reduces atherosclerotic lesions in double-knockout mice (ApoE(-/-)/ICAM-1(-/-)) fed a fat or a chow diet. *Arterioscler Thromb Vasc Biol*, *20*(12), 2630-2635.
- Braun, A., Trigatti, B. L., Post, M. J., Sato, K., Simons, M., Edelberg, J. M., . . . Krieger, M. (2002). Loss of SR-BI expression leads to the early onset of occlusive atherosclerotic coronary artery disease, spontaneous myocardial infarctions, severe cardiac dysfunction, and premature death in apolipoprotein E-deficient mice. *Circ Res*, *90*(3), 270-276.
- Braun, A., Yesilaltay, A., Acton, S., Broschat, K. O., Krul, E. S., Napawan, N., . . . Krieger, M. (2008). Inhibition of intestinal absorption of cholesterol by

ezetimibe or bile acids by SC-435 alters lipoprotein metabolism and extends the lifespan of SR-BI/apoE double knockout mice.

Atherosclerosis, 198(1), 77-84. doi: 10.1016/j.atherosclerosis.2007.10.012

Braun, A., Zhang, S., Miettinen, H. E., Ebrahim, S., Holm, T. M., Vasile, E., . . .

Krieger, M. (2003). Probucol prevents early coronary heart disease and death in the high-density lipoprotein receptor SR-BI/apolipoprotein E double knockout mouse. *Proc Natl Acad Sci U S A*, 100(12), 7283-7288.

Breslow, J. L. (1996). Mouse models of atherosclerosis. *Science*, 272(5262), 685-688.

Cai, L., Ji, A., de Beer, F. C., Tannock, L. R., & van der Westhuyzen, D. R.

(2008). SR-BI protects against endotoxemia in mice through its roles in glucocorticoid production and hepatic clearance. *J Clin Invest*, 118(1), 364-375. doi: 10.1172/JCI31539

Cai, L., Wang, Z., Meyer, J. M., Ji, A., & van der Westhuyzen, D. R. (2012).

Macrophage SR-BI regulates LPS-induced pro-inflammatory signaling in mice and isolated macrophages. *J Lipid Res*, 53(8), 1472-1481. doi: 10.1194/jlr.M023234

Caligiuri, G., Nicoletti, A., Poirier, B., & Hansson, G. K. (2002). Protective

immunity against atherosclerosis carried by B cells of hypercholesterolemic mice. *J Clin Invest*, 109(6), 745-753. doi: 10.1172/JCI7272

- Canton, J., Neculai, D., & Grinstein, S. (2013). Scavenger receptors in homeostasis and immunity. *Nat Rev Immunol*, *13*(9), 621-634. doi: 10.1038/nri3515
- Cao, G., Zhao, L., Stangl, H., Hasegawa, T., Richardson, J. A., Parker, K. L., & Hobbs, H. H. (1999). Developmental and hormonal regulation of murine scavenger receptor, class B, type 1. *Mol Endocrinol*, *13*(9), 1460-1473.
- Chamberlain, J., Francis, S., Brookes, Z., Shaw, G., Graham, D., Alp, N. J., . . . Crossman, D. C. (2009). Interleukin-1 regulates multiple atherogenic mechanisms in response to fat feeding. *PLoS One*, *4*(4), e5073. doi: 10.1371/journal.pone.0005073
- Chatzizisis, Y. S., Coskun, A. U., Jonas, M., Edelman, E. R., Feldman, C. L., & Stone, P. H. (2007). Role of endothelial shear stress in the natural history of coronary atherosclerosis and vascular remodeling: molecular, cellular, and vascular behavior. *J Am Coll Cardiol*, *49*(25), 2379-2393. doi: 10.1016/j.jacc.2007.02.059
- Covey, S. D., Krieger, M., Wang, W., Penman, M., & Trigatti, B. L. (2003). Scavenger receptor class B type I-mediated protection against atherosclerosis in LDL receptor-negative mice involves its expression in bone marrow-derived cells. *Arterioscler Thromb Vasc Biol*, *23*(9), 1589-1594.

- Cybulsky, M. I., Iiyama, K., Li, H., Zhu, S., Chen, M., Iiyama, M., . . . Milstone, D. S. (2001). A major role for VCAM-1, but not ICAM-1, in early atherosclerosis. *J Clin Invest*, *107*(10), 1255-1262. doi: 10.1172/JCI11871
- Daniels, T. F., Killinger, K. M., Michal, J. J., Wright, R. W., Jr., & Jiang, Z. (2009). Lipoproteins, cholesterol homeostasis and cardiac health. *Int J Biol Sci*, *5*(5), 474-488.
- Dansky, H. M., Barlow, C. B., Lominska, C., Sikes, J. L., Kao, C., Weinsaft, J., . . . Smith, J. D. (2001). Adhesion of monocytes to arterial endothelium and initiation of atherosclerosis are critically dependent on vascular cell adhesion molecule-1 gene dosage. *Arterioscler Thromb Vasc Biol*, *21*(10), 1662-1667.
- Daugherty, A. (2002). Mouse models of atherosclerosis. *Am J Med Sci*, *323*(1), 3-10.
- Davi, G., & Patrono, C. (2007). Platelet activation and atherothrombosis. *N Engl J Med*, *357*(24), 2482-2494. doi: 10.1056/NEJMra071014
- Deanfield, J. E., Halcox, J. P., & Rabelink, T. J. (2007). Endothelial function and dysfunction: testing and clinical relevance. *Circulation*, *115*(10), 1285-1295. doi: 10.1161/CIRCULATIONAHA.106.652859
- Dole, V. S., Matuskova, J., Vasile, E., Yesilaltay, A., Bergmeier, W., Bernimoulin, M., . . . Krieger, M. (2008). Thrombocytopenia and platelet abnormalities in high-density lipoprotein receptor-deficient mice. *Arterioscler Thromb Vasc Biol*, *28*(6), 1111-1116. doi: 10.1161/ATVBAHA.108.162347

Du, F., Zhou, J., Gong, R., Huang, X., Pansuria, M., Virtue, A., . . . Yang, X. F.

(2012). Endothelial progenitor cells in atherosclerosis. *Front Biosci (Landmark Ed)*, *17*, 2327-2349.

Fazio, S., & Linton, M. F. (2001). Mouse models of hyperlipidemia and atherosclerosis. *Front Biosci*, *6*, D515-525.

Feng, H., Guo, L., Wang, D., Gao, H., Hou, G., Zheng, Z., . . . Li, X. A. (2011).

Deficiency of scavenger receptor BI leads to impaired lymphocyte homeostasis and autoimmune disorders in mice. *Arterioscler Thromb Vasc Biol*, *31*(11), 2543-2551. doi: 10.1161/ATVBAHA.111.234716

Feng, Y., Jacobs, F., Van Craeyveld, E., Brunaud, C., Snoeys, J., Tjwa, M., . . .

De Geest, B. (2008). Human ApoA-I transfer attenuates transplant arteriosclerosis via enhanced incorporation of bone marrow-derived endothelial progenitor cells. *Arterioscler Thromb Vasc Biol*, *28*(2), 278-283. doi: 10.1161/ATVBAHA.107.158741

Feng, Y., Schouteden, S., Geenens, R., Van Duppen, V., Herijgers, P., Holvoet,

P., . . . Verfaillie, C. M. (2012). Hematopoietic stem/progenitor cell proliferation and differentiation is differentially regulated by high-density and low-density lipoproteins in mice. *PLoS One*, *7*(11), e47286. doi: 10.1371/journal.pone.0047286

Feng, Y., van Eck, M., Van Craeyveld, E., Jacobs, F., Carlier, V., Van Linthout,

S., . . . De Geest, B. (2009). Critical role of scavenger receptor-BI-expressing bone marrow-derived endothelial progenitor cells in the

- attenuation of allograft vasculopathy after human apo A-I transfer. *Blood*, 113(3), 755-764. doi: 10.1182/blood-2008-06-161794
- Fernandez-Hernando, C., Ackah, E., Yu, J., Suarez, Y., Murata, T., Iwakiri, Y., . . . Sessa, W. C. (2007). Loss of Akt1 leads to severe atherosclerosis and occlusive coronary artery disease. *Cell Metab*, 6(6), 446-457.
- Gao, M., Zhao, D., Schouteden, S., Sorci-Thomas, M. G., Van Veldhoven, P. P., Eggermont, K., . . . Feng, Y. (2014). Regulation of high-density lipoprotein on hematopoietic stem/progenitor cells in atherosclerosis requires scavenger receptor type BI expression. *Arterioscler Thromb Vasc Biol*, 34(9), 1900-1909. doi: 10.1161/ATVBAHA.114.304006
- Getz, G. S., & Reardon, C. A. (2006). Diet and murine atherosclerosis. *Arterioscler Thromb Vasc Biol*, 26(2), 242-249.
- Gilibert, S., Galle-Treger, L., Moreau, M., Saint-Charles, F., Costa, S., Ballaire, R., . . . Huby, T. (2014). Adrenocortical scavenger receptor class B type I deficiency exacerbates endotoxic shock and precipitates sepsis-induced mortality in mice. *J Immunol*, 193(2), 817-826. doi: 10.4049/jimmunol.1303164
- Goldstein, J. L., & Brown, M. S. (2009). The LDL receptor. *Arterioscler Thromb Vasc Biol*, 29(4), 431-438. doi: 10.1161/ATVBAHA.108.179564
- Guo, L., Song, Z., Li, M., Wu, Q., Wang, D., Feng, H., . . . Li, X. A. (2009). Scavenger Receptor BI Protects against Septic Death through Its Role in

Modulating Inflammatory Response. *J Biol Chem*, 284(30), 19826-19834.

doi: 10.1074/jbc.M109.020933

Guo, L., Zheng, Z., Ai, J., Huang, B., & Li, X. A. (2014). Hepatic scavenger receptor BI protects against polymicrobial-induced sepsis through promoting LPS clearance in mice. *J Biol Chem*, 289(21), 14666-14673.

doi: 10.1074/jbc.M113.537258

Hajra, L., Evans, A. I., Chen, M., Hyduk, S. J., Collins, T., & Cybulsky, M. I. (2000). The NF-kappa B signal transduction pathway in aortic endothelial cells is primed for activation in regions predisposed to atherosclerotic lesion formation. *Proc Natl Acad Sci U S A*, 97(16), 9052-9057.

Harder, C., Lau, P., Meng, A., Whitman, S. C., & McPherson, R. (2007).

Cholesteryl ester transfer protein (CETP) expression protects against diet induced atherosclerosis in SR-BI deficient mice. *Arterioscler Thromb Vasc Biol*, 27(4), 858-864. doi: 10.1161/01.ATV.0000259357.42089.dc

Hartvigsen, K., Binder, C. J., Hansen, L. F., Rafia, A., Juliano, J., Horkko, S., . . .

Li, A. C. (2007). A diet-induced hypercholesterolemic murine model to study atherogenesis without obesity and metabolic syndrome. *Arterioscler Thromb Vasc Biol*, 27(4), 878-885. doi:

10.1161/01.ATV.0000258790.35810.02

Hegele, R. A. (2009). Plasma lipoproteins: genetic influences and clinical implications. *Nat Rev Genet*, 10(2), 109-121. doi: 10.1038/nrg2481

- Herman, G. E. (2003). Disorders of cholesterol biosynthesis: prototypic metabolic malformation syndromes. *Hum Mol Genet*, *12 Spec No 1*, R75-88.
- Hildebrand, R. B., Lammers, B., Meurs, I., Korporaal, S. J., De Haan, W., Zhao, Y., . . . Van Eck, M. (2010). Restoration of high-density lipoprotein levels by cholesteryl ester transfer protein expression in scavenger receptor class B type I (SR-BI) knockout mice does not normalize pathologies associated with SR-BI deficiency. *Arterioscler Thromb Vasc Biol*, *30(7)*, 1439-1445. doi: 10.1161/ATVBAHA.110.205153
- Hoekstra, M., Meurs, I., Koenders, M., Out, R., Hildebrand, R. B., Kruijt, J. K., . . . Van Berkel, T. J. (2008). Absence of HDL cholesteryl ester uptake in mice via SR-BI impairs an adequate adrenal glucocorticoid-mediated stress response to fasting. *J Lipid Res*, *49(4)*, 738-745. doi: 10.1194/jlr.M700475-JLR200
- Holm, T. M., Braun, A., Trigatti, B. L., Brugnara, C., Sakamoto, M., Krieger, M., & Andrews, N. C. (2002). Failure of red blood cell maturation in mice with defects in the high-density lipoprotein receptor SR-BI. *Blood*, *99(5)*, 1817-1824.
- Hopkins, P. N. (2013). Molecular biology of atherosclerosis. *Physiol Rev*, *93(3)*, 1317-1542. doi: 10.1152/physrev.00004.2012
- Huby, T., Doucet, C., Dachet, C., Ouzilleau, B., Ueda, Y., Afzal, V., . . . Lesnik, P. (2006). Knockdown expression and hepatic deficiency reveal an

atheroprotective role for SR-BI in liver and peripheral tissues. *J Clin Invest*, 116(10), 2767-2776. doi: 10.1172/JCI26893

Iiyama, K., Hajra, L., Iiyama, M., Li, H., DiChiara, M., Medoff, B. D., & Cybulsky, M. I. (1999). Patterns of vascular cell adhesion molecule-1 and intercellular adhesion molecule-1 expression in rabbit and mouse atherosclerotic lesions and at sites predisposed to lesion formation. *Circ Res*, 85(2), 199-207.

Ishibashi, S., Brown, M. S., Goldstein, J. L., Gerard, R. D., Hammer, R. E., & Herz, J. (1993). Hypercholesterolemia in low density lipoprotein receptor knockout mice and its reversal by adenovirus-mediated gene delivery. *J Clin Invest*, 92(2), 883-893.

Ishibashi, S., Goldstein, J. L., Brown, M. S., Herz, J., & Burns, D. K. (1994). Massive xanthomatosis and atherosclerosis in cholesterol-fed low density lipoprotein receptor-negative mice. *J Clin Invest*, 93(5), 1885-1893.

Ji, Y., Jian, B., Wang, N., Sun, Y., Moya, M. L., Phillips, M. C., . . . Tall, A. R. (1997). Scavenger receptor BI promotes high density lipoprotein-mediated cellular cholesterol efflux. *J Biol Chem*, 272(34), 20982-20985.

Ji, Y., Wang, N., Ramakrishnan, R., Sehayek, E., Huszar, D., Breslow, J. L., & Tall, A. R. (1999). Hepatic scavenger receptor BI promotes rapid clearance of high density lipoprotein free cholesterol and its transport into bile. *J Biol Chem*, 274(47), 33398-33402.

- Jian, B., de la Llera-Moya, M., Ji, Y., Wang, N., Phillips, M. C., Swaney, J. B., . . . Rothblat, G. H. (1998). Scavenger receptor class B type I as a mediator of cellular cholesterol efflux to lipoproteins and phospholipid acceptors. *J Biol Chem*, 273(10), 5599-5606.
- Karackattu, S. L., Picard, M. H., & Krieger, M. (2005). Lymphocytes are not required for the rapid onset of coronary heart disease in scavenger receptor class B type I/apolipoprotein E double knockout mice. *Arterioscler Thromb Vasc Biol*, 25(4), 803-808. doi: 10.1161/01.ATV.0000158310.64498.ac
- Karackattu, S. L., Trigatti, B., & Krieger, M. (2006). Hepatic lipase deficiency delays atherosclerosis, myocardial infarction, and cardiac dysfunction and extends lifespan in SR-BI/apolipoprotein E double knockout mice. *Arterioscler Thromb Vasc Biol*, 26(3), 548-554.
- Kimura, T., Tomura, H., Mogi, C., Kuwabara, A., Damirin, A., Ishizuka, T., . . . Okajima, F. (2006). Role of scavenger receptor class B type I and sphingosine 1-phosphate receptors in high density lipoprotein-induced inhibition of adhesion molecule expression in endothelial cells. *J Biol Chem*, 281(49), 37457-37467.
- Kocher, O., Yesilaltay, A., Shen, C. H., Zhang, S., Daniels, K., Pal, R., . . . Krieger, M. (2008). Influence of PDZK1 on lipoprotein metabolism and atherosclerosis. *Biochim Biophys Acta*, 1782(5), 310-316. doi: 10.1016/j.bbadis.2008.02.004

- Korporaal, S. J., Meurs, I., Hauer, A. D., Hildebrand, R. B., Hoekstra, M., Cate, H. T., . . . Van Eck, M. (2011). Deletion of the high-density lipoprotein receptor scavenger receptor BI in mice modulates thrombosis susceptibility and indirectly affects platelet function by elevation of plasma free cholesterol. *Arterioscler Thromb Vasc Biol*, *31*(1), 34-42. doi: 10.1161/ATVBAHA.110.210252
- Kozarsky, K. F., Donahee, M. H., Glick, J. M., Krieger, M., & Rader, D. J. (2000). Gene transfer and hepatic overexpression of the HDL receptor SR-BI reduces atherosclerosis in the cholesterol-fed LDL receptor-deficient mouse. *Arterioscler Thromb Vasc Biol*, *20*(3), 721-727.
- Kozarsky, K. F., Donahee, M. H., Rigotti, A., Iqbal, S. N., Edelman, E. R., & Krieger, M. (1997). Overexpression of the HDL receptor SR-BI alters plasma HDL and bile cholesterol levels. *Nature*, *387*(6631), 414-417.
- Krieger, M. (1999). Charting the fate of the "good cholesterol": identification and characterization of the high-density lipoprotein receptor SR-BI. *Annu Rev Biochem*, *68*, 523-558.
- Kuhlencordt, P. J., Gyurko, R., Han, F., Scherrer-Crosbie, M., Aretz, T. H., Hajjar, R., . . . Huang, P. L. (2001). Accelerated atherosclerosis, aortic aneurysm formation, and ischemic heart disease in apolipoprotein E/endothelial nitric oxide synthase double-knockout mice. *Circulation*, *104*(4), 448-454.
- Kyaw, T., Tay, C., Krishnamurthi, S., Kanellakis, P., Agrotis, A., Tipping, P., . . . Toh, B. H. (2011). B1a B lymphocytes are atheroprotective by secreting

natural IgM that increases IgM deposits and reduces necrotic cores in atherosclerotic lesions. *Circ Res*, 109(8), 830-840. doi:

10.1161/CIRCRESAHA.111.248542

Kzhyshkowska, J., Neyen, C., & Gordon, S. (2012). Role of macrophage scavenger receptors in atherosclerosis. *Immunobiology*, 217(5), 492-502.

doi: 10.1016/j.imbio.2012.02.015

Langer, H. F., & Gawaz, M. (2008). Platelet-vessel wall interactions in atherosclerotic disease. *Thromb Haemost*, 99(3), 480-486. doi:

10.1160/TH07-11-0685

LaRosa, J. C., Pedersen, T. R., Somaratne, R., & Wasserman, S. M. (2013).

Safety and effect of very low levels of low-density lipoprotein cholesterol on cardiovascular events. *Am J Cardiol*, 111(8), 1221-1229. doi:

10.1016/j.amjcard.2012.12.052

Ley, K., Miller, Y. I., & Hedrick, C. C. (2011). Monocyte and macrophage dynamics during atherogenesis. *Arterioscler Thromb Vasc Biol*, 31(7),

1506-1516. doi: 10.1161/ATVBAHA.110.221127

Li, J., & Ley, K. (2015). Lymphocyte migration into atherosclerotic plaque.

Arterioscler Thromb Vasc Biol, 35(1), 40-49. doi:

10.1161/ATVBAHA.114.303227

Li, X. A., Guo, L., Asmis, R., Nikolova-Karakashian, M., & Smart, E. J. (2006).

Scavenger receptor BI prevents nitric oxide-induced cytotoxicity and

endotoxin-induced death. *Circ Res*, 98(7), e60-65. doi:

10.1161/01.RES.0000219310.00308.10

- Li, X. A., Titlow, W. B., Jackson, B. A., Giltiay, N., Nikolova-Karakashian, M., Uittenbogaard, A., & Smart, E. J. (2002). High density lipoprotein binding to scavenger receptor, Class B, type I activates endothelial nitric-oxide synthase in a ceramide-dependent manner. *J Biol Chem*, 277(13), 11058-11063.
- Libby, P. (2002). Inflammation in atherosclerosis. *Nature*, 420(6917), 868-874. doi: 10.1038/nature01323
- Libby, P. (2009). Molecular and cellular mechanisms of the thrombotic complications of atherosclerosis. *J Lipid Res*, 50 Suppl, S352-357. doi: 10.1194/jlr.R800099-JLR200
- Libby, P., Ridker, P. M., & Maseri, A. (2002). Inflammation and atherosclerosis. *Circulation*, 105(9), 1135-1143.
- Linsel-Nitschke, P., & Tall, A. R. (2005). HDL as a target in the treatment of atherosclerotic cardiovascular disease. *Nat Rev Drug Discov*, 4(3), 193-205. doi: 10.1038/nrd1658
- Llodra, J., Angeli, V., Liu, J., Trogan, E., Fisher, E. A., & Randolph, G. J. (2004). Emigration of monocyte-derived cells from atherosclerotic lesions characterizes regressive, but not progressive, plaques. *Proc Natl Acad Sci U S A*, 101(32), 11779-11784. doi: 10.1073/pnas.0403259101

- Lusis, A. J. (2000). Atherosclerosis. *Nature*, 407(6801), 233-241. doi:
10.1038/35025203
- Lusis, A. J., Fogelman, A. M., & Fonarow, G. C. (2004). Genetic basis of
atherosclerosis: part I: new genes and pathways. *Circulation*, 110(13),
1868-1873. doi: 10.1161/01.CIR.0000143041.58692.CC
- Ma, Y., Ashraf, M. Z., & Podrez, E. A. (2010). Scavenger receptor BI modulates
platelet reactivity and thrombosis in dyslipidemia. *Blood*, 116(11), 1932-
1941. doi: 10.1182/blood-2010-02-268508
- Meurs, I., Hoekstra, M., van Wanrooij, E. J., Hildebrand, R. B., Kuiper, J.,
Kuipers, F., . . . Van Eck, M. (2005). HDL cholesterol levels are an
important factor for determining the lifespan of erythrocytes. *Exp Hematol*,
33(11), 1309-1319. doi: 10.1016/j.exphem.2005.07.004
- Miettinen, H. E., Rayburn, H., & Krieger, M. (2001). Abnormal lipoprotein
metabolism and reversible female infertility in HDL receptor (SR-BI)-
deficient mice. *J Clin Invest*, 108(11), 1717-1722.
- Mineo, C., Yuhanna, I. S., Quon, M. J., & Shaul, P. W. (2003). High density
lipoprotein-induced endothelial nitric-oxide synthase activation is mediated
by Akt and MAP kinases. *J Biol Chem*, 278(11), 9142-9149.
- Montecucco, F., Quercioli, A., & Mach, F. (2009). Ezetimibe/simvastatin. *Expert
Opin Drug Saf*, 8(6), 715-725. doi: 10.1517/14740330903282745
- Nakagawa-Toyama, Y., Zhang, S., & Krieger, M. (2012). Dietary manipulation
and social isolation alter disease progression in a murine model of

coronary heart disease. *PLoS One*, 7(10), e47965. doi:

10.1371/journal.pone.0047965

Neculai, D., Schwake, M., Ravichandran, M., Zunke, F., Collins, R. F., Peters, J.,

. . . Dhe-Paganon, S. (2013). Structure of LIMP-2 provides functional

insights with implications for SR-BI and CD36. *Nature*, 504(7478), 172-

176. doi: 10.1038/nature12684

Nes, W. D. (2011). Biosynthesis of cholesterol and other sterols. *Chem Rev*,

111(10), 6423-6451. doi: 10.1021/cr200021m

Noor, R., Shuaib, U., Wang, C. X., Todd, K., Ghani, U., Schwindt, B., & Shuaib,

A. (2007). High-density lipoprotein cholesterol regulates endothelial

progenitor cells by increasing eNOS and preventing apoptosis.

Atherosclerosis, 192(1), 92-99. doi: 10.1016/j.atherosclerosis.2006.06.023

Paigen, B., Morrow, A., Brandon, C., Mitchell, D., & Holmes, P. (1985). Variation

in susceptibility to atherosclerosis among inbred strains of mice.

Atherosclerosis, 57(1), 65-73.

Pei, Y., Chen, X., Aboutouk, D., Fuller, M. T., Dadoo, O., Yu, P., . . . Trigatti, B. L.

(2013). SR-BI in bone marrow derived cells protects mice from diet

induced coronary artery atherosclerosis and myocardial infarction. *PLoS*

One, 8(8), e72492. doi: 10.1371/journal.pone.0072492

Petoumenos, V., Nickenig, G., & Werner, N. (2009). High-density lipoprotein

exerts vasculoprotection via endothelial progenitor cells. *J Cell Mol Med*,

13(11-12), 4623-4635. doi: 10.1111/j.1582-4934.2008.00472.x

- Phillips, M. C. (2013). New insights into the determination of HDL structure by apolipoproteins: Thematic review series: high density lipoprotein structure, function, and metabolism. *J Lipid Res*, *54*(8), 2034-2048. doi: 10.1194/jlr.R034025
- Piedrahita, J. A., Zhang, S. H., Hagan, J. R., Oliver, P. M., & Maeda, N. (1992). Generation of mice carrying a mutant apolipoprotein E gene inactivated by gene targeting in embryonic stem cells. *Proc Natl Acad Sci U S A*, *89*(10), 4471-4475.
- Plump, A. S., Smith, J. D., Hayek, T., Aalto-Setälä, K., Walsh, A., Verstuyft, J. G., . . . Breslow, J. L. (1992). Severe hypercholesterolemia and atherosclerosis in apolipoprotein E-deficient mice created by homologous recombination in ES cells. *Cell*, *71*(2), 343-353.
- Rader, D. J., & Daugherty, A. (2008). Translating molecular discoveries into new therapies for atherosclerosis. *Nature*, *451*(7181), 904-913. doi: 10.1038/nature06796
- Raffai, R. L., Loeb, S. M., & Weisgraber, K. H. (2005). Apolipoprotein E promotes the regression of atherosclerosis independently of lowering plasma cholesterol levels. *Arterioscler Thromb Vasc Biol*, *25*(2), 436-441.
- Raffai, R. L., & Weisgraber, K. H. (2002). Hypomorphic apolipoprotein E mice: a new model of conditional gene repair to examine apolipoprotein E-mediated metabolism. *J Biol Chem*, *277*(13), 11064-11068.

- Reardon, C. A., & Getz, G. S. (2001). Mouse models of atherosclerosis. *Curr Opin Lipidol*, 12(2), 167-173.
- Ridker, P. M. (2014). LDL cholesterol: controversies and future therapeutic directions. *Lancet*, 384(9943), 607-617. doi: 10.1016/S0140-6736(14)61009-6
- Rigotti, A., Edelman, E. R., Seifert, P., Iqbal, S. N., DeMattos, R. B., Temel, R. E., . . . Williams, D. L. (1996). Regulation by adrenocorticotrophic hormone of the in vivo expression of scavenger receptor class B type I (SR-BI), a high density lipoprotein receptor, in steroidogenic cells of the murine adrenal gland. *J Biol Chem*, 271(52), 33545-33549.
- Rigotti, A., Miettinen, H. E., & Krieger, M. (2003). The role of the high-density lipoprotein receptor SR-BI in the lipid metabolism of endocrine and other tissues. *Endocr Rev*, 24(3), 357-387.
- Rigotti, A., Trigatti, B. L., Penman, M., Rayburn, H., Herz, J., & Krieger, M. (1997). A targeted mutation in the murine gene encoding the high density lipoprotein (HDL) receptor scavenger receptor class B type I reveals its key role in HDL metabolism. *Proc Natl Acad Sci U S A*, 94(23), 12610-12615.
- Robbins, C. S., Chudnovskiy, A., Rauch, P. J., Figueiredo, J. L., Iwamoto, Y., Gorbатов, R., . . . Swirski, F. K. (2012). Extramedullary hematopoiesis generates Ly-6C(high) monocytes that infiltrate atherosclerotic lesions.

Circulation, 125(2), 364-374. doi:

10.1161/CIRCULATIONAHA.111.061986

Rodrigueza, W. V., Thuahnai, S. T., Temel, R. E., Lund-Katz, S., Phillips, M. C., & Williams, D. L. (1999). Mechanism of scavenger receptor class B type I-mediated selective uptake of cholesteryl esters from high density lipoprotein to adrenal cells. *J Biol Chem*, 274(29), 20344-20350.

Seetharam, D., Mineo, C., Gormley, A. K., Gibson, L. L., Vongpatanasin, W., Chambliss, K. L., . . . Shaul, P. W. (2006). High-density lipoprotein promotes endothelial cell migration and reendothelialization via scavenger receptor-B type I. *Circ Res*, 98(1), 63-72.

Selathurai, A., Deswaerte, V., Kanellakis, P., Tipping, P., Toh, B. H., Bobik, A., & Kyaw, T. (2014). Natural killer (NK) cells augment atherosclerosis by cytotoxic-dependent mechanisms. *Cardiovasc Res*, 102(1), 128-137. doi: 10.1093/cvr/cvu016

Silver, D. L. (2002). A carboxyl-terminal PDZ-interacting domain of scavenger receptor B, type I is essential for cell surface expression in liver. *J Biol Chem*, 277(37), 34042-34047.

Sary, H. C., Chandler, A. B., Dinsmore, R. E., Fuster, V., Glagov, S., Insull, W., Jr., . . . Wissler, R. W. (1995). A definition of advanced types of atherosclerotic lesions and a histological classification of atherosclerosis. A report from the Committee on Vascular Lesions of the Council on

Arteriosclerosis, American Heart Association. *Circulation*, 92(5), 1355-1374.

Stary, H. C., Chandler, A. B., Glagov, S., Guyton, J. R., Insull, W., Jr., Rosenfeld, M. E., . . . Wissler, R. W. (1994). A definition of initial, fatty streak, and intermediate lesions of atherosclerosis. A report from the Committee on Vascular Lesions of the Council on Arteriosclerosis, American Heart Association. *Circulation*, 89(5), 2462-2478.

Steinberg, D. (1997). Low density lipoprotein oxidation and its pathobiological significance. *J Biol Chem*, 272(34), 20963-20966.

Sumi, M., Sata, M., Miura, S., Rye, K. A., Toya, N., Kanaoka, Y., . . . Nagai, R. (2007). Reconstituted high-density lipoprotein stimulates differentiation of endothelial progenitor cells and enhances ischemia-induced angiogenesis. *Arterioscler Thromb Vasc Biol*, 27(4), 813-818. doi: 10.1161/01.ATV.0000259299.38843.64

Sun, Y., Wang, N., & Tall, A. R. (1999). Regulation of adrenal scavenger receptor-BI expression by ACTH and cellular cholesterol pools. *J Lipid Res*, 40(10), 1799-1805.

Swirski, F. K., Libby, P., Aikawa, E., Alcaide, P., Luscinskas, F. W., Weissleder, R., & Pittet, M. J. (2007). Ly-6Chi monocytes dominate hypercholesterolemia-associated monocytosis and give rise to macrophages in atheromata. *J Clin Invest*, 117(1), 195-205.

- Swirski, F. K., & Nahrendorf, M. (2013). Leukocyte behavior in atherosclerosis, myocardial infarction, and heart failure. *Science*, 339(6116), 161-166. doi: 10.1126/science.1230719
- Tabas, I. (2010). Macrophage death and defective inflammation resolution in atherosclerosis. *Nat Rev Immunol*, 10(1), 36-46. doi: 10.1038/nri2675
- Tall, A. R., Yvan-Charvet, L., Westerterp, M., & Murphy, A. J. (2012). Cholesterol efflux: a novel regulator of myelopoiesis and atherogenesis. *Arterioscler Thromb Vasc Biol*, 32(11), 2547-2552. doi: 10.1161/ATVBAHA.112.300134
- Trigatti, B., Rayburn, H., Vinals, M., Braun, A., Miettinen, H., Penman, M., . . . Krieger, M. (1999). Influence of the high density lipoprotein receptor SR-BI on reproductive and cardiovascular pathophysiology. *Proc Natl Acad Sci U S A*, 96(16), 9322-9327.
- Trigatti, B., Rigotti, A., & Krieger, M. (2000). The role of the high-density lipoprotein receptor SR-BI in cholesterol metabolism. *Curr Opin Lipidol*, 11(2), 123-131.
- Trigatti, B. L., Krieger, M., & Rigotti, A. (2003). Influence of the HDL receptor SR-BI on lipoprotein metabolism and atherosclerosis. *Arterioscler Thromb Vasc Biol*, 23(10), 1732-1738.
- Tso, C., Martinic, G., Fan, W. H., Rogers, C., Rye, K. A., & Barter, P. J. (2006). High-density lipoproteins enhance progenitor-mediated endothelium repair

in mice. *Arterioscler Thromb Vasc Biol*, 26(5), 1144-1149. doi:
10.1161/01.ATV.0000216600.37436.cf

Ueda, Y., Gong, E., Royer, L., Cooper, P. N., Francone, O. L., & Rubin, E. M. (2000). Relationship between expression levels and atherogenesis in scavenger receptor class B, type I transgenics. *J Biol Chem*, 275(27), 20368-20373.

Uittenbogaard, A., Shaul, P. W., Yuhanna, I. S., Blair, A., & Smart, E. J. (2000). High density lipoprotein prevents oxidized low density lipoprotein-induced inhibition of endothelial nitric-oxide synthase localization and activation in caveolae. *J Biol Chem*, 275(15), 11278-11283.

Van Eck, M., Bos, I. S., Hildebrand, R. B., Van Rij, B. T., & Van Berkel, T. J. (2004). Dual role for scavenger receptor class B, type I on bone marrow-derived cells in atherosclerotic lesion development. *Am J Pathol*, 165(3), 785-794.

Van Eck, M., Twisk, J., Hoekstra, M., Van Rij, B. T., Van der Lans, C. A., Bos, I. S., . . . Van Berkel, T. J. (2003). Differential effects of scavenger receptor BI deficiency on lipid metabolism in cells of the arterial wall and in the liver. *J Biol Chem*, 278(26), 23699-23705.

Vergnes, L., Phan, J., Strauss, M., Tafuri, S., & Reue, K. (2003). Cholesterol and cholate components of an atherogenic diet induce distinct stages of hepatic inflammatory gene expression. *J Biol Chem*, 278(44), 42774-42784. doi: 10.1074/jbc.M306022200

- Wang, X., Collins, H. L., Ranalletta, M., Fuki, I. V., Billheimer, J. T., Rothblat, G. H., . . . Rader, D. J. (2007). Macrophage ABCA1 and ABCG1, but not SR-BI, promote macrophage reverse cholesterol transport in vivo. *J Clin Invest*, 117(8), 2216-2224.
- Webb, N. R., Connell, P. M., Graf, G. A., Smart, E. J., de Villiers, W. J., de Beer, F. C., & van der Westhuyzen, D. R. (1998). SR-BII, an isoform of the scavenger receptor BI containing an alternate cytoplasmic tail, mediates lipid transfer between high density lipoprotein and cells. *J Biol Chem*, 273(24), 15241-15248.
- Weber, C., Zernecke, A., & Libby, P. (2008). The multifaceted contributions of leukocyte subsets to atherosclerosis: lessons from mouse models. *Nat Rev Immunol*, 8(10), 802-815. doi: 10.1038/nri2415
- Westerterp, M., Gourion-Arsiquaud, S., Murphy, A. J., Shih, A., Cremers, S., Levine, R. L., . . . Yvan-Charvet, L. (2012). Regulation of hematopoietic stem and progenitor cell mobilization by cholesterol efflux pathways. *Cell Stem Cell*, 11(2), 195-206. doi: 10.1016/j.stem.2012.04.024
- Whitman, S. C. (2004). A practical approach to using mice in atherosclerosis research. *Clin Biochem Rev*, 25(1), 81-93.
- Witztum, J. L., & Lichtman, A. H. (2014). The influence of innate and adaptive immune responses on atherosclerosis. *Annu Rev Pathol*, 9, 73-102. doi: 10.1146/annurev-pathol-020712-163936

- Won, D., Zhu, S. N., Chen, M., Teichert, A. M., Fish, J. E., Matouk, C. C., . . .
Cybulsky, M. I. (2007). Relative reduction of endothelial nitric-oxide
synthase expression and transcription in atherosclerosis-prone regions of
the mouse aorta and in an in vitro model of disturbed flow. *Am J Pathol*,
171(5), 1691-1704.
- Xiao, C., Hsieh, J., Adeli, K., & Lewis, G. F. (2011). Gut-liver interaction in
triglyceride-rich lipoprotein metabolism. *Am J Physiol Endocrinol Metab*,
301(3), E429-446. doi: 10.1152/ajpendo.00178.2011
- Yesilaltay, A., Daniels, K., Pal, R., Krieger, M., & Kocher, O. (2009). Loss of
PDZK1 causes coronary artery occlusion and myocardial infarction in
Paigen diet-fed apolipoprotein E deficient mice. *PLoS One*, 4(12), e8103.
doi: 10.1371/journal.pone.0008103
- Yesilaltay, A., Dokshin, G. A., Busso, D., Wang, L., Galiani, D., Chavarria, T., . . .
Krieger, M. (2014). Excess cholesterol induces mouse egg activation and
may cause female infertility. *Proc Natl Acad Sci U S A*, 111(46), E4972-
4980. doi: 10.1073/pnas.1418954111
- Yu, H., Zhang, W., Yancey, P. G., Koury, M. J., Zhang, Y., Fazio, S., & Linton, M.
F. (2006). Macrophage apolipoprotein E reduces atherosclerosis and
prevents premature death in apolipoprotein E and scavenger receptor-
class BI double-knockout mice. *Arterioscler Thromb Vasc Biol*, 26(1), 150-
156.

- Yu, X. H., Fu, Y. C., Zhang, D. W., Yin, K., & Tang, C. K. (2013). Foam cells in atherosclerosis. *Clin Chim Acta*, 424, 245-252. doi: 10.1016/j.cca.2013.06.006
- Yuhanna, I. S., Zhu, Y., Cox, B. E., Hahner, L. D., Osborne-Lawrence, S., Lu, P., . . . Shaul, P. W. (2001). High-density lipoprotein binding to scavenger receptor-BI activates endothelial nitric oxide synthase. *Nat Med*, 7(7), 853-857.
- Yvan-Charvet, L., Pagler, T., Gautier, E. L., Avagyan, S., Siry, R. L., Han, S., . . . Tall, A. R. (2010). ATP-binding cassette transporters and HDL suppress hematopoietic stem cell proliferation. *Science*, 328(5986), 1689-1693. doi: 10.1126/science.1189731
- Zhang, Q., Yin, H., Liu, P., Zhang, H., & She, M. (2010). Essential role of HDL on endothelial progenitor cell proliferation with PI3K/Akt/cyclin D1 as the signal pathway. *Exp Biol Med (Maywood)*, 235(9), 1082-1092. doi: 10.1258/ebm.2010.010060
- Zhang, S., Picard, M. H., Vasile, E., Zhu, Y., Raffai, R. L., Weisgraber, K. H., & Krieger, M. (2005). Diet-induced occlusive coronary atherosclerosis, myocardial infarction, cardiac dysfunction, and premature death in scavenger receptor class B type I-deficient, hypomorphic apolipoprotein ER61 mice. *Circulation*, 111(25), 3457-3464.

- Zhang, S. H., Reddick, R. L., Piedrahita, J. A., & Maeda, N. (1992). Spontaneous hypercholesterolemia and arterial lesions in mice lacking apolipoprotein E. *Science*, 258(5081), 468-471.
- Zhang, W., Yancey, P. G., Su, Y. R., Babaev, V. R., Zhang, Y., Fazio, S., & Linton, M. F. (2003). Inactivation of macrophage scavenger receptor class B type I promotes atherosclerotic lesion development in apolipoprotein E-deficient mice. *Circulation*, 108(18), 2258-2263.
- Zhou, J., Moller, J., Danielsen, C. C., Bentzon, J., Ravn, H. B., Austin, R. C., & Falk, E. (2001). Dietary supplementation with methionine and homocysteine promotes early atherosclerosis but not plaque rupture in ApoE-deficient mice. *Arterioscler Thromb Vasc Biol*, 21(9), 1470-1476.
- Zhu, W., Saddar, S., Seetharam, D., Chambliss, K. L., Longoria, C., Silver, D. L., . . . Mineo, C. (2008). The scavenger receptor class B type I adaptor protein PDZK1 maintains endothelial monolayer integrity. *Circ Res*, 102(4), 480-487. doi: 10.1161/CIRCRESAHA.107.159079